TITLE AN INVESTIGATION INTO THE RELATIONSHIPS BETWEEN PROCESSING, ORIENTATION AND PROPERTIES OF LOW DENSITY POLYETHYLENE FILMS

AUTHOR BAHARIN BIN AZAHARI

INSTITUTION and DATE Polytechnic of North London (1990) (CNAA)

AN INVESTIGATION INTO THE RELATIONSHIPS BETWEEN PROCESSING, ORIENTATION AND PROPERTIES OF LOW DENSITY POLYETHYLENE FILMS

BAHARIN BIN AZAHARI (BSc, MSc)

A thesis submitted in partial fulfilment of the requirements of the Council for National Academic Awards for the degree of Doctor of Philosophy

September 1990

Sponsored by the Polytechnic of North London in collaboration with BP Chemicals Ltd

ABSTRACT

AN INVESTIGATION INTO THE RELATIONSHIPS BETWEEN PROCESSING, ORIENTATION AND PROPERTIES OF LOW DENSITY POLYETHYLENE FILMS

by

Baharin B. Azahari

The effect of changing processing conditions on the mechanical properties of LDPE, LLDPE and blends of LDPE and LLDPE blown films was studied. The results were analysed by relating the change in mechanical properties with the change in the residual strain of the manufactured films. The residual strain was measured by using a shrinkage method.

The residual strain of the films was found to depend on the processing conditions used to manufacture the films and on the proportion of LLDPE in the blend. Increasing the blow-up ratio, *BUR*, or the haul-off speed, *HOS*, increased the residual strain in the extrusion or machine direction, *MD*, and the residual strain in the direction perpendicular to the machine direction, *TD*, of the films. On the other hand, increasing the freeze line height, *FLH*, and the screw speed, *SS*, reduced the residual strain in both directions of the films. Increasing LLDPE composition in the blend also resulted in the decrease in the residual strain in both directions of the films.

The measured mechanical properties were found to depend on the residual strain in both *MD* and *TD*. In the case of tensile strength and elongation at break it was possible to correlate all measurements with a single function of the residual strain in the direction of test and the perpendicular direction. For yield strength, tensile modulus, tear and impact the dependence was more complex.

ACKNOWLEDGEMENTS

I would like to thank my supervisors, D.J. Dunning and Dr. B.W. Burgar, for their invaluable help and advice throughout the project. Also I would like to thank BP Chemicals, especially Dr. John Torkington, for supplying me with the materials for the project.

An expression of thank is also due to Universiti Sains Malaysia and Jabatan Perkhidmatan Awam Malaysia for sponsoring me and also thanks to all the technicians at London School of Polymer Technology, especially Percy, for helping me with my work.

Finally, I would like to dedicate this thesis to my wife, Suria, and my son, Mohd. Barzaki, for their patience and understanding in me throughout the project.

ERRATA

Page 1 line 8, "application" should be "applications".

Page 2 line 2, "degree" should be "degrees".

Page 4 line 5, "by which" should be "at which".

Page 15 line 22, "crystal" should be "crystals".

Page 56 line 3, "different" should be "difference".

Page 56 line 15, "to study" should be "of studying".

Page 56 line 20, "use shrinkage method" should be "use a shrinkage method".

Page 63 line 13, "110" should be "105".

Page 72 line 5, "as a mean of" should be "as a means of".

Page 82 line 9, "than" should be "then".

Page 92 line 13, "hold" should be "held".

Page 95 line 2, "110" should be "105".

Page 118 line 22, "10^{-2}" should be "10^{-3}".

Page 128 line 5, "discussed" should be "discusses".

Page 134 lines 1 and 2, "EB_{MD}" should be "Eb_{MD}".

Page 134 line 3, "EB_{TD}" should be "Eb_{TD}".

Page 160 line 5, "eventhough" should be "even though".

Page 170 line 19, "that" should be "than".

Page 170 last line, "anymore" should be " any more".

Page 227 line 2, "eventhough" should be "even though".

Page 229 line 12, "eventhough" should be "even though".

Page 246 line 16, "eventhough" should be "even though".

Page 262 line 4, "dependent" should be "dependence".

Page 266 line 11, "direction" should be "directions".

Page 267 line 4, "time" should be "times".

Page 267 line 11, "molecules" should be "molecular".

Page 268 line 12, "limitting" should be "limiting".

CONTENTS

CHAPTER 1.0

INTRODUCTION, LITERATURE SURVEY AND OBJECTIVES OF PROJECT

1.1 Introduction

Polyethylene (PE) films are widely used in packaging because of their price and properties. PE films are cheap and have adequate optical and mechanical properties. Good optical properties are important in display packaging. Application such as plastic bags need good mechanical properties to ensure the bags do not tear or split easily. The mechanical properties of the films are made up of:

a) tensile properties;
b) tear properties; and
c) impact properties.

The mechanical properties are dependent on the type of resin used to make the film and also on the choice of processing conditions.

There are three types of PE resins that are available:

a) low density polyethylene (LDPE);
b) linear low density polyethylene (LLDPE); and
c) high density polyethylene (HDPE).

LDPE has branched molecules, whilst LLDPE and HDPE have

linear molecules. The difference in structure gives rise to different degree of crystallinity and mechanical properties of the films made from LDPE and LLDPE or HDPE. HDPE has the highest degree of crystallinity followed by LDPE. The crystallinity in LLDPE varies depending on the level of comonomer used to make the resin. Films made from LLDPE and HDPE usually have better mechanical properties than LDPE films except the impact strength. The impact strength of HDPE is poorer than that of LDPE. However, LDPE films have better optical properties than LLDPE and HDPE films. To get films of moderate optical and good mechanical properties blends of LDPE and LLDPE are used.

Processing conditions also effect film properties. One effect of changing processing conditions is to change the orientation of the films. Since the mechanical properties depend on the orientation, changing the processing conditions changes the mechanical properties of the films.

The orientation of the films could be studied by several methods, such as:

a) x-ray diffraction;
b) birefringence;
c) infra-red dichroism; and
d) shrinkage.

Of these methods, the x-ray method is widely used to study orientation. The other methods are used in conjunction

with the x-ray method. In this project, however, the shrinkage method is employed to study the orientation. Using this method the residual strain of the film is evaluated and this strain is used as a measure of the orientation of the films.

1.2 Film Blowing Process

Before proceeding into a detailed study of the PE blown film process, I will outline the blowing process and the variables used in describing the process.

The blowing process is shown diagramatically in Figure 1.1. In this process the molten polymer is extruded through a circular die in a tubular form. The die can either be the bottom-fed die, side-fed or a spiral mandrel die (1). As the melt emerges from the die it is blown into a bubble. The bubble is cooled by blowing cool air onto the outside of the bubble. The bubble is fed into the nip rolls which flatten it and prevent air escaping from the bubble. Thus the air pressure inside the bubble is maintained. The flattened bubble is then fed into the winding rolls. The size of the bubble is determined by the amount of air introduced into it. The ratio of the bubble diameter to the die exit gap diameter is called the blow-up ratio, BUR.

The position where the molten polymer solidifies is called the freeze line. The vertical distance from this

point to the die lip is called the <u>freeze line height</u>, *FLH*. The *FLH* can be adjusted by controlling the cooling air velocity blowing onto the outside of the bubble. The *FLH* will be lowered if the air velocity is increased.

The speed by which the bubble is being pulled by the nip rolls is called the <u>haul-off speed</u>, *HOS*. If other processing conditions are kept constant, increasing the *HOS* will reduce the film thickness.

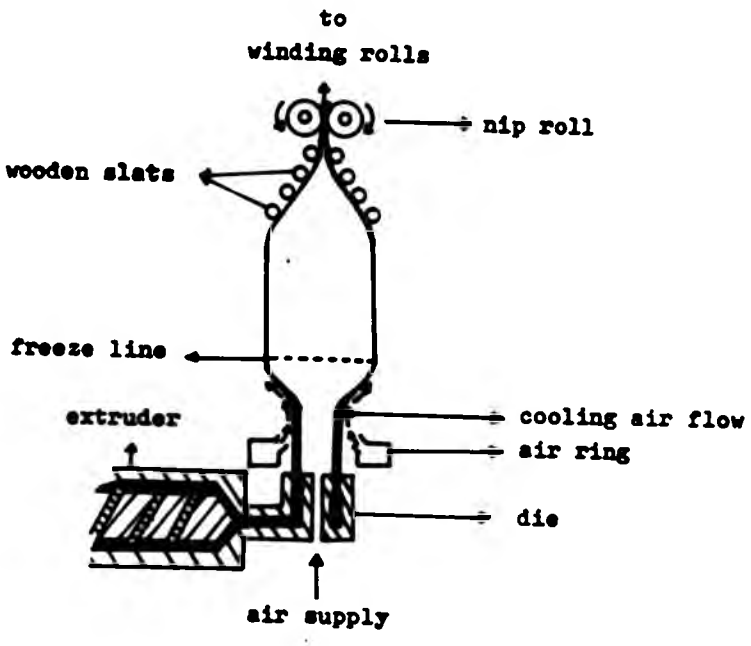

Figure 1.1. Sketch of the film blowing process.

The extruder output rate is controlled by the extruder screw speed, *SS*. Increasing the *SS* will increase the output rate. This will result in the increase of film thickness, the *FLH* and the melt temperature if the *BUR*, the *HOS* and cooling air velocity are kept constant.

Another processing variable is the melt temperature, *MT*. The *MT* could be increased by increasing the *SS* or the barrel and die temperatures.

Each of the processing variables will affect the orientation which arises due to deformation in the molten region of the bubble between the die and freeze line. This is because the orientation in the film is controlled by the following stresses:

a) shear stress during the passage of molten polymer in the die;
b) the transverse stress created by blowing-up of the film bubble after it leaves the die; and
c) the machine direction stress imposed by the haul-off unit.

The relatively slow cooling of PE melt allows molecular relaxation to occur up to the point at which it solidifies (freeze line). Therefore, the orientation present immediately before the freeze line is the most important since there is no further opportunity for molecular relaxation to take place. From the above

argument it is clear that increasing the variables like the *FLN* and the *MT*, will relax the orientation, while the variables like the *BUR* and the *NOS* will change the relative amount of orientation in the extrusion or machine direction, *MD*, and the transverse direction, *TD*, of the film.

1.3 Deformation in the Molten Region

The deformation taking place in the molten region modifies the mechanical properties of the film. This is because the deformation taking place here affects the orientation frozen into the solidified film.

1.3.1 Theoretical Studies

An early study of the deformation in the molten region was the model set up by *Pearson and Petrie (2,3,5)*. Using this model a lot of work has been done on the deformation in the molten region *(4 - 17)*. The model was set up by making a few assumptions:

a) the flow in the molten region is steady;
b) the polymer melt is incompressible and Newtonian;
c) the blowing process is isothermal; and
d) the effects of gravity and inertia on the melt are negligible.

The assumptions that the molten polymer is Newtonian and the blowing process is isothermal are not true. The molten polymer is non-Newtonian and the blowing process is not isothermal.

1.3.2 Experimental Studies

Petrie (4) used the model to predict the bubble shape of LDPE blown film. Using the assumptions that the blowing process is isothermal and the melt is Newtonian, *Petrie* found that the predicted bubble shape has a long neck and sudden blow-up. The predicted bubble shape did not agree with the experimentally measured bubble shape which has a short neck and gradual expansion. However, when the measured temperature profile and the standard viscosity-temperature relation of the melt are included into the model (i.e. non-isothermal condition), the predicted bubble shape is nearly the same as the measured bubble shape. *Petrie* also found that the effect of gravity is small but significant on bubble shape, and rather large on the velocity profile.

The work done by *Luo and Tanner (7)* further proves that the assumption of an isothermal blowing process in the theory does not give results which agree with experimental observations. *Luo and Tanner* used the non-isothermal *Maxwell model* to predict the bubble shape,

film thickness, bubble temperature, axial and circumferential stresses and circumferential strain rate of LDPE blown film. The predicted results are in good agreement with the experimentally measured results.

Han and Park (17,18) used the non-isothermal power law fluid model to predict the bubble shape, axial tension and film thickness. The relationship between predicted and experimentally obtained results are reasonable.

Kanai et al. (11,12,14) measured the bubble velocity and strain rate profiles of LDPE, LLDPE and HDPE blown films using a motion picture technique to measure strain rates and velocity profiles. Also they measured the temperature profile of the bubble using the infra-red thermometer. The velocity and strain rate profiles for LDPE are shown in Figure 1.2 *(11)*. It can be seen from Figure 1.2 that the velocity in the *MD*, V_z, increases with the axial distance, *z*, and reaches the maximum value just before the freeze line and levels off beyond the freeze line. The point of maximum V_z corresponds to the point of rapid bubble inflation. Beyond the freeze line the melt solidifies and the element is frozen in into the film and moves off with the velocity of the haul-off unit. This explains why V_z is not zero even beyond the freeze line. The velocity in the *TD*, V_y, reaches the maximum value at the same point as V_z. However, V_y goes to zero after the freeze line. This is because V_y corresponds to the velocity of the element due to bubble expansion. After

the freeze line the bubble stops expanding and V_y, therefore, returns to zero.

From the strain rates profiles, Figure 1.2, it is observed that the strain rates in both directions reached the maximum values before the freeze line. The strain rate in the *MD* is d_{11} and that in the *TD* is d_{22}. After the freeze line both strain rates returned to zero. Comparing the strain rates profiles and the velocity profiles, it can be seen that the maxima of the two profiles are located within the same region, near the freeze line.

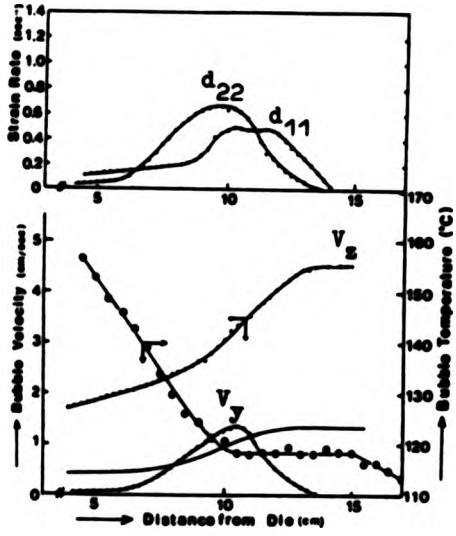

Figure 1.2. Local velocities (V_z,V_y), deformation rates (d_{11},d_{22}) and temperature profiles along the length of the bubble of LDPE blown film with drawdown ratio of 4.0, BUR of 3.5 and FLH of 12.0 cm. (11) Kanai et al.

The effect of increasing the *FLH* on the strain rates profiles is shown in Figure 1.3 *(11)*. The maximum value of d_{11} decreases and shifts further up the bubble as the *FLH* increases. The decrease in d_{11} is due to the molecular relaxation explained before in Section 1.1 and the shift of the maximum d_{11} is due to the increase in the *FLH*. Since the maximum stress occurs in the region prior to the freeze line, due to the increase in the viscosity of the melt before solidification, increasing the *FLH* increases the position of maximum d_{11}. The maximum value of d_{22} is not affected much by increasing *FLH* but is shifted further up the bubble as the *FLH* increases. This is because the *BUR* of the film is kept constant.

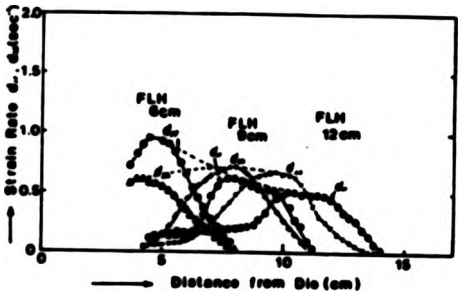

Figure 1.3. Effect of increasing FLH on the strain rates profiles of LDPE blown film of drawdown ratio of 4.0 and BUR of 3.5. (11) Kanai et al.

The effect of increasing the BUR on the strain rates profiles is shown in Figure 1.4 (11). Increasing the BUR from 3.5 to 4.5 has little effect on the maximum value of d_{11} but increases the maximum value of d_{22} from around 0.7 sec^{-1} to around 0.9 sec^{-1}. This shows that the deformation in the TD is controlled by the BUR of the film.

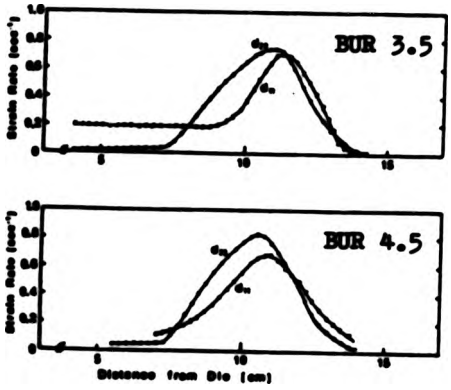

Figure 1.4. Effect of BUR on the strain rates profiles of LLDPE blown film of drawdown ratio of 4.0 and FLH of 12.0 cm. (11) Kanai et al.

1.4 Bubble Cooling

In contrast to the assumptions made by Pearson and Petrie, the film blowing process is not isothermal (4,5,7,10,11,17-22). The temperature of the polymer melt decreases as it travels from the die lip to the freeze line, shown in Figure 1.5 (11). The plateau region is due

to crystallisation.

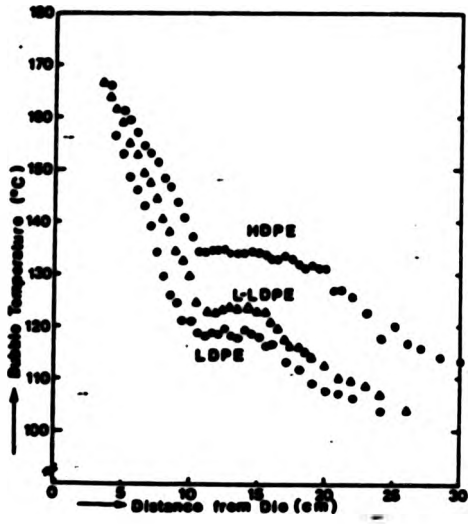

Figure 1.5. Temperature profiles of LDPE, LLDPE and HDPE blown films of drawdown ratio of 4.0, BUR of 3.5 and FLH of 12.0 cm. (11) Kanai et al.

The bubble cooling process is brought about by these three heat transfer processes:

a) conduction;

b) convection; and

c) radiation.

The main heat transfer process responsible for bubble cooling is by convection *(18,54)* brought about by blowing cooling air on the bubble surface. The bubble cools faster when the cooling air velocity is increased. The cooling

rate of the bubble affects the bubble neck geometry *(20)*. Slow rate of cooling will result in long-necked bubble, whilst faster rate of cooling produces short-necked bubble.

The processing conditions also affect the bubble cooling. Increasing the output rate, *SS*, while keeping other processing conditions the same, will result in longer cooling zone, i.e. longer neck *(20)*. The cooling zone is also increased by increasing the melt temperature *(20)* because as the melt temperature is increased the amount of heat that needs to be dissipated between the die and the freeze line is also increased. Increasing the *NOS*, keeping the *SS* and die gap constant, results in the increase of the *FLH* and thus result in lower rate of cooling. On the other hand, increasing the *BUR* and keeping the other conditions constant will reduce film thickness. This results in the increase in bubble cooling rate *(20)*.

1.5 Orientation

A polymer is said to be oriented when the polymer molecules are aligned preferentially in one or more directions. Orientation requires a considerable mobility of large segments of the molecules and this cannot occur below the glass transition temperature, Tg, of the polymer. Orientation can be achieved by cold stretching or during a fabrication process. During cold stretching heat

will be generated and this will raise the temperature at the area of stretching to above the Tg. The orientation of the polymer is responsible for the anisotropic behaviour of the fabricated polymer *(27,29-31,49)*.

There are two types of orientation:

a) uniaxial; and
b) biaxial.

In uniaxial orientation the polymer molecules are aligned in one direction, usually the stress direction. This kind of orientation is usually encountered in polymer fibres and produces strength in one direction only, the orientation direction. Uniaxial orientation is not suitable for film because this type of film will be weak along the line parallel to the direction of orientation.

Biaxial orientation takes place when the polymer molecules are aligned in more than one direction. It is usually encountered in film blowing whereby the molten polymer is stretched in the transverse direction as well as in the extrusion direction. The biaxially oriented film is found to be tougher and less liable to splitting than uniaxially oriented film.

There are several methods available to study the orientation in PE films. These are:

a) x-ray diffraction *(23,24,26,28,32,35-37,41,43-46)*;

b) birefringence *(23,25,32,33,39-42,44-46)*;

c) infra-red dichroism *(23,32,38,42,47)*; and

d) shrinkage *(49-60)*.

The x-ray diffraction method measures the orientation of the crystallographic axes of the crystallites in the film, whereas the infra-red dichroism method can be used to measure the orientation of the crystalline and amorphous regions by looking at the dichroic ratio of infra-red absorption bands associated with each region. The birefringence method measures the orientation of the polymer molecules in the sample. On the other hand, the shrinkage method measures the amount of stretching, strain, the shrunk film needs to restore it to its original state.

The most commonly used method to study orientation is the x-ray method. The other methods are usually used to support the result obtained with the x-ray method.

1.5.1 X-Ray Method

Polyethylene is a semi-crystalline polymer and this means that only part of its molecules crystallise. The initial part that crystallises acts as a nucleus from which larger crystal can grow. In crystalline regions the molecules are evenly spaced in a regular repeating arrangement. The basic building block of this structure is

known as the unit cell.

The unit cell of PE is orthorhombic and is defined by three unequal, perpendicular axes, *a*, *b*, and *c* as shown in Figure 1.6 *(34)*. The *c*-axis is in the same direction as the carbon backbone of the molecules and has a dimension of about 2.534 Å. The *a*-axis is about 7.400 Å and *b*-axis is is 4.930 Å *(50)*. By studying the orientation of these axes, the orientation of the crystallites in the film can be studied. This is usually done by using the x-ray diffraction method.

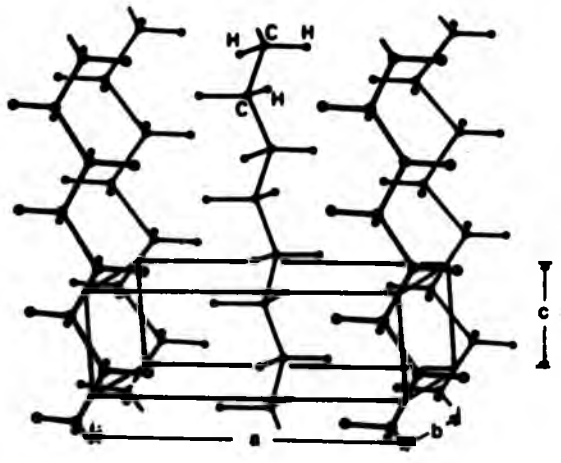

Figure 1.6. The unit cell of PE crystallite showing the crystallographic axes. (34) Keller

When x-rays are passed through the film sample, the x-rays are diffracted by the crystalline region. Therefore, by studying the x-ray diffraction pattern the orientation of the crystallites in the film can be deduced. The orientation of the crystallites in the film is usually presented in terms of the pole figures *(28,32,35-37,41,43,45,46)*, which are the stereographic projections of the diffracted intensities of normals to the crystallographic planes. The reflection of *(200)* plane corresponds to the *a*-axis, while the *(020)* plane is due to the *b*-axis. The c-axis is represented by the reflection of *(002)* plane.

The work done on crystallite orientation of LDPE and HDPE films so far showed that the orientation depends on the processing conditions *(23,26,28,32,36,41,45)*, type of resin used *(28,36,43,44)* and also on the stress state during blowing *(35,36,37,46)*. There are three types of crystallite orientation:

a) type *I* or relaxed fibre orientation *(23,32,45)*;
b) type *II* or row orientation *(24,32)*; and
c) type *III* which is the modified row orientation *(26,32)*.

In type *I*, the *a*-axis is oriented along the *MD* and the *b*- and *c*-axes are randomly oriented perpendicular to the *a*-axis. However, in type *II*, the *b*-axis is oriented

perpendicular to the *MD* and the *a*- and *c*-axes are oriented randomly around it. In type *III*, the *b*-axis is oriented perpendicular to the *MD* but the *a*- and *c*-axes are tilted at an angle to the *MD*. The distinction between type *I* and type *II* is not so clear. Figure 1.7 *(32)* shows the different types of crystallite orientation.

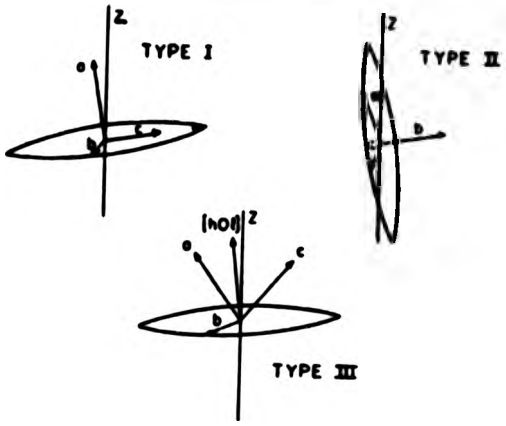

Figure 1.7. The three types of crystallite orientation of PE film. The Z direction refers to the MD. (32) Nagasawa et al.

The work done by Choi et al. *(41)* on HDPE blown film showed that uniaxially stretched films exhibited type *II* orientation. However, samples with constant *BUR* showed type *III* orientation. This is in agreement with that obtained by Holmes et al. *(26)* and Lindenmeyer et al. *(28)*.

The effect of the *FLH* on the orientation was studied by *Desper (32)*. The results obtained showed that increasing the quenching rate (lower *FLH*) of LDPE blown films resulted in type *I* orientation. This is also observed by *Gilbert et al. (45)*.

The effect of stress state during blowing on the orientation of crystallites was studied by *Maddams and Preedy (35-37)*. Low *MT* results in high stress condition. High stress condition is also observed with HDPE melt. Under low stress condition *a*- and *c*-axes are randomly oriented in the *MD-SN* plane (due to lamellae twisting in the film), whereas at high stress the *a*-axis is oriented along the *SN* and *c*-axis along the *MD*. The *SN* direction is the direction normal to the plane or thickness of the film.

1.5.2 Birefringence

Birefringence measures the polarisability of the polymer molecules. The polarisability in the direction of stress, *MD*, of an oriented polymer molecule is different from the polarisability in the direction perpendicular to it. The difference between the polarisability in these two directions gives rise to a difference between the refractive index in these directions. The difference in the refractive indices is called the birefringence *(40)*.

There are three principal refractive indices in the

film (n_1, n_2 and n_3). The refractive index in the *MD* is n_1, whereas the refractive index in the *TD* is n_2. The refractive index in the *SN* is denoted by n_3.

In the uniaxially oriented film, n_1 does not equal to n_2 or n_3 but n_2 is equal to n_3. Therefore the birefringence is given by

$$\Delta n_{12} = n_1 - n_2 \qquad (1.1)$$

This is called the in-plane birefringence.

In the biaxially oriented film, $n_1 \neq n_2 \neq n_3$. Therefore the birefringence of the biaxially oriented film is made up of the in-plane birefringence and the out-of-plane birefringences,

$$\Delta n_{13} = n_1 - n_3 \qquad (1.2)$$

$$\Delta n_{23} = n_2 - n_3 \qquad (1.3)$$

The measured birefringence is made up of the birefringence of the crystalline and amorphous regions *(32)* and also the form birefringence *(25)*. The form birefringence arises due to the presence of two phases (crystalline and amorphous), each having a different refractive index. The form birefringence only constitute around 5% of the measured birefringence and is usually ignored.

The birefringence is affected by the drawdown ratio of

the film, V_L/V_o (33,39,41,42,44,46), that is the ratio of the velocity of an element at the freeze line, V_L, to the velocity at the die, V_o. The effect is illustrated in Figure 1.8 (41).

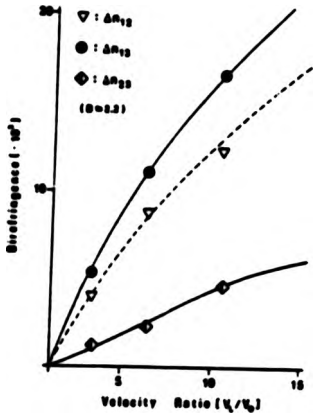

Figure 1.8. Effect of increasing drawdown ratio (velocity ratio) on the birefringence of HDPE films of BUR of 2.2. (41) Choi et al.

It can be seen from Figure 1.8 that increasing the drawdown ratio increases Δn_{12}, Δn_{13} and Δn_{23}. Since the *BUR* of the films is kept constant, the increase in V_L/V_o of the films is achieved by the increase in *MOS*. Increasing the *MOS* results in the increase of the orientation in the *MD*. The increase in the orientation is reflected by the increase in the refractive index in the *MD*, i.e. n_1. The orientation in the *TD*, however, does not increase because the *BUR* is kept constant at 2.2.

Therefore the value of Δn_{12} will increase with increasing V_L/V_O. The orientation in the *SN* decreases with increasing V_L/V_O and therefore the value of Δn_{13} increases with increasing V_L/V_O. Increasing V_L/V_O of the films will also increase the value of Δn_{23} of the films. This is because value of n_2 remains the same with increasing V_L/V_O but the value of n_3 decreases with increasing V_L/V_O. The result of this is to increase the value of Δn_{23} of the films.

The effect of increasing the *BUR* on the in-plane birefringence, Δn_{12}, of HDPE blown films is shown in Figure 1.9 *(45)*. It is observed that increasing the *BUR* decreases the in-plane birefringence of the films, except the *Unifos DMDS 2900* sample. This decrease is expected since increasing the *BUR* will increase the orientation in the *TD*, therefore the in-plane birefringence will be reduced.

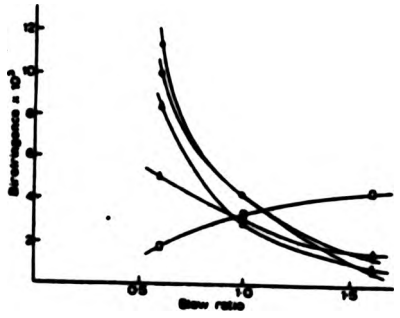

Figure 1.9. Effect of BUR on the in-plane birefringence of HDPE films. The films are: (●) Wacker DF 5071G; (○) Wacker FF 5551G; (△) Hostalen GM 9255F; (▲) Hostalen GF 7740F2 and (□) Unifos DMDS 2900. (45) Gilbert et al.

Figure 1.10 *(45)* shows the effect of increasing the *FLH* on the in-plane birefringence of HDPE films. It can be seen that increasing the *FLH* decreases the in-plane birefringence of the films, except the *Hostalen GF 7740F2* and *Unifos DMDS 2900* films. The decrease of the in-plane birefringence with increasing *FLH* is due to the increase in the time for relaxation of the stretched molecules and crystallites reorientation.

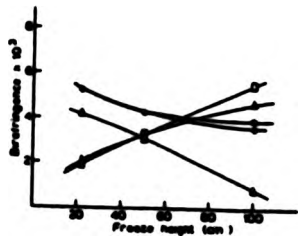

Figure 1.10. Effect of FLH on the in-plane birefringence of HDPE films. The films are: (●) Wacker DF 5071G; (○) Wacker FF 5551G; (△) Hostalen GM 9255F; (▲) Hostalen GF 7740F2 and (□) Unifos DMDS 2900.(45) Gilbert et al.

1.5.3 Infra-red Dichroism

When an infra-red beam is passed through a film peaks are produced in the infra-red spectrum. These peaks are produced due to the absorption of the light wave in the sample. The absorption of the light wave takes place when the frequency of the waves is equal to the natural

frequency of vibration of the electrons in the film sample. The absorbance at a given frequency, A, is given by *(42)*

$$A = \log(I_o/I) \qquad (1.4)$$

where I_o is the incident beam intensity and I is the transmitted beam intensity.

In infra-red dichroism method, the infra-red beam is polarised parallel to the *MD* and at right angles to it. The ratio of the absorbances of the polarised infra-red beam parallel and perpendicular to the stretching direction is called the dichroic ratio *(42)*. The value of dichroic ratio can vary from zero (due to no absorption in parallel direction) to infinity (due to no absorption in perpendicular direction). If the dichroic ratio is smaller than 1.0 the band is called a perpendicular band. However, if the dichroic ratio is larger than 1.0 it is called parallel band.

In PE there are infra-red-absorbing groups which coincide with the crystallographic axes and thus it is possible to establish the orientation of the individual crystallographic axes in PE from the values of dichroic ratios.

The work done by Holmes *et al. (23)* on the PE flat film showed that, from the dichroic ratio of 729 cm^{-1} band, the c-axis is oriented at right angles to the

stretching direction, *MD*, while the *a*-axis is oriented parallel to the *MD*. The *b*-axis, on the other hand, is oriented randomly in a plane at right angles to the *a*-axis. They also found that the *c*-axis in the amorphous region is oriented at right angles to that in the crystalline region (cross orientation).

Desper (32) studied the dichroic ratios of 722-733 cm^{-1} (CH_2-rocking doublet), 1300 and 1380 cm^{-1} bands (amorphous bands) and 1468-1480 cm^{-1} bands (CH_2- bending doublet) of blown LDPE films. From the results it was concluded that increasing the quenching rate of the films resulted in the *a*-axis to be oriented along the *MD* and the *c*-axis is shifted from being oriented nearly along the *MD* to perpendicular to the *MD*. This agrees with the results obtained by using the x-ray diffraction method.

The results of the work done by *Parikh and Knight (47)* showed that the dichroic ratio of 720 cm^{-1} band, *b*-axis, decreases as the crystals become oriented more in the *MD*. The opposite effect is observed for the dichroic ratio of 730 cm^{-1} band, *a*-axis.

1.5.4 Shrinkage

The shrinkage of the film is due to the orientation frozen into the film brought about by the stresses during deformation *(49,51,53)*. On reheating the film above its melting point, the film reverts towards its unstrained

state and thus shrinkage takes place. Samuels *(50)* showed that the shrinkage of polyethylene terephthalate fibre is proportional to the orientation in the amorphous region. The plot was shown to be linear.

The *MD* orientation of the film is introduced into the film during the passage of the molten polymer through the die and also by extension brought about by the haul-off unit *(51)*. The *TD* orientation, on the other hand, is introduced by bubble inflation *(51)*. The orientation is frozen into the film at the freeze line where the melt solidifies.

The amount of shrinkage in each direction will depend on the processing conditions *(51,53,55)*, shrink medium temperature *(52-54,56,58,59)*, sample heating time *(57,59)* and also on the type of resin used to manufacture the film *(51,53)*.

The *BUR* has the greatest influence on the relationship between the *MD* and the *TD* shrinkage *(51,53,55)*. Increasing the *BUR* of the film increases the *TD* shrinkage and reduces the *MD* shrinkage. This effect is shown in Figure 1.11 *(51)*.

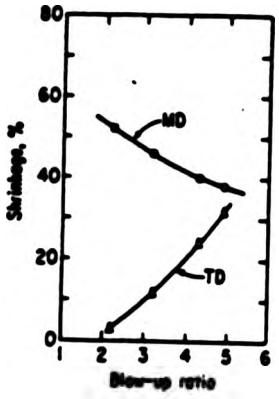

Figure 1.11. Effect of BUR on the shrinkage of LDPE film at shrinkage temperature of 104°C. (51) Steffen

The effect of increasing the *FLH* on the shrinkage of LDPE films is to increase the *TD* and reduces the *MD* shrinkage *(51,55)*. This is shown in Figure 1.12 *(51)*. The reduction in the *MD* shrinkage with increasing *FLH* is due to the increase in relaxation of orientation at high *FLH*. At high *FLH* the blowing takes place at a distance further away from the die. Therefore the temperature at this point is lower and thus the relaxation of orientation in the *TD* is reduced. This results in the increase in the *TD* shrinkage.

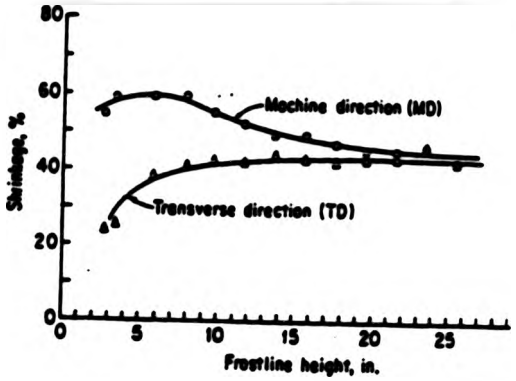

Figure 1.12. Effect of FLH on the shrinkage of LDPE film at shrinkage temperature of 104°C. (51) Steffen

The film thickness also affects the shrinkage of the film. Increasing the film thickness decreases shrinkage *(51,59)*. This is because increasing film thickness will result in the increase in the time needed to cool the film. The increase in cooling time results in the increase in the relaxation of orientation in the film and thus reduces shrinkage. However, the work done by *Steffen (51)* on the effect of film thickness on shrinkage showed that the effect depends on the melt index, *MI*, of the resin. The effect of film thickness on shrinkage is less for low *MI* resin than the effect on high *MI* resin.

The shrinkage of the film is also affected by the extrusion melt temperature, *MT*, *(51)*. Decreasing the *MT* increases the stress in the bubble due to the deformation (blowing process) taking place at low temperature. This results in the increase in the shrinkage of the film. The increase in shrinkage, however, is small.

The shrinkage also depends on the temperature at which

the test is done *(52-54,56-59)* and also on the time the test piece is heated *(57,59)*. At constant heating time, the shrinkage increases with temperature. The same is true with increasing heating time at a constant temperature.

1.5.5 Summary of the Methods Used to Measure Orientation

The results obtained with x-ray and infra-red methods are consistent with each other. This is shown by the results obtained by *Desper (32)* who investigated the effect of increasing quenching rate (decreasing *FLH*) of LDPE blown films. Both methods showed that films with low *FLH* have type *I* orientation.

The orientation measured by birefringence method can be compared with the result obtained by shrinkage method. The results obtained by *Gilbert (45)* on the effect of increasing the *BUR* and *FLH* on the orientation of HDPE films using birefringence method, Figures 1.9 and 1.10, are consistent with the results obtained by *Steffen (51)* using the shrinkage method, Figures 1.11 and 1.12.

1.5.6 Structure of Blown Polyethylene Film

The mechanical properties of the film may be affected by the crystalline structure of the film. The type of structure formed depends on the crystallisation conditions. PE single crystals have been obtained by

slowly cooling a very dilute polymer solution, 0.01% PE in xylene at 85°C *(61)*. These crystals are in the shape of hollow pyramids. However, if the PE is crystallised from melt, spherulitic structures will be formed *(60,63)*. The spherulites are made up of twisted ribbon-like lamellae radially arranged around the centres of the spherulites. The polymer molecules in the lamellae are arranged in a folded form. On the other hand, a 'row-nucleated' structure will be produced if crystallisation takes place in a flowing melt *(41,46,62,67,68)* such as encountered in film blowing process. This structure is made up of alternating layers of lamellae and amorphous regions. The amorphous regions consist of polymer molecules that are excluded from the lamellae during crystallisation, such as chain ends, and tie molecules which connect adjacent lamellae together.

From the work done on the orientation of PE films, it is found that the orientation of the axes depends on the processing conditions used to manufacture the films. From these results, White *et al.* *(41,46)* proposed the possible structure of the PE films. The structure of PE films is the 'row-nucleated' structure as shown in Figure 1.13 *(41)*.

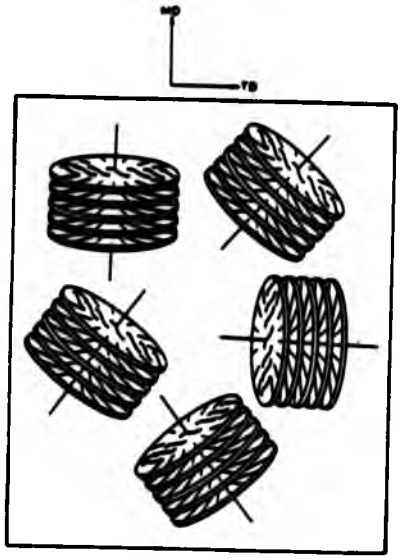

Figure 1.13. The 'row-nucleated' structure of PE blown film. (41) Choi et al.

When the film sample is deformed, separation of lamellae will take place. As the lamellae separate the tie molecules will be extended *(60,64-66,68,69,118)*. As the tie molecules are extended, the lamellae will be twisted so that they will be oriented along the stretching direction. On further deformation, however, the lamellae are broken off and the fragments are incorporated to form the fibrillar structure (61-63,68) like those encountered in fibre.

1.6 Material for the Polyethylene Blown Film Process

There are three types of PE resin that can be used to manufacture blown films. These are

a) low density polyethylene (LDPE);
b) linear low density polyethylene (LLDPE); and
c) high density polyethylene (HDPE).

Of these three resins, only LDPE and LLDPE will be discussed at great length because they are used in this project.

LDPE is polymerised by a high temperature, 200 -280^{o}C, and high pressure, 1000 - 3000 kg/cm^{2}, process *(81,83)*. LLDPE, on the other hand, is produced by copolymerisation of ethylene and α-olefins with *Ziegler* catalyst (Ti-based catalyst) or *Phillips* catalysts (Cr-based catalyst systems) under low temperature, 60 - 200^{o}C, and low pressure, 5 - 200 kg/cm^{2} *(81,83)*.

LDPE has long-chain branches, *LCB*, and short-chain branches, *SCB*, *(70,77-79,81,83)*, whereas LLDPE is a linear polymer with *SCB* originated from the α-olefin used as a comonomer *(70,78,79,81,83)*. LLDPE has bigger crystallite size than LDPE *(79,81)* because of its linear structure and the melting point of LLDPE is 10^{o}C higher than LDPE at the same density *(70,78)*. The difference in the structure between LDPE and LLDPE results in the

difference in rheological and mechanical properties of these two resins.

1.6.1 Rheological Properties of Low Density Polyethylene and Linear Low Density Polyethylene

The processability of a polymer is related to its rheological properties. The rheological properties depend on the molecular weight, *MW*, molecular weight distribution, *MWD*, and *LCB* of the resin. Resins with narrow *MWD* and low *LCB* gives maximum drawdown and better blowability as discussed below.

LDPE has high amount of *LCB* and wider *MWD* than LLDPE *(70,73,78,82,87,88)* and therefore its melt is strain hardening *(70, 82-84)*. This is evident from Figure 1.14 *(83)*. It can be seen from Figure 1.14 that the extensional viscosity of LDPE is higher than that of LLDPE. Also the extensional viscosity of LDPE increases with deformation. This phenomenum is called strain hardening, which gives rise to bubble stability of LDPE blown film. LLDPE, on the other hand, shows less strain hardening behaviour. The behaviour of LLDPE gives rise to greater drawdown and bubble instability if care is not taken during blowing.

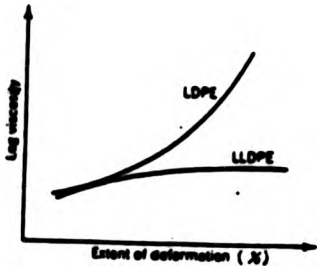

Figure 1.14. The extensional viscosity of LDPE and LLDPE. (83) James

Eventhough LLDPE has lower extensional viscosity than LDPE, its shear viscosity in blown film grade is higher than that of LDPE, at shear stresses in the die and extruder *(70,71,77-79,83,87,88)*. This is illustrated in Figure 1.15 *(79)*. LLDPE has higher shear viscosity because of its narrow *MWD* and also the absence of *LCB* in the molecules. The higher melt shear viscosity of LLDPE results in the increase in screw torque during extrusion and also heat generation in the melt.

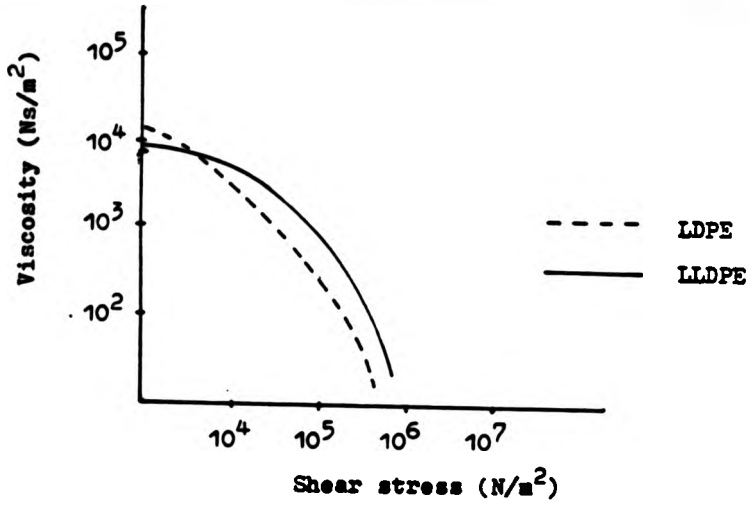

Figure 1.15. Shear viscosity of LDPE and LLDPE. (79) Gray

The dynamic viscoelastic properties of the two resins are also different *(81,85)*. From Figure 1.16 *(81)* it can be seen that the storage modulus, *G'*, and the loss modulus, *G"*, curves for LLDPE are steeper than that of LDPE. This suggests that the distribution of relaxation times is broader in LDPE as compared with that in LLDPE due to broader *MWD* and *LCB* in LDPE.

The melt flow rate of LLDPE is lower than that of LDPE for a given *MW*, as shown in Figure 1.17 *(81)*. This difference is due to the difference in the molecular dimensions between LDPE and LLDPE. At the same *MW*, LDPE has smaller molecular dimensions than LLDPE because LDPE molecules have *LCB*.

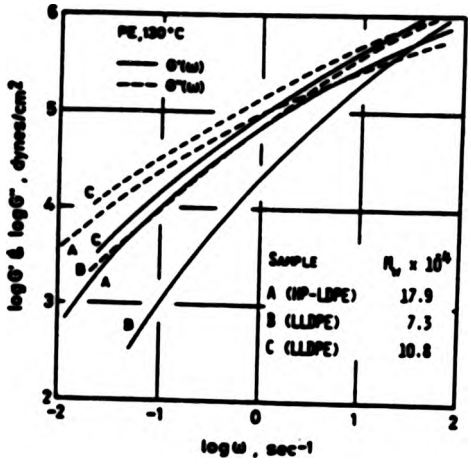

Figure 1.16. The storage modulus, G', and loss modulus, G", of LDPE and two LLDPE resins as a function of frequency at temperature of 130°C. (81) Furumiya et al.

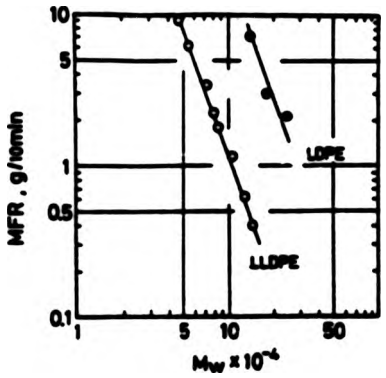

Figure 1.17. Melt flow rate of LDPE and LLDPE as a function of weight-average molecular weight. (81) Furumiya et al.

The melt tension, a measure of the force needed to stretch the molten polymer, of LLDPE is lower than LDPE, at the same melt flow rate, MFR, *(70,80)*. This is shown in Figure 1.18 *(81)*. The lower melt tension of LLDPE leads to bubble instability in the blown bubble. The low melt tension also results in low shrinkage of LLDPE films compared with LDPE films *(70,80)*.

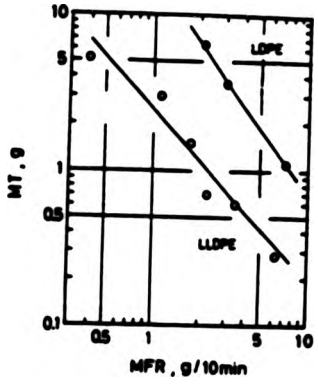

Figure 1.18. Melt tension as a function of melt index of LDPE and LLDPE. (81) Furumiya et al.

1.6.2 Mechanical Properties of Low Density Polyethylene and Linear Low Density Polyethylene

The mechanical properties of these two resins depend on the structure of the resin. Differences in the structure between LDPE and LLDPE gives rise to the differences in the mechanical properties.

The tensile strength, elongation at break, tear strength and impact strength of LLDPE films are claimed to be higher than those of LDPE films *(70,73-75,78,81,83,86, 89)*. This is shown in Table 1.1 *(86)*. In this table the mechanical properties of LDPE and LLDPE films made with the same *BUR* and *MT* are compared.

Table 1.1. Mechanical properties of LDPE and LLDPE films. (86) Siegmann et al.

	LLDPE		LDPE	
	MD	TD	MD	TD
Tensile strength (MPa)	38	35	24	20
Yield strength (MPa)	—	14	—	10
Elongation (%)	625	680	400	560
Dart drop impact (gr)		250		120
Elmendorf tear (gr/μ)	32	52	12	16

The high elongation at break of LLDPE film is due to the absence of *LCB (72,76,77,79,81)*. The absence of *LCB* results in the reduction in the amount of entanglement of molecules. The entanglement acts as a cross-link thereby reducing the effective length of chains between fixed points. The shorter the chain the less it is extendible and therefore will break quickly. Therefore reducing entanglement increases elongation at break.

1.6.3 Blends of Polyethylene

Since its introduction, LLDPE has had a great impact on the film market, due to its better mechanical

properties. However, there are a few drawbacks with LLDPE. These are:

a) to process LLDPE on conventional LDPE extruders, machine modification is needed to prevent the reduction of output and heat and pressure (torque) build-up in the extruder which could lead to bubble cooling problem and screw abrasion;
b) LLDPE films have inferior optical properties and therefore are not suitable for displaying purposes; and
c) LLDPE films have greater drawdown than LDPE films and this gives rise to bubble instability if care is not taken during blowing and also may lead to reduced output rates.

The drawbacks mentioned above have been overcome by blending LLDPE with LDPE. Blends of up to 25% LLDPE are used with conventional LDPE extruders without machine modification *(92)*.

The maximum output rate, obtainable while maintaining bubble stability, of the extruder is reduced when LLDPE is used *(93,94,99)*. This effect is shown in Figure 1.19 *(99)*. It could be seen that the maximum output rate of LLDPE is half that of LDPE. The decrease in the maximum output rate with increasing LLDPE is due to the increase in bubble instability. In section 1.6.2 it was pointed out that the

extensional viscosity of LLDPE is lower than that of LDPE. The lower extensional viscosity of LLDPE may result in bubble instability.

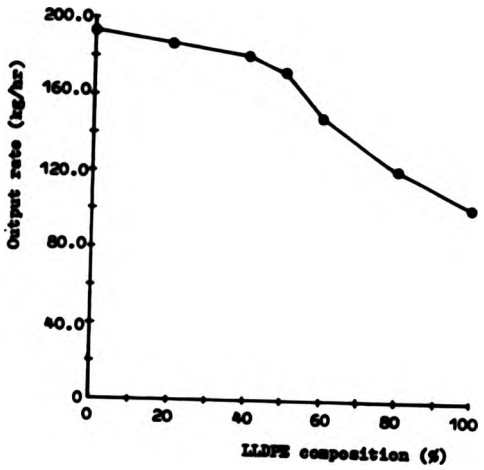

Figure 1.19. Effect of blending on the output rate of an extruder. The resins are: (a) LDPE of MI = 1.0 g/10 min and density = 919 kg/m^3; and (b) LLDPE of MI = 1.0 g/10 min and density = 920 kg/m^3. (99) Veasey

Blending LDPE with LLDPE also affects the shear viscosity *(91,95,100,101,103)*. This is illustrated by Figure 1.20 *(103)*. It can be seen that the shear viscosity of LLDPE is lower than that of LDPE at low shear rate. At higher shear rate, the viscosity switches over.

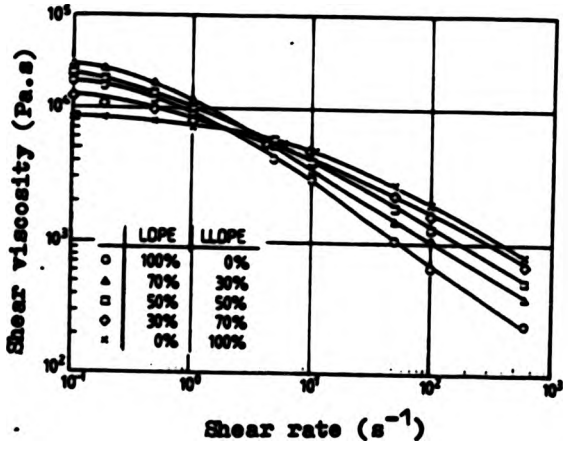

Figure 1.20. Effect of blending on the shear viscosity at temperature of 190°C.(103) Schule et al.

The drawdown ratio of the blown film is affected by blending *(79,82,92,93,97)*. Increasing LLDPE proportion, in a blend with low MFR LDPE, increases the drawdown ratio as shown in Figure 1.21 *(97)*. The increase in drawdown ratio is due to the decrease in the extensional viscosity of LLDPE melt. The decrease in extensional viscosity increases the melt extensibility before bubble rupture. This results in the increase in drawdown ratio of the film.

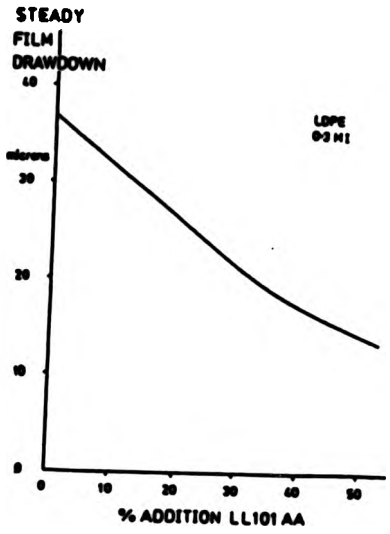

Figure 1.21. Effect of blending on the film drawdown. (97) Davies

Blending LLDPE with LDPE also affects the torque exerted by the melt on the screw *(90,98,100,104)*. Increasing LDPE composition in the blend reduces the torque on the screw, as shown in Figure 1.22 *(98)*. The torque exerted by the melt depends on the shear viscosity of the melt. Since increasing LDPE reduces the shear viscosity, this results in the reduction of the torque.

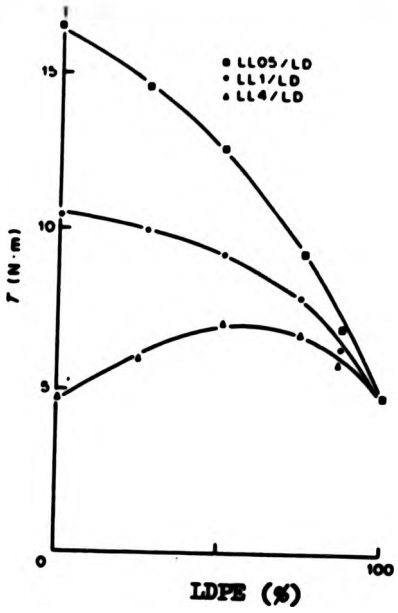

Figure 1.22. Effect of blending on the torque experience by the extruder screw. The resins used are: (a) LDPE of MI = 2.9 g/10 min and density = 921.5 kg/m^3; (b) LLDPE05 of MI = 0.53 g/10 min and density = 921.6 kg/m^3; (c) LLDPE1 of MI = 1.1 g/10 min and density = 923.7 kg/m^3; and (d) LLDPE4 of MI = 4.3 g/10 min and density = 938.3 kg/m^3. (98) La Mantia et al.

Blends of LDPE and LLDPE form a semi-compatible mixture. This is evident from the thermogram of LDPE, LLDPE and blend of LDPE and LLDPE, as shown in Figure 1.23 *(103)*. From Figure 1.23 it could be seen that the thermogram of the blend consists of two peaks. This means that two types of crystal are produced, each with different melt temperature. The size of the melting peaks is proportional to the ratios of the components in the blends *(96,102)*, as shown in Figure 1.24 *(96)*.

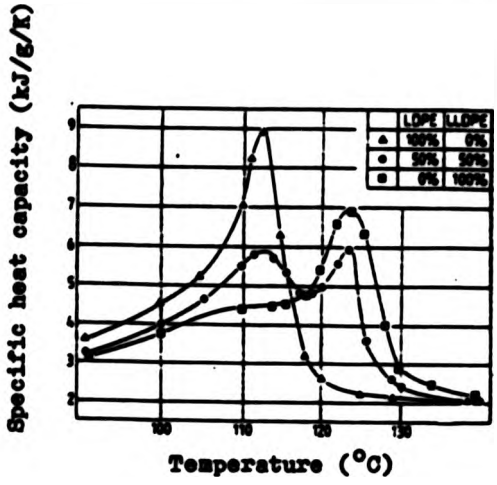

Figure 1.23. Melting behaviour of LDPE, LLDPE and blended films at constant heating rate of 10 K/min.
(103) Schulz et al.

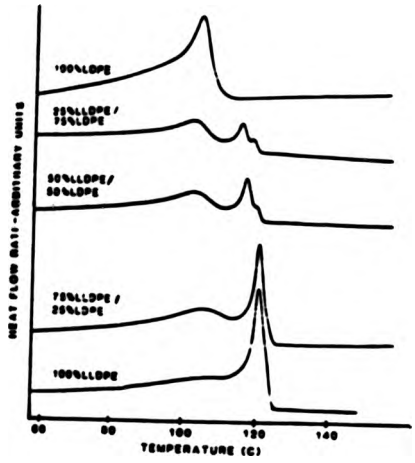

Figure 1.24. Melting behaviour as a function of LLDPE composition in the blend. (96) Bonotto et al.

The mechanical properties of the films are also affected by blending. Usually the mechanical properties, except the tear strength, decrease with increasing LDPE composition in the blends. Increasing the LDPE content in the blend decreases the tensile strength of the film *(91-99,101,104)*. This is illustrated in Figure 1.25 *(98)*, which shows the effect of LDPE composition on the *MD* tensile strength.

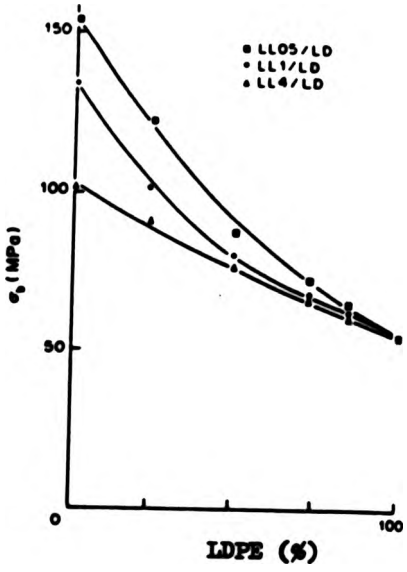

Figure 1.25. Effect of blending on the tensile strength. The resins are: (a) LDPE of MI = 2.9 g/10 min and density = 921.5 kg/m^3; (b) LLDPE05 of MI = 0.53 g/10 min and density = 921.6 kg/m^3; (c) LLDPE1 of MI = 1.1 g/10 min and density = 923.7 kg/m^3; and (d) LLDPE4 of MI = 4.3 g/10 min and density = 938.3 kg/m^3.(98) La Mantia et al.

The elongation at break of the films is also affected by the composition of the blend. Increasing LDPE composition in the blend results in the decrease in the elongation at break of the film *(91-96,98,99,101,103-105)*. This effect is shown in Figure 1.26 *(98)*.

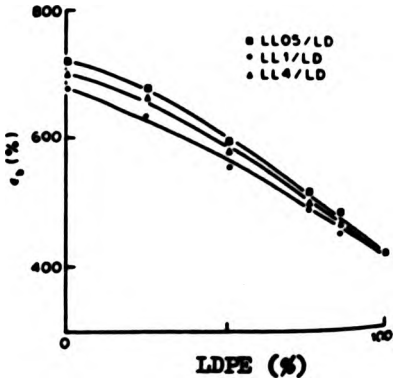

Figure 1.26. Effect of blending on the elongation at break. The resins are: (a) LDPE of MI = 2.9 g/10 min and density = 921.5 kg/m^3; (b) LLDPE05 of MI = 0.53 g/10 min and density = 921.6 kg/m^3; (c) LLDPE1 of MI = 1.1 g/10 min and density = 923.7 kg/m^3; and (d) LLDPE4 of MI = 4.3 g/10 min and density = 938.3 kg/m^3.(98) La Mantia et al.

The results of blending on the impact strength, however, are mixed. The results published so far showed that the impact strength decreases slightly with increasing LLDPE composition *(91-94,96,97)*, as shown in Figure 1.27 *(92)*.

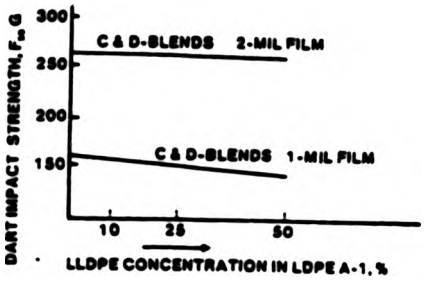

Figure 1.27. Effect of blending on the impact strength. The resins are: (a) LDPE A-1 of MI = 0.24 g/10 min and density = 918 kg/m^3; (b) LLDPE C of MI = 1.0 g/10 min and density = 920 kg/m^3; and (c) LLDPE D of MI = 1.0 g/10 min and density = 920 kg/m^3.(92) Mancokivell

The effect of composition on the *Elmendorf* tear strength is not straight forward. The *MD Elmendorf* tear strength decreases with increasing LLDPE composition up to around 70% LLDPE *(91,93,95,96,99)*. It increases again after 70% LLDPE composition in the blend. This is shown in Figure 1.28 *(91)*. The tear strength in the *TD*, however, does not show this behaviour. It increases with increasing LLDPE composition in the film.

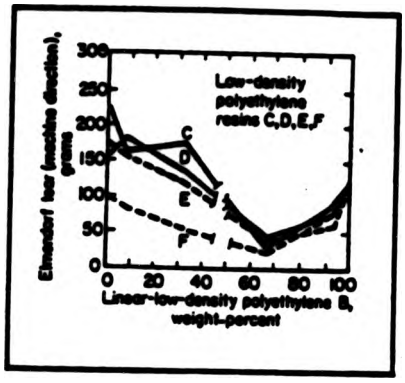

Figure 1.28. Effect of blending on the MD Elmendorf tear strength. The resins are: (a) LLDPE B of MI = 20 g/min and density = 918 kg/m^3; (b) LDPE C of MI = 20 g/min and density = 922 kg/m^3; (c) LDPE D of MI = 25 g/min and density = 918 kg/m^3; (d) LDPE E of MI = 13 g/min, density = 925 kg/m^3 and contains 3 weight-percent EVA; and (e) LDPE F of MI = 25 g/min, density = 926 kg/m^3 and contains 9 weight-percent EVA.(91) Speed

1.7 Effect of Processing Conditions on the Mechanical Properties of Polyethylene Films

The mechanical properties of the films are affected by the processing conditions used to manufacture the films. These processing conditions are *BUR, FLH, NOS, SS* and *MT*. These processing conditions will affect the net residual orientation of the film *(106,109)*. Since the mechanical properties of the film depend on the orientation, changing the processing conditions will affect the mechanical properties of the film. Changing processing conditions may

also affect the crystal morphology of the polyethylene films which can also alter mechanical properties.

1.7.1 Effect of Blow-up Ratio on Mechanical Properties

The *BUR* of the film determines the size of the blown film bubble. Increasing the *BUR* increases the size of the bubble. Therefore it is clear that increasing the *BUR* will increase the orientation in the *TD* *(107)*. This is because increasing the *BUR* will increase the stretching along the *TD*. The result of this increase in the *TD* stretching is to increase the orientation in the *TD*. As the orientation in the *TD* increases the orientation in the *MD* is reduced. The change in the net orientation due to increasing the *BUR* is reflected in the mechanical properties of the film.

Increasing the *BUR* results in the increase in the *TD* tensile strength and reduces the *MD* tensile strength *(107,108)*, Figure 1.29 *(108)*. The *MD* elongation at break, on the other hand, increases with *BUR*, while the *TD* elongation at break decreases with increasing *BUR (108)*.

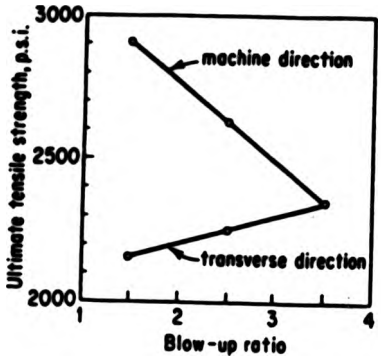

Figure 1.29. Effect of BUR on the tensile strength of PE film.(108) Pilaro et al.

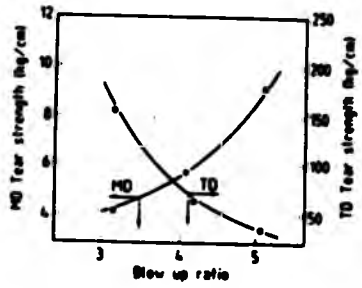

Figure 1.30. Effect of BUR on the tear strength of PE film.(116) Kanai

The effect of increasing the *BUR* on the tear strength is the opposite to the effect on tensile strength. Increasing the *BUR* increases the *MD* tear strength and decreases the *TD* tear strength *(107,116)*, as shown in Figure 1.30 *(116)*.

The impact strength of the film also increases with increasing *BUR (107,111-113,116)*, Figure 1.31 *(116)*. This is because increasing the *BUR* results in balanced film. Balanced film has balanced strength and therefore it will not split on impact. Instead it will puncture. Therefore it can be said that changing the *BUR* also changes the impact failure mode of the films. This results in increased impact strength.

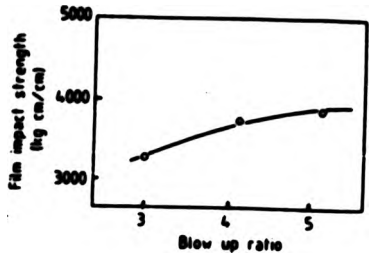

Figure 1.31. Effect of BUR on the impact strength of HDPE film.(116) Kanai

1.7.2 Effect of Freeze Line Height on Mechanical Properties

Some of the orientation taking place during blowing relaxes before the melt reaches the freeze line *(106,109)*. The amount of relaxation depends on the *FLH*, if the resins used are the same. The higher the *FLH* the more will be the relaxation of the orientation. Therefore at higher *FLH*, the *MD* orientation will be reduced but not the *TD* orientation. This is because at higher *FLH* the sideways blowing process, which is near the freeze line, takes place further from the die and so at lower temperatures, compared with blowing process at low *FLH*. Therefore the amount of *TD* relaxation is reduced. This gives rise to the increase in the *TD* orientation.

The effect of increasing the *FLH* on the mechanical properties of the film is the same as the effect of increasing the *BUR* on the mechanical properties.

Increasing the *FLH* increases the tensile strength in the *TD* and reduces the *MD* tensile strength *(114,115)*. The elongation at break in the *MD* increases with increasing *FLH* but not the *TD* elongation at break *(115)*.

The effect of increasing the *FLH* on the tear strength is shown in Figure 1.32 *(116)*. The *MD* tear strength increases with increasing *FLH* and the opposite is observed for the *TD* tear strength *(114,116)*. The increase in the *MD* tear strength is due to the increase in the *TD* orientation brought about by increasing the *FLH*. The *MD* tear strength measures the energy needed to break the molecules oriented perpendicular to the *MD* and therefore depends on the *TD* orientation.

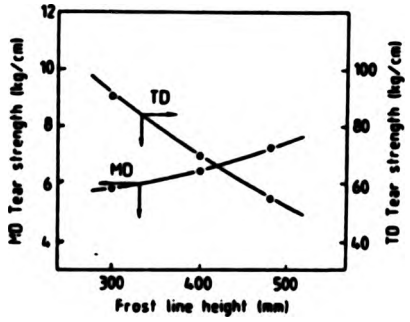

Figure 1.32. Effect of *FLH* on the tear strength of PE film. (116) Kanai

The impact strength of the film increases with increasing *FLH (107,113,116)*. This is shown in Figure 1.33 *(116)*. When the *FLH* is increased the film produced is more balanced and thus has higher impact strength.

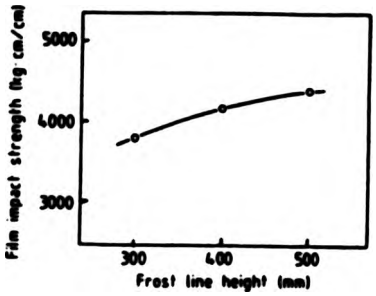

Figure 1.33. Effect of *FLH* on the impact strength of PE film.(116) Kanai

1.7.3 Effect of Screw Speed on Mechanical Properties

Increasing the *SS* results in thicker films, if the other processing conditions are kept constant *(110)*.

From the work published to date on the effect of the *SS* on the mechanical properties, no clear conclusion could be drawn. Some results showed that increasing the *SS* increases the mechanical properties *(110)*. Other results showed a mixed effect *(107)*.

1.7.4 Effect of Haul-off Speed on Mechanical Properties

Increasing the *HOS* will result in the increase in the *MD* orientation if other processing conditions are kept constant. Therefore, the effect of increasing the *HOS* on mechanical properties is the opposite to that observed with the *BUR*.

1.7.5 Effect of Melt Temperature on Mechanical Properties

The effect of increasing the *MT* is to increase the relaxation of orientation *(110)*. This effect is the same as increasing the *FLH* except that the relaxation is higher. Therefore increasing the *MT* increases the *MD* Elmendorf tear strength and improves impact strength *(109)*.

1.8 Summary

The published work on blown PE films has, so far, concentrated on the following areas:

a) effect of processing conditions on the properties of the films;

b) effect of processing conditions on the deformation of the molten films during their manufacture and the subsequent residual orientation in the film; and

c) effect of blending on the properties of the film.

The results published in the above areas do not quantitatively relate processing conditions to film structure (i.e. orientation and crystallinity) and hence their effects on the properties of the films. Rather, the explanations of the effect of processing conditions on properties are qualitative and given in terms of factors (such as orientation) which are inferred rather than measured.

1.9 Objectives of the Project

The general objective of the project is to relate the mechanical properties of LDPE and LLDPE films and blend films of the two to their processing conditions through a quantitative measure of film structure. It was thought that the residual orientation in the film would be the most important factor affecting properties. The main objectives were therefore to:

a) establish an experimentally suitable method for determining orientation in blown films;
b) determine how the orientation depended on processing conditions; and
c) relate the mechanical properties to the orientation measurements.

It was expected that this would draw together much of the work that has been reported, which separately examines the

processing-structure-properties relationship.

The orientation in each direction of the film (MD or TD) is important because the different in the orientation will result in an anisotropic behaviour. Therefore it is important to keep the orientation level the same when comparing the properties of the films. It was therefore the aim to study the interaction of orientations in both directions on the properties.

The thickness of the film affects the properties such as elongation at break of the films because this property is not evaluated by dividing it with thickness. Thicker films have greater elongation at break. Therefore it is important to keep the thickness of the films constant when comparing the properties of several batches of films.

The most common method to study the orientation mentioned in the literature is the x-ray method. This method is not easy to use and the interpretation of the results is difficult. Other methods such as shrinkage is easy but not widely used.

It is the aim of this project to use shrinkage method to study orientation of the films. Also samples of constant thickness and orientation in one direction are produced with the help of the annealing method. It is hoped that by keeping the thickness constant, the effect of thickness on the properties of the films could be eliminated.

CHAPTER 2.0

EXPERIMENTAL

2.1 Introduction

The experimental work of this project consists of three parts. These parts are:

a) sample preparation;
b) evaluation of residual strain of the sample; and
c) mechanical properties testing.

The samples preparation is made up of film manufacture and annealing. In film manufacture, films were produced from LDPE, LLDPE and blends of 75% LDPE/25% LLDPE and 25% LDPE/75% LLDPE. For each material a range of films was made by changing the processing conditions. Films of either constant *MD* or *TD* residual strain and variable residual strain in the other direction could not be produced by changing the processing conditions alone. Therefore, an annealing method was devised and used to modify the film residual strain to desired values.

The residual strain values of the samples were evaluated from the shrinkage obtained by shrinkage tests.

The mechanical properties of the samples were measured by mechanical testing. The test includes tensile, tear

and impact tests.

2.2 Materials

2.2.1 Polyethylene

The materials used to manufacture the films, supplied by BP Chemical, were:

a) LDPE (*LD5320MN*); and

b) LLDPE (*LL0209AA*).

Their grade characteristics as supplied by BP are shown in Table 2.1.

Table 2.1. The melt flow rate and density of LDPE and LLDPE resins used to manufacture the films.

Resin	Melt flow rate (g/10 min)	Density (kg/m^3)
LDPE	2.0	920.0
LLDPE	0.9	920.0

2.2.2 Silicone Oil

The silicone oil used in this project was the high boiling point silicone oil obtained from Aldrich Chemical Company.

2.3 Equipments

2.3.1 Film Extruder

The films were manufactured using a blown film extruder manufactured by Queens Machinery. The details are shown in Table 2.2.

Table 2.2. Details of the extruder used to manufacture the blown films.

Screw diameter		40.0 mm
Screw length to diameter ratio		26:1
Die diameters		37.0 mm
	and	100.0 mm
Die gaps		1.0 mm
	and	2.0 mm
Screw speed range		22-122 rpm
Haul-off speed range		5.0-85.0 m/min

2.3.2 Hot Plate for Shrinkage Test

A regulated hot plate was used to heat the sample and the silicone oil in the shrinkage test. The temperature was controlled by adjusting the temperature setting knob.

2.3.3 Thermocouple

A thermocouple in a needle probe, obtained from

Digitron Instrumentation Ltd., was used to measure the temperature of the silicone oil and also the temperature of the molten PE resin.

2.3.4 Oven for Annealing

An oven, fitted with a fan, was used in the annealing process. The fan was used to circulate the air in the oven so that the sample could be heated effectively and uniformly. For efficient temperature control, a relay system was connected to the oven. This system could control the temperature of the oven to within $\pm$ 1°C of the set temperature.

2.3.5 Tensile Tester

The tensile test was carried out using an *Instron* tensile testing machine which was fitted with a 100.0 N load cell.

2.3.6 Impact Tester

A *Rosand Instrumented Impact Tester* was used in the impact strength test. This machine has a striker of weight 8.0 kg and attached to this striker are the hemispherical impacting head of diameter 3.5 cm and a load cell. The impacting head punctures the film sample after the striker

is released. The drop height of the striker could be adjusted according to the type of sample used and for film the height was chosen to be 0.75 metre.

2.4 Preparation of Films

The blown films were manufactured using the blown film extruder described in Section 2.3.1. The blown film bubble is cooled by a blower which sucks in air from the surroundings and blows it onto the bubble surface. The speed of the cooling air is controlled by adjusting the air intake opening of the blower.

Films of various sizes were produced by altering the processing conditions. For each run of the extruder the processing conditions were recorded. The processing conditions that could be altered were:

a) blow-up ratio;
b) die diameter and gap;
c) freeze line height;
d) haul-off speed;
e) melt temperature; and
f) screw speed and output rate.

The processing conditions used to make each film are shown in Chapter 4.0.

The melt temperature, *MT*, was measured using a thermocouple, in a needle probe, to measure the temperature of the molten polymer at the die lip. Four readings were taken at several places around the circumference of the die and the average *MT* was evaluated. The *MT* was altered by changing the temperature settings on the extruder barrel and die.

The output rate of the extruder at a given screw speed, *SS*, was evaluated by weighing the extrudates taken at 30.0 seconds intervals. Three extrudates were collected and their average weight expressed as the output rate of the extruder at a given *SS*. The unit used for the output rate is kilogram/hour/metre of die circumference.

The haul-off speed, *HOS*, of the haul-off unit was measured by timing a certain number of revolutions of the nip rolls and measuring their radius. With these values *HOS* could be evaluated.

The films produced were LDPE, LLDPE and blends of 75% LDPE/25% LLDPE and 25% LDPE/75% LLDPE films. The blends were prepared by weighing the appropriate amount of each resin, LDPE and LLDPE, and mixing the granules by shaking in a bag.

2.5 Annealing of Samples

Annealing involves heating the film sample at its elevated temperature in the oven to relax the residual strain of the sample. The reduction in residual strain of the sample depends on the duration of heating and the temperature of annealing. The longer the annealing time the more reduction in residual strain. Therefore by annealing the sample at several temperatures below and above its melting temperature, Tm, for several annealing times, samples of different residual strain values could be obtained. Also, the thickness of the sample could be kept constant if the sample is prevented from shrinking during annealing. Temperatures between 110 and 130^{o}C were used.

To prevent the films from shrinking they were placed on glass plates, 30.0 by 30.0 cm, during heating in the oven. In this way the samples did not shrink and the thickness of the samples remained constant.

The glass plate was heated in the oven at the chosen annealing temperature for about 2.0 minutes. Then the plate was taken out and film sample was placed gently on the plate. The air trapped between the sample and the plate was displaced by using a rubber roller. The roller was used to prevent scratching the film sample. The plate and sample were then heated in the oven for five minutes. After that they were taken out and the remainder of the

trapped air was removed. Then the plate and the sample were heated in the oven for the rest of the chosen annealing time.

After annealing the film and the plate were taken out and placed on a rack to cool to the room temperature.

2.6 Shrinkage Test and the Evaluation of Residual Strain of the Samples

The shrinkage test aimed to measure the change in size of a sample after heating to a state under which its residual strain relaxes completely. The residual strain could be calculated from the size change as described later.

The biggest problem encountered in the shrinkage test was the wrinkling of the test piece during heating. This effect could be eliminated by using a petri dish. The dish was filled with a small amount of high boiling point silicone oil, described in Section 2.2.2, just enough to cover the bottom of the dish. The silicone oil allowed the test piece to shrink freely in the heated petri dish. The wrinkling of the sample was eliminated by dropping several drops of hot silicone oil on the test piece during the shrinkage process.

In this project the shrinkage test was carried out at a temperature of 130 $\pm$ 2^{o}C. The heating was done using the hot plate mentioned in Section 2.3.2.

The film sample was cut into a 50.0 by 50.0 mm square and its thickness was measured. The shrinkage of the sample was calculated by evaluating the change in its length, along the *MD* and the *TD*, after heating. The percentage shrinkage of the samples in each direction is given by

$$\text{Percentage shrinkage} = \frac{Lo - L}{Lo} \times 100 \qquad (2.1)$$

where *Lo* is the length before heating and *L* is the length after heating.

The residual strain of the sample was evaluated using the following equations:

$$(\varepsilon_{MD}) = (S_{MD}^{4/3} \times S_{TD}^{2/3}) - 1 \qquad (2.2)$$

$$(\varepsilon_{TD}) = (S_{TD}^{4/3} \times S_{MD}^{2/3}) - 1 \qquad (2.3)$$

where ε is the residual strain and S is the shrink ratio and the subscripts *MD* and *TD* refer to the value in the direction *MD* and *TD*, respectively. The shrink ratio is related to the shrinkage of the sample and the relationship is shown by equation 2.4.

$$S = \frac{1}{1 - (\text{shrinkage}/100)} = \frac{Lo}{L} \qquad (2.4)$$

The derivation of these equations is shown in Appendix 1.0.

Other workers have shown that the shrinkage of the sample depends on the shrinkage temperature *(51-53,55,57,58)* and heating time *(56,58)*. This was also observed in the results here. It was thought that the continuing increase of shrinkage with heating time, at constant shrinkage temperature, is not due to the residual strain of the sample, as will be shown later in Chapter 3.0. In order to determine the true residual strain in the samples it is necessary to know the shrinkage at zero heating time. This is achieved by extrapolation described in Appendix 2.0.

2.7 Tensile Properties Testing

Five test pieces were cut, from each film sample, along the *MD* and the *TD*. The test piece was cut in a strip form of dimensions 100.0 by 10.0 mm. The thickness of each test piece was measured at three places along its length and the average thickness was recorded.

Each test piece was placed between the grips of the Instron which were set at 50.0 mm apart. The test was performed at room temperature by pulling the test piece at a cross-head speed of 500.0 mm/min and with a full scale load generally set at 20.0 N (thicker samples needed a greater load). The load-extension curve of the sample was

recorded on a chart. The speed of this chart was set at the same speed as the cross-head speed. From the load-extension curve, the tensile strength, elongation at break, yield stress and tensile modulus were evaluated. A typical load-extension curve is shown in Figure 2.1.

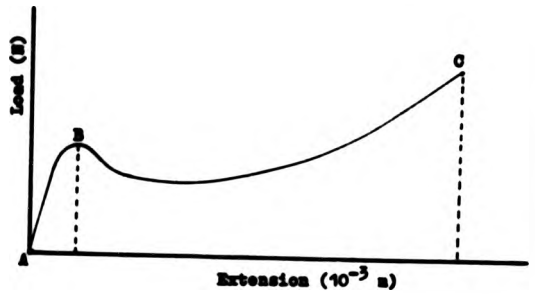

Figure 2.1. A typical stress-strain curve of PE film.

The tensile strength is the measure of the stress at point *C*, where the sample breaks. This is evaluated by dividing the load at break with the original cross-sectional area of the test piece.

The elongation at break, *Eb*, of the test piece is the total extension from point *A* to point *C* expressed as a percentage of initial grip separation, i.e.

$$Eb = \frac{\text{Extension}}{\text{Initial grip separation}} \times 100 \qquad (2.5)$$

The yield point is point *B* on the curve. The yield stress is the measure of stress at this point. This is

calculated by dividing the load at point *B* with the original cross-sectional area of the test piece. Some test pieces, typically those pulled in the *MD*, do not show a clear yield point. The yield point of this type of test piece was determined by drawing two tangents to the load-extension curve - one is drawn to the initial linear portion of the curve and the other to the later part of the curve. The point where the two tangents meet is taken as the yield point of the test piece.

The tensile modulus of the test piece is the ratio of tensile stress to the corresponding strain at the linear portion of the curve (part of the curve after point *A* and before point *B*). To evaluate the tensile modulus, a point is chosen along the initial linear portion of the load-extension curve. The load and extension at this point are noted. The ratio of the stress to the corresponding extension at the chosen point is the tensile modulus of the test piece.

2.8 Tear Strength Testing

The tear strength of the films was evaluated by using the trouser tear test method. The shape and dimensions of the trouser test piece are shown in Figure 2.2.

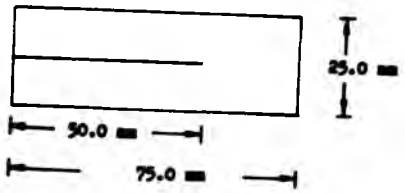

Figure 2.2. The shape and dimensions of trouser tear strength test piece.

Five test pieces were cut in each direction and the thickness was measured along the uncut length of the test piece. Three readings were taken and the average thickness was recorded.

The tearing test was done by using an *Instron* tensile testing machine fitted with a 100.0 N load cell. Each test piece was placed between the grips which were set at 50.0 mm apart. The test piece was pulled at a cross-head speed of 200.0 mm/min to propagate the tear. Full scale load was 20.0 N. The tearing curve of each test piece was plotted by the machine on the chart which was set at the same speed as the cross-head speed.

The tear strength of the test piece was calculated by dividing the maximum tearing load, obtained from the tearing curve, with the average test piece thickness. The direction of the initial cut along the test piece was used to identify the tear direction in subsequent discussion.

2.9 Impact Strength Testing

The thickness of the film sample to be tested was measured and the average value evaluated. The sample was then placed at the bottom of the machine directly below the striker and held in place by means of a pair of clamps.

The load cell detects the impact forces as the sample fails. The force signal is integrated to obtain failure energy. The force signal is also transmitted to a BBC computer. This has been programmed to plot the impact curve. A typical impact curve is shown in Figure 2.3.

The impact curve is a plot of the impact force as a function of the distance travelled by the impacting head after it touches the film surface. The first peak, at 50.0 mm in the example, is the impact curve of the film sample. The second peak is due to the vibration of the machine and is usually ignored. The word 'round' at the top right hand corner refers to the hole made by the impacting head on the sample.

The impact strength of the film sample was taken as either the force at the peak per unit sample thickness or the failure energy per unit sample thickness. The values of maximum impact force and the failure energy of the sample are printed by the computer as shown in Figure 2.3.

ROSAND IMPACT ANALYSIS SYSTEM

Drive: 1
Sample: LDPE
Details: BUR5.7.110.28'
Date: 08/03/89
Time: 15:18:41
Temp: 20 deg C
Velocity: 3.683 m/s
Filter frequency: 1 kHz

PEAK INFORMATION
Force at cursor=59.61 N
Deflection at cursor=46.16mm
Energy at cursor=1.131 J

FAILURE INFORMATION
Deflection at failure=77.21mm
Energy at failure=1.742 J

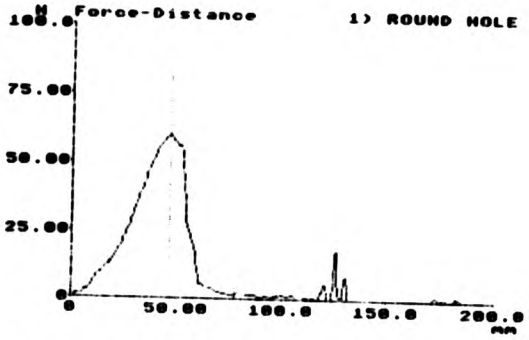

Figure 2.3. A typical impact curve obtained by using a Rosand Instrumented Impact Tester.

CHAPTER 3.0

RESULTS OF PRELIMINARY STUDIES

3.1 Introduction

The preliminary studies were designed to investigate:

a) the shrinkage test as a mean of measuring residual strains in PE films made by blown film extrusion;
b) the effect of processing conditions on residual strains; and
c) the effect of residual strains on mechanical properties.

Films were made using the equipment and materials described in Chapter 2.0. The 37.0×10^{-3} m diameter die was used and the die gap was set at 2.0×10^{-3} m. The results of the various investigations are described below.

3.2 Determination of Residual Strains in Polyethylene Films

Two films were prepared using the conditions shown in Table 3.1.

Table 3.1. The processing conditions used to manufacture LDPE films to study the effect of shrinkage time on the residual strain.

Die diameter	(10^{-3}m)	37.0
Die gap	(10^{-3}m)	2.0
FLH	(10^{-3}m)	100.0
SS	(rpm)	22.0
Output rate	(kg/hr/m die cir.)	59.0
Melt temperature	(^{o}C)	165.0

Sample	Haul-off speed (10^{-3}m/s)	Blow-up ratio
1A	83.0	2.4
1B	167.0	4.7

The residual strain values of these two films as a function of shrinkage time were evaluated using the method described in Section 2.6. Basically, squares of film were immersed in silicone oil and relaxation allowed to take place for a given time. The dimensions of the film were measured and the residual strain of the sample was calculated using the equations shown in Section 2.6 of Chapter 2.0. The results are shown in Table 3.2 and Figure 3.1.

Table 3.2. Effect of shrinkage time on the apparent residual strain of LDPE films.

Shrinkage time (min)	Sample 1A			Sample 1B		
	Average thickness (10^{-6} m)	Residual strain (apparent)		Average thickness (10^{-6} m)	Residual strain (apparent)	
		MD	TD		MD	TD
1.0	33.3	18.18	3.16	71.7	7.34	3.69
2.0	35.0	19.72	3.46	80.0	7.87	3.92
5.0	36.7	20.12	3.63	80.0	8.45	4.13
10.0	33.3	24.04	4.30	78.3	8.99	4.30
20.0	28.3	29.75	5.33	78.3	9.84	4.70
30.0	35.0	34.37	6.19	75.0	10.93	5.28
45.0	30.0	42.98	7.37	70.0	11.93	5.69
95.0	36.7	55.16	8.80	80.0	14.19	6.49

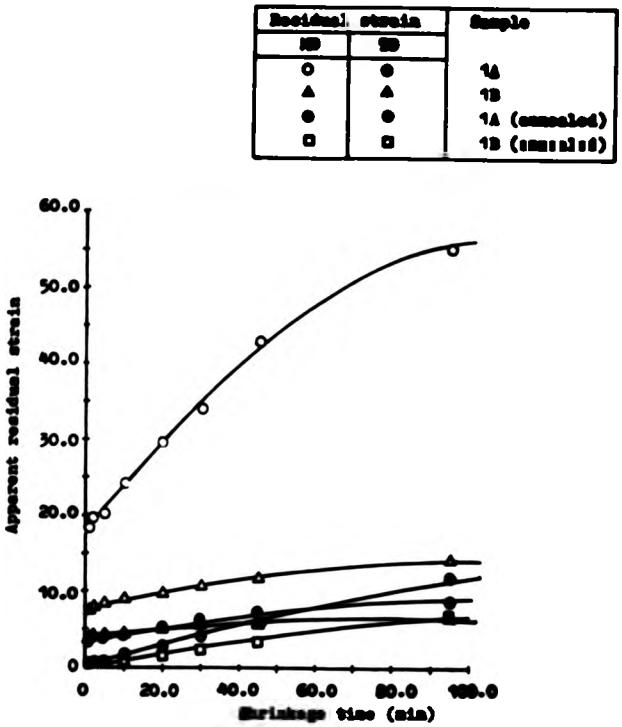

Figure 3.1. Plot of the effect of shrinkage time on the apparent residual strain of samples 1A and 1B and also the annealed samples 1A and 1B.

The residual strain appears to increase with shrinkage time. It is thus not clear at what time the sample can be considered to have fully shrunk and therefore what is the original residual strain value. It is thought that the apparent increase of residual strain with increasing shrinkage time is not due to the relaxation of residual strain. It may be due to a 'flow' process, possibly caused by surface tension forces. The

true relaxation of residual strain takes place at very beginning of the shrinkage time as shown in Figure 3.2. Therefore the residual strain values measured are called the apparent residual strain of the films.

To prove that the increase in shrinkage and hence the apparent residual strain with shrinkage time is not due to the relaxation of residual strain in the sample, the two films were annealed at 133.0 ± 2°C for 2.0 hours to completely relax all the residual strain in the films. The apparent residual strain values of these annealed films were then evaluated by shrinkage testing and the results are shown in Table 3.3. The results in Table 3.3 are also plotted in Figure 3.1.

Table 3.3. Effect of shrinkage time on the apparent residual strain of annealed LDPE films annealed at 133 ± 2°C for 2.0 hours.

	Annealed sample 1A			Annealed sample 1B		
Shrinkage time (min)	Average thickness (10^{-6} m)	Residual strain (apparent)		Average thickness (10^{-6} m)	Residual strain (apparent)	
		MD	TD		MD	TD
1.0	31.7	0.29	0.29	65.0	0.14	0.14
2.0	36.7	0.51	0.51	61.7	0.23	0.24
5.0	35.0	0.93	0.93	60.0	0.50	0.50
10.0	36.7	1.52	1.52	66.7	0.94	0.93
20.0	33.3	2.75	2.79	75.0	1.67	1.68
30.0	30.0	4.09	4.15	78.3	2.36	2.36
45.0	36.7	5.91	5.97	80.0	3.42	3.41
90.0	35.0	11.83	11.77	70.0	6.74	6.73

From Figure 3.1 it can be seen that the apparent residual strain of the annealed films increases with increasing shrinkage time. The apparent residual strain in the *MD* is the same as the apparent residual strain in the *TD* for each sample. However, the thinner film sample has higher apparent residual strain than the thicker sample. Also it is noticed that the increase in the apparent residual strain with shrinkage time is greater with the thinner film than the thicker one.

The annealed samples have almost zero apparent residual strain at zero shrinkage time. This means that the samples have no residual strain after they have been annealed for 2.0 hours, that is, they are completely relaxed. However, the apparent residual strain values of these samples seemed to increase with increasing shrinkage time. Since the samples have no residual strain in it, the observed increase in the apparent residual strain values with shrinkage time is not due to relaxation of the residual strain of the samples but due to some kind of flow process that takes place in the heated samples. The flow process is possibly due to surface tension converting the flat molten sample into a more spherical shape. Therefore the apparent residual strain values measured is the sum of the true residual strain of the film and the 'flow' effect as shown in Figure 3.2. The true residual strain value of the film is the value extrapolated to zero shrinkage time.

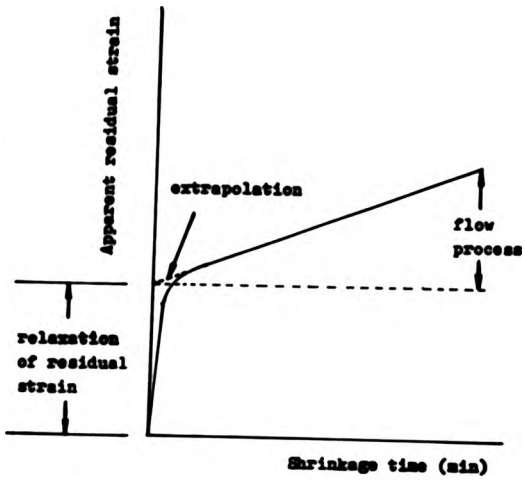

Figure 3.2. Plot of apparent residual strain against shrinkage time showing the extrapolation, the relaxation of residual strain and flow process.

3.3 Effect of Changing Processing Conditions on the Residual Strains of Polyethylene Films

The effect of changing the processing conditions on the residual strain of 50% LDPE/50% LLDPE blend films showed that changing one condition affected the residual strain in both directions of the films. The effect of changing the *BUR*, *HOS*, *FLH*, and *SS* on the residual strain of these films is shown in Figures 3.3 to 3.6.

Increasing the *BUR* of the films from 1.5 to around 3.5 increases the residual strain in both directions of the films. This is illustrated in Figure 3.3.

Increasing the *BUR*, at constant *HOS* and *FLH*, increases the stress along the *TD* of the film bubble. This results in the increase in orientation along the *TD* which is shown by the increase in the residual strain in the *TD*. When the *BUR* is increased the bubble will expand and will reduce the *FLH*. However, since the *HOS* and *FLH* are kept constant, this will induce stress along the *MD*. This explains the increase in the residual strain along the *MD* with increasing *BUR*.

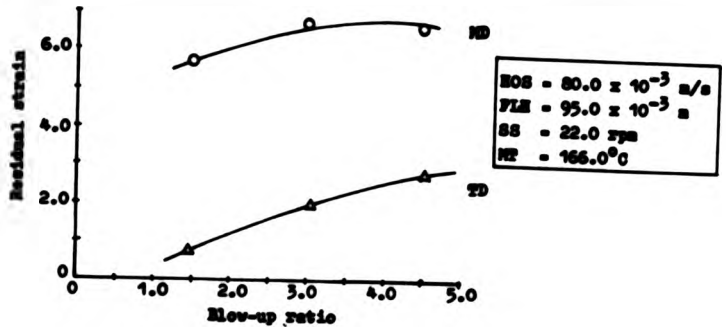

Figure 3.3. Effect of increasing BUR on the residual strain of LDPE films.

The effect of increasing the *HOS* at constant *BUR* on the residual strain of the films is shown in Figure 3.4. It can be seen that increasing the *HOS* increases the residual strain in both directions. Increasing the *HOS* increases the orientation along the *MD*. As the *HOS* is increased, the bubble will become smaller due to increased

stretching along the *MD*. However, since the *BUR* is kept constant, this prevented the bubble from becoming smaller and thus induced stress along the *TD*. This is shown by the increase in the residual strain in the *TD* of the films.

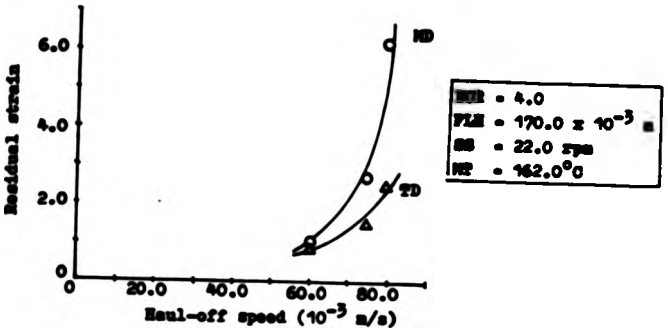

Figure 3.4. Effect of increasing HOS on the residual strain of LDPE films.

Figure 3.5 shows the effect of increasing the *FLH* on the residual strain of LDPE films. The effect of increasing the *FLH* on the residual strain is the opposite to that observed with the *BUR* and the *HOS*. Increasing the *FLH* reduces the residual strain in the *MD* and increases the residual strain in the *TD* slightly. This is because increasing the *FLH* increases the relaxation of the stretched polymer molecules due to the deformation taking place during the passage of the polymer melt in the die. This increased relaxation results in the decrease in the orientation along the *MD*. This is shown by the decrease in the residual strain in the *MD*. At higher *FLH*, the blowing

of the bubble takes place at a distance further away from the die and thus the temperature at this point is lower compared with lower *FLH* bubble. Therefore the relaxation of the stretched molecules is reduced. This results in the increase in the *TD* residual strain. The increase, however, is small.

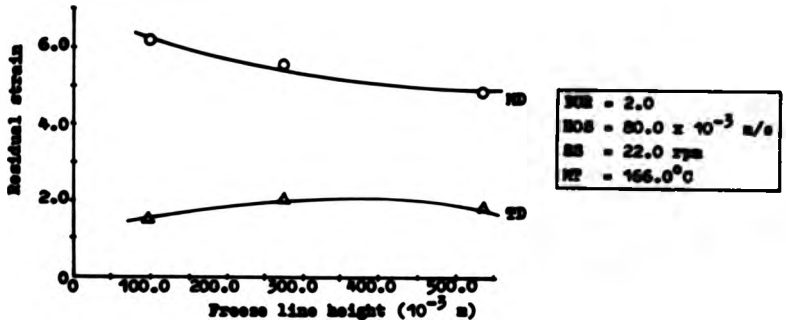

Figure 3.5. Effect of increasing FLH on the residual strain of LDPE films.

The effect of increasing the *SS* on the residual strain of LDPE films is shown in Figure 3.6. It could be seen that increasing the *SS* decreases the residual strain in both directions of the films. This is because increasing the *SS* keeping other processing conditions constant will increase the *MT*. Increase in the *MT* results in the increase in the relaxation of the stretched molecules. Therefore the residual strain in both directions will also be reduced.

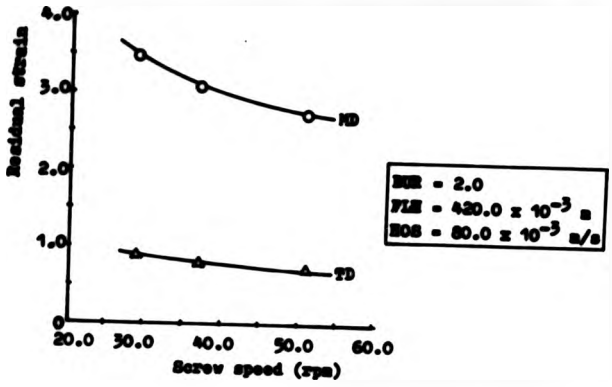

Figure 3.6. Effect of increasing SS on the residual strain of LDPE films.

3.4 Effect of Blending on the Residual Strains

The effect of LLDPE composition in the blend on the residual strain of the PE films is shown in Figure 3.7. The *BUR* and the *FLH* were kept constant but the *HOS* and the *SS* were varied to get films of various thickness and residual strains. A graph of residual strain against thickness was plotted. The residual strain values of all the films at thickness of around 250 x 10^{-6} m were noted from the graph. These values were than plotted as a function of LLDPE composition to produce Figure 3.7.

It is observed that the residual strain in both directions decreases with increasing LLDPE composition in the blend. The reduction is due to the linear structure of LLDPE molecules. The linear structure results in lesser

amount of molecular entanglement which could prevent the stretched molecules from relaxing after deformation.

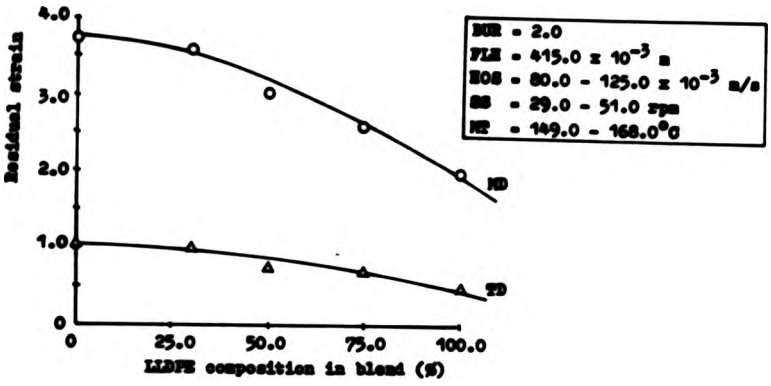

Figure 3.7. Residual strain as a function of LLDPE composition in the blend.

3.5 Effect of Residual Strains on the Mechanical Properties

The effects of residual strain on the mechanical properties of LDPE, LLDPE and blends of 75% LDPE/25% LLDPE, 50% LDPE/50% LLDPE and 25% LDPE/75% LLDPE films are shown in Figures 3.8 to 3.13. These films were produced with the same processing conditions mentioned in section 3.4. In these figures the mechanical property in a given direction of each sample is plotted against its respective residual strain values, i.e. the *MD* tensile strength is plotted against the *MD* residual strain etc. It is important to note here that in this preliminary work, films of various residual strain values were obtained by changing the thickness. This means that samples with

higher residual strain in both directions were thinner than the films with lower residual strains.

It should be emphasised that due to the extent of scattering of the results, it is difficult to draw lines through the points. However, for the purpose of indicating trends it has been assumed that the points represent a family of related curves and lines have been drawn on this basis. It is to be understood that the lines are not to be considered as significantly in the correct place.

The tensile strength of the films as a function of residual strain is shown in Figure 3.8. It can be seen that increasing the residual strain in the test direction increases the tensile strength in that direction. Also it is observed that the tensile strength in a given direction increases with increasing LLDPE composition in the blends.

The effect of increasing the residual strain on the elongation at break is shown in Figure 3.9. It is observed that increasing the residual strain in one direction generally decreases the elongation at break in that direction. The elongation at break of LLDPE-rich films is greater than that of LDPE-rich films.

The effect of residual strain on the yield stress and tensile modulus of the films is shown in Figure 3.10 and 3.11, respectively. These figures show that the results are scattered.

The tear strength of the films as a function of residual strain is shown in Figure 3.12. It is observed

that the *MD* tear strength slightly decreases with increasing *MD* residual strain. Also the tear strength increases with increasing LLDPE composition in the films.

The effect of increasing the *MD* or the *TD* residual strain on the impact strength of LDPE, LLDPE and blends of LDPE/LLDPE films is shown in Figure 3.13. The impact strength, impact force and failure energy, increases with increasing the *MD* and the *TD* residual strain.

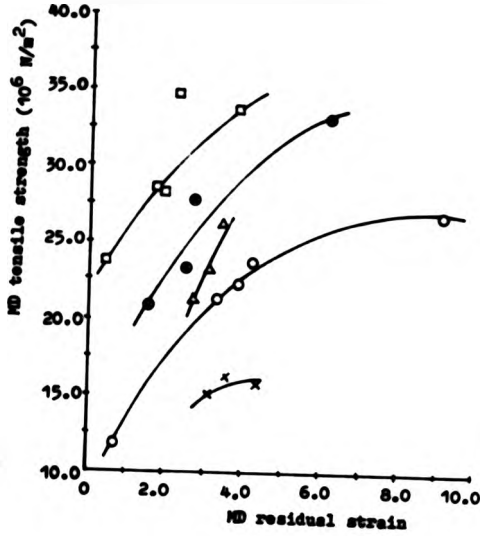

(a)

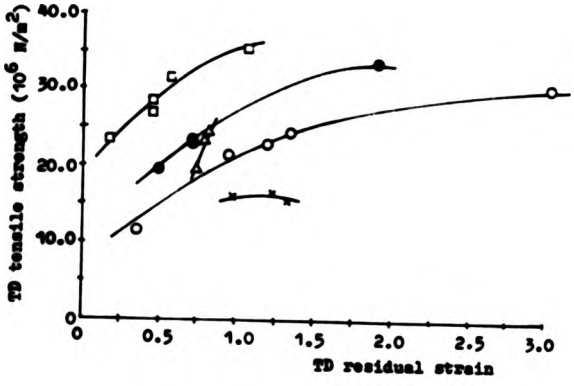

(b)

Figure 3.8. Plots of tensile strength in each direction as a function of residual strain of: (×) LDPE; (○) 75% LDPE/ 25% LLDPE; (△) 50% LDPE/50% LLDPE; (●) 25% LDPE/75% LLDPE; and (□) LLDPE films.

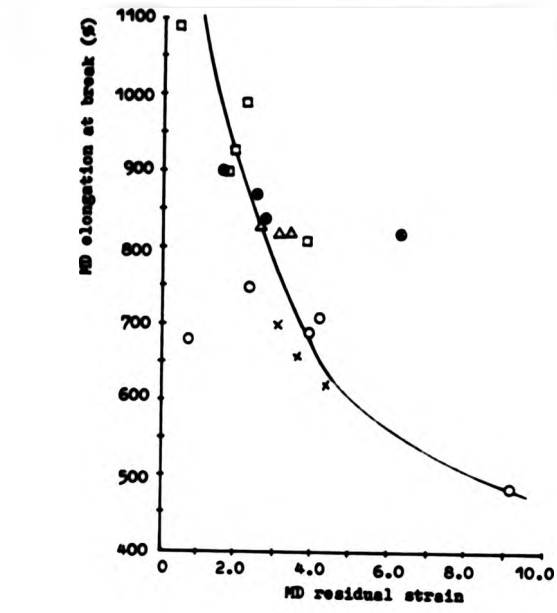

(a)

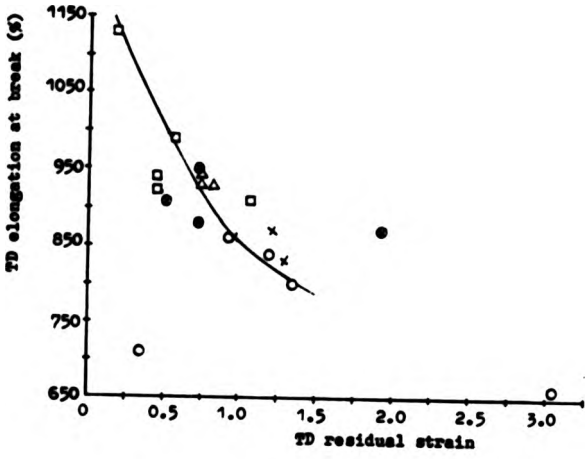

(b)

Figure 3.9. Plots of elongation at break in each direction as a function of residual strain of: (×) LDPE; (○) 75% LDPE/25% LLDPE; (△) 50% LDPE/50% LLDPE; (●) 25% LDPE/75% LLDPE; and (□) LLDPE films.

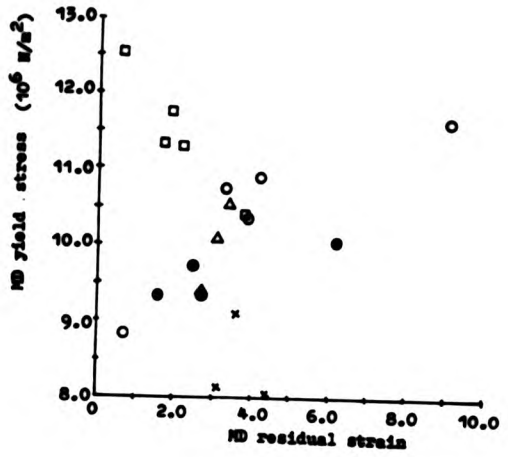

(a)

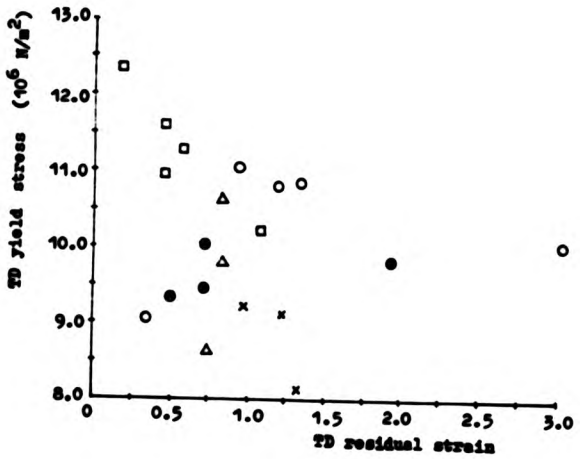

(b)

Figure 3.10. Plots of yield stress in each direction as a function of residual strain of: (×) LDPE; (○) 75% LDPE/ 25% LLDPE; (△) 50% LDPE/50% LLDPE; (●) 25% LDPE/75% LLDPE; and (□) LLDPE films.

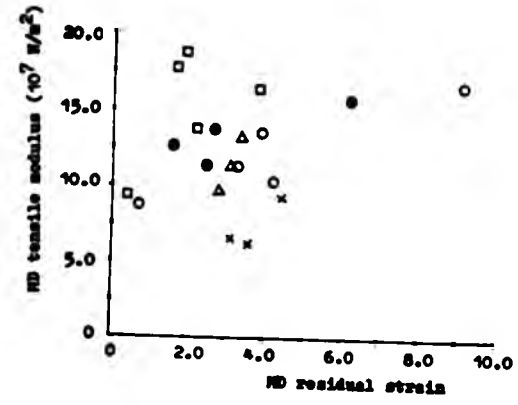

(a)

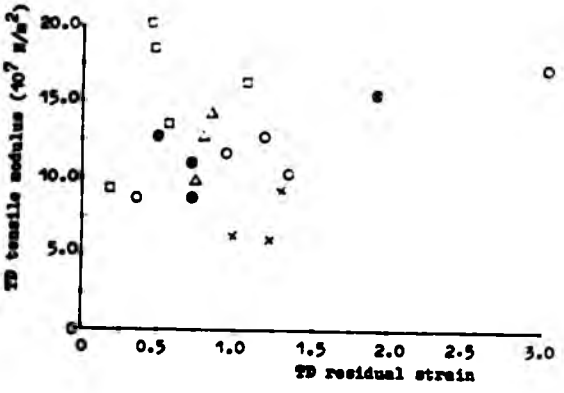

(b)

Figure 3.11. Plots of tensile modulus in each direction as a function of residual strain of: (×) LDPE; (○) 75% LDPE/ 25% LLDPE; (△) 50% LDPE/50% LLDPE; (●) 25% LDPE/75% LLDPE; and (□) LLDPE films.

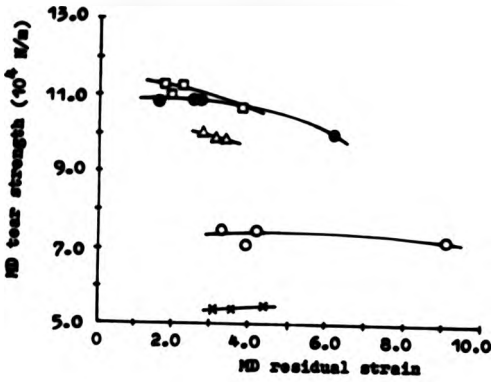

(a)

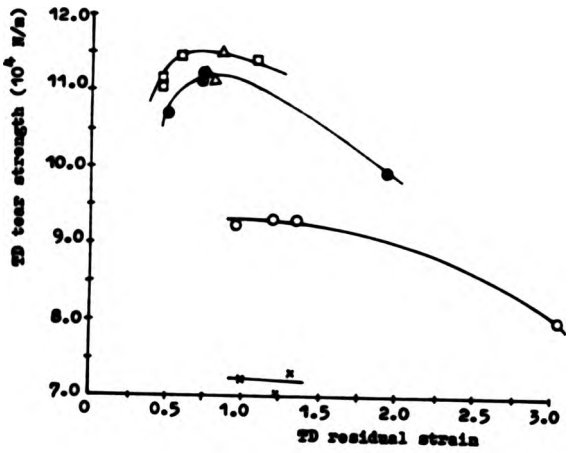

(b)

Figure 3.12. Plots of tear strength in each direction as a function of residual strain of: (×) LDPE; (O) 75% LDPE/25% LLDPE; (Δ) 50% LDPE/50% LLDPE; (●) 25% LDPE/75% LLDPE; and (□) LLDPE films.

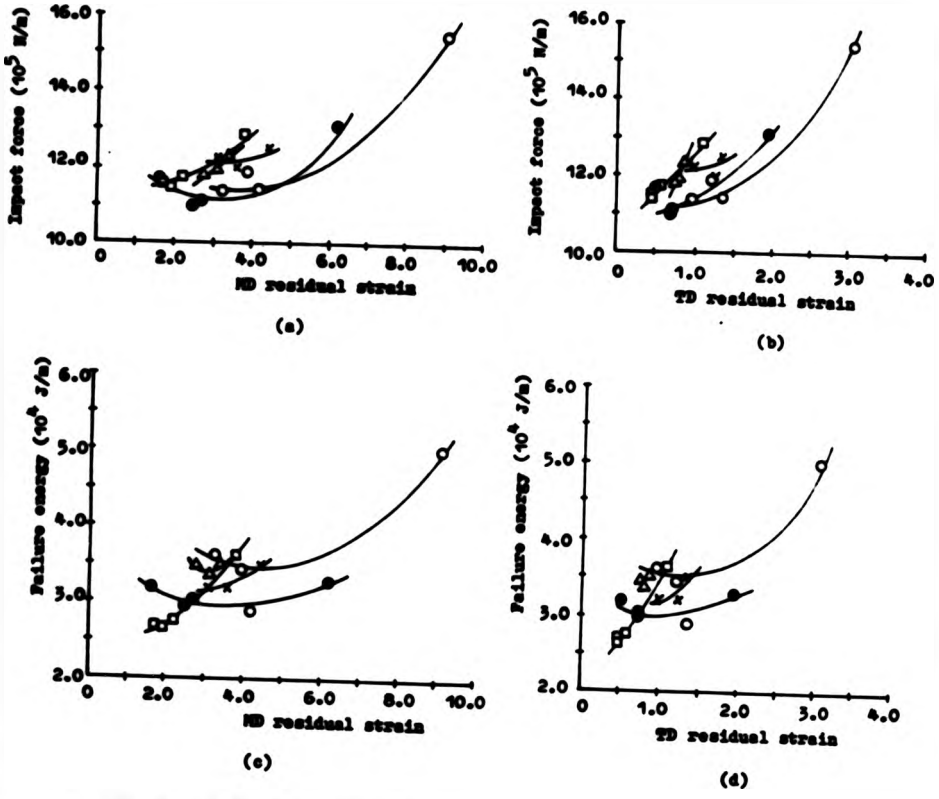

Figure 3.13. Plots of impact strength (impact force and failure energy) as a function of residual strain of: (x) LDPE; (O) 75% LDPE/25% LLDPE; (Δ) 50% LDPE/50% LLDPE; (●) 25% LDPE/75% LLDPE; and (□) LLDPE films.

3.6 Summary of Preliminary Results

It is seen that the mechanical property results obtained in the preliminary studies are very inconclusive. There is often such a large scattering of points that it

is impossible to even attempt to draw lines on some of the graphs.

It is thought that this large scatter of values arises from the difficulty of preparing samples which vary in only one parameter. The parameters that were varied include:

a) the *MD* residual strain;
b) the *TD* residual strain; and
c) the thickness of sample.

It was not possible to prepare samples by the blown film process which had, for example, the *MD* residual strain as a variable, but with the *TD* residual strain and the thickness hold at constant value. This means that samples had three interdependent variables affecting the properties of the films. It is thought that this explains the nature of the poor correlation obtained in the graphs.

It is thought that the problem of preparing films with one variable is the origin of the conflicting data in the literature, and the major cause of the lack of understanding of the blown film process and its effect on properties.

The results described in the next chapters attempt to overcome the problems of multivariable films and hence derive a clearer understanding of the blown film process than has previously been reported in the literature.

CHAPTER 4.0

EFFECT OF ANNEALING TEMPERATURE AND TIME ON THE RESIDUAL STRAINS OF POLYETHYLENE FILMS

4.1 Introduction

In order to perform mechanical tests on samples with residual strain values which could not be obtained simply by modifying the processing conditions during film production, films were annealed at temperatures close to their melting point to allow controlled relaxation of the residual strain to a desired value. To enable the preparation of films of desired residual strain, the relaxation process was studied and the results are covered in this chapter.

Film samples were annealed at several annealing temperatures and times according to the procedure described in section 2.3. The residual strain of the annealed samples was evaluated using the shrinkage method described in section 2.4. The results showing residual strain as a function of annealing temperature and time for LDPE, LLDPE and blends of LDPE and LLDPE films will now be given.

4.2 Effect of Annealing Temperature and Time on the Residual Strains of Low Density Polyethylene Films

Five LDPE films were produced by changing the *NOS* and the *BUR* to get films of thickness of around 35.0 ± 5 micron. The processing conditions used to produce these films are shown in Table 4.1.

Table 4.1. The processing conditions used to manufacture LDPE films to study the effect of annealing temperature and time on the residual strain.

Die diameter	(10^{-3}m)	37.0
Die gap	(10^{-3}m)	2.0
FLH	(10^{-3}m)	200.0
SS	(rpm)	22.0
Output rate	(kg/hr/m die cir.)	60.0
Melt temperature	(^{o}C)	163.0

Sample	Haul-off speed (10^{-3} m/s)	Blow-up ratio
2A	375.0	0.9
2B	250.0	1.3
2C	167.0	2.5
2D	125.0	3.8
2E	96.0	5.7

The films were annealed over an annealing temperature range of 110 - 115°C and an annealing time range of 0 - 60 minutes. The results of annealing on the residual strain of LDPE films are shown in Table 4.2. These results are plotted in Figure 4.1.

Table 4.2. Effect of annealing temperature and time on the residual strain of LDPE films.

Annealing temperature (°C)	Annealing time (min)	Sample 2A			Sample 2B			Sample 2C			Sample 2D			Sample 2E		
		Average thickness (10^{-6}m)	Residual strain		Average thickness (10^{-6}m)	Residual strain		Average thickness (10^{-6}m)	Residual strain		Average thickness (10^{-6}m)	Residual strain		Average thickness (10^{-6}m)	Residual strain	
			MD	TD		MD	TD		MD	TD		MD	TD		MD	TD
105	0.0	36.7	20.33	1.89	-	-	-	-	-	-	-	-	-	35.7	13.06	7.38
	10.0	35.7	18.50	1.73	-	-	-	-	-	-	-	-	-	33.0	13.06	7.29
	20.0	36.3	18.02	1.62	-	-	-	-	-	-	-	-	-	33.3	12.54	6.81
	30.0	35.7	17.07	1.55	-	-	-	-	-	-	-	-	-	34.7	12.28	6.63
	45.0	35.7	16.73	1.50	-	-	-	-	-	-	-	-	-	35.4	11.88	5.94
	60.0	33.7	16.72	1.43	-	-	-	-	-	-	-	-	-	31.3	11.48	5.77
110	0.0	36.7	20.33	1.89	33.0	19.59	2.60	30.0	19.15	5.66	32.7	18.25	5.79	35.7	13.06	7.38
	5.0	-	-	-	-	-	-	-	-	-	-	-	-	31.7	13.03	7.22
	10.0	37.0	17.92	1.48	36.3	17.15	2.07	32.0	17.64	4.72	33.7	15.85	4.64	33.3	11.63	6.61
	15.0	-	-	-	-	-	-	-	-	-	-	-	-	32.0	11.71	6.41
	20.0	36.7	13.57	1.03	34.7	14.12	1.65	31.7	13.34	3.21	34.3	12.63	3.55	31.0	10.78	5.25
	25.0	-	-	-	-	-	-	-	-	-	-	-	-	31.7	10.66	5.65
	30.0	36.3	13.35	0.98	38.3	12.23	1.38	31.3	13.04	3.10	31.7	12.26	3.55	38.0	9.81	4.98
	35.0	-	-	-	-	-	-	-	-	-	-	-	-	32.3	9.66	5.45
	45.0	35.3	12.80	1.04	36.3	11.95	1.31	33.0	12.72	3.10	33.0	11.54	3.35	32.0	9.24	4.87
	60.0	36.3	11.64	0.99	39.0	11.83	1.21	31.0	12.02	2.88	32.7	11.57	3.21	36.3	8.15	3.87
115	0.0	-	-	-	33.0	19.59	2.60	30.0	19.15	5.66	32.7	18.25	5.79	35.7	13.06	7.38
	10.0	-	-	-	37.7	12.84	1.19	31.0	15.49	3.90	33.0	12.93	3.65	35.0	9.69	4.70
	20.0	-	-	-	39.0	5.92	0.29	30.3	4.32	0.70	30.3	5.31	0.91	30.8	2.79	1.15
	30.0	-	-	-	40.0	5.94	0.33	30.7	4.17	0.51	33.0	4.83	0.72	39.0	2.47	0.97
	45.0	-	-	-	40.0	4.77	0.28	31.0	4.09	0.44	32.7	4.35	0.68	31.0	1.76	0.95
	60.0	-	-	-	40.0	4.41	0.29	33.3	4.00	0.38	34.3	4.00	0.55	39.3	1.75	0.68

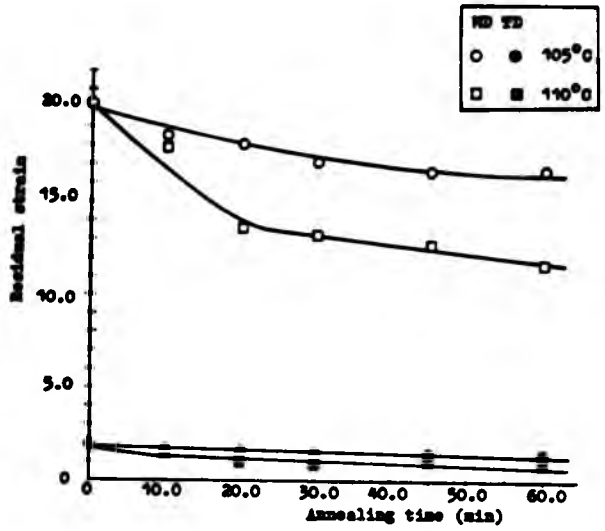

Figure 4.1(a) Sample 2A

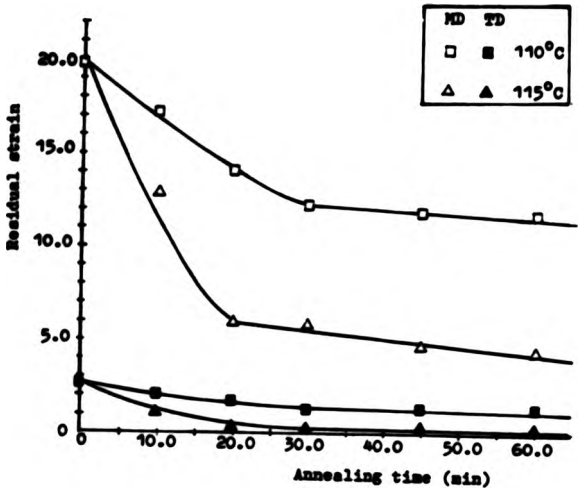

Figure 4.1(b) Sample 2B

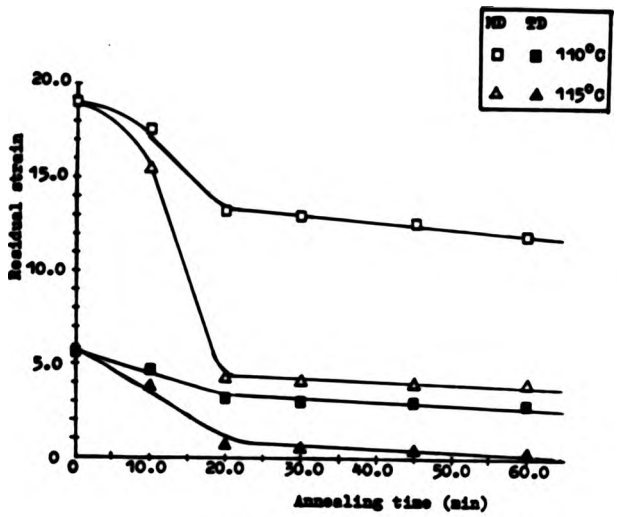

Figure 4.1(c) Sample 2C

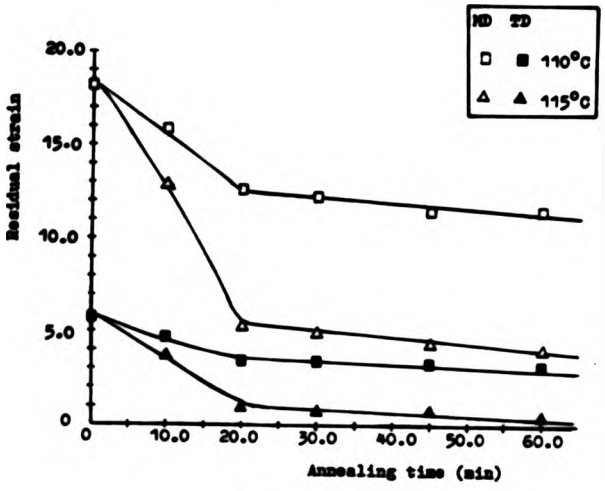

Figure 4.1(d) Sample 2D

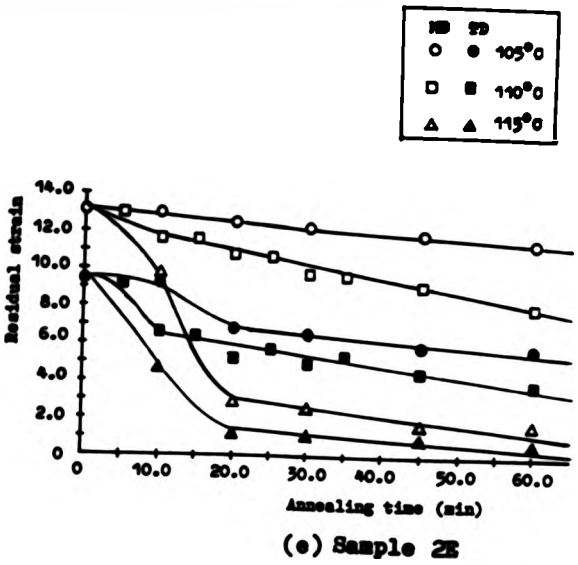

(e) Sample 2E

Figure 4.1. Residual strain of LDPE films as a function of annealing temperature and time. The plots are for: (a) sample 2A; (b) sample 2B; (c) sample 2C; (d) sample 2D; and (e) sample 2E.

When sample 2A was annealed at 115°C, small holes were formed in the sample. Shrinkage test could not be done on this sample and therefore it was rejected.

From Figure 4.1, it can be seen that increasing the annealing time, at constant annealing temperature, reduces the residual strain in both directions of the films. The same effect is observed with increasing annealing temperature at constant annealing time.

4.3 Effect of Annealing Temperature and Time on the Residual Strains of Blended Films

Two 75% LDPE/25% LLDPE blend films were produced by changing the processing conditions as shown in Table 4.3. The thickness of the films was kept constant at 35.0 ± 5 micron.

Table 4.3. The processing conditions used to produce 75% LDPE/25% LLDPE blend films.

Die diameter	(10^{-3} m)	37.0
Die gap	(10^{-3} m)	2.0
FLH	(10^{-3} m)	10.0
SS	(rpm)	15.0
Output rate	(kg/hr/m die cir.)	36.8
Melt temperature	(^{o}C)	155.0

Sample	Haul-off speed (10^{-3}m/s)	Blow-up ratio
3A	146.0	1.6
3B	125.0	3.4

The samples were annealed at annealing temperatures of 115^{o}C, 120^{o}C and 125^{o}C and an annealing time range of 0 - 60 minutes. The results of annealing are shown in Table 4.4 and plotted in Figure 4.2.

As observed with LDPE films, the effect of increasing annealing temperature and time is to reduce the residual strain of 75% LDPE/25% LLDPE blend films.

Table 4.4. Residual strain of 75% LDPE/25% LLDPE blend films as a function of annealing temperature and time.

Annealing temperature (°C)	Annealing time (min)	Sample 3A			Sample 3B		
		Average thickness (10^{-6}m)	Residual strain		Average thickness (10^{-6}m)	Residual strain	
			MD	TD		MD	TD
115	0.0	36.7	18.51	1.91	33.3	14.55	3.26
	10.0	37.3	15.08	1.44	36.7	12.61	2.49
	20.0	38.0	14.03	1.29	31.7	9.52	1.91
	30.0	36.0	13.20	1.13	35.0	9.67	1.67
	45.0	34.3	12.83	1.16	32.0	9.65	1.57
	60.0	36.0	12.68	1.18	34.0	9.38	1.51
120	0.0	36.7	18.51	1.91	33.3	14.55	3.26
	10.0	37.0	12.61	1.06	31.0	9.83	2.18
	20.0	37.7	8.30	0.57	36.0	5.57	0.83
	30.0	36.0	7.27	0.47	35.7	5.31	0.74
	45.0	36.0	7.08	0.36	35.0	5.20	0.62
	60.0	37.0	6.84	0.35	37.0	5.07	0.64
125	0.0	36.7	18.51	1.91	33.3	14.55	3.26
	10.0	35.3	9.38	0.60	35.7	5.23	0.76
	20.0	34.0	4.08	0.39	36.3	1.33	0.16
	30.0	35.0	3.92	0.29	36.0	1.20	0.15
	45.0	36.0	1.74	0.20	36.7	1.20	0.13
	60.0	35.0	1.23	0.21	34.0	1.19	0.14

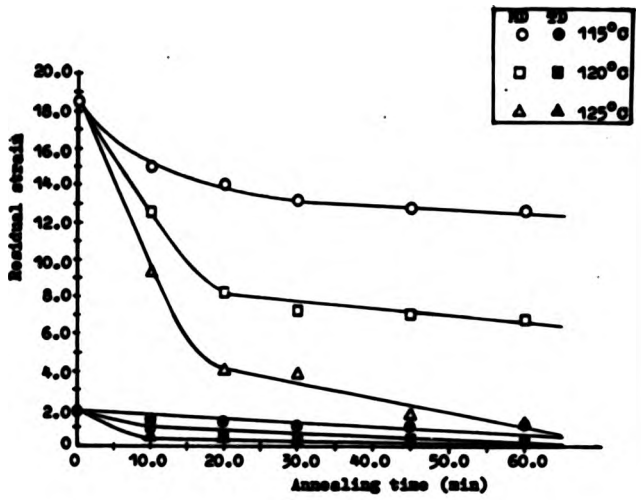

(a) Sample 3A

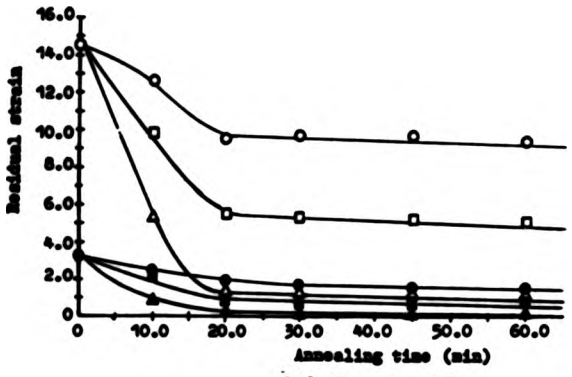

(b) Sample 3B

Figure 4.2. Residual strain of 75% LDPE/25% LLDPE blend films as a function of annealing temperature and time. The plots are for: (a) sample 3A; and (b) sample 3B.

Two 25% LDPE/75% LLDPE blend films of thickness 35.0 ± 5 micron were produced by using the processing variable shown in Table 4.5.

Table 4.5. The processing conditions used to produce 25% LDPE/75% LLDPE blend films.

Die diameter	(10^{-3} m)	37.0
Die gap	(10^{-3} m)	2.0
FLH	(10^{-3} m)	100.0
SS	(rpm)	19.0
Output rate	(kg/hr/m die cir.)	44.7
Melt temperature	(^{o}C)	157.0

Sample	Haul-off speed (10^{-3}m/s)	Blow-up ratio
4A	167.0	1.8
4B	125.0	3.3

The film samples were annealed at annealing temperatures of 120°C, 125°C and 130°C. The annealing time range was 0 - 60 minutes for each sample except at the annealing temperature of 130°C where after 30.0 minutes it was found that the residual strain of the films was nearly zero. The effect of annealing temperature and time on the residual strain of 25% LDPE/75% LLDPE blend films is shown in Table 4.6 and Figure 4.3.

From Figure 4.3, it can be seen that increasing the annealing time and temperature reduces the residual strain of the 25% LDPE/75% LLDPE blend films.

Table 4.6. Residual strain of 25% LDPE/75% LLDPE blend films as a function of annealing temperature and time.

Annealing temperature (°C)	Annealing time (min)	Sample 4A			Sample 4B		
		Average thickness (10^{-6}m)	Residual strain		Average thickness (10^{-6}m)	Residual strain	
			MD	TD		MD	TD
120	0.0	36.3	14.95	1.60	34.0	11.60	3.40
	10.0	36.7	12.82	1.33	32.7	10.97	2.74
	20.0	36.7	11.64	1.17	30.3	8.76	2.20
	30.0	37.7	11.26	1.16	39.0	8.50	1.67
	45.0	35.8	11.20	1.13	36.7	8.45	1.55
	60.0	36.3	11.15	1.10	32.7	8.16	1.38
125	0.0	36.3	14.95	1.60	34.0	11.60	3.40
	10.0	34.3	11.57	1.14	33.3	9.40	2.30
	20.0	36.7	7.24	0.65	34.0	5.43	1.19
	30.0	36.7	7.30	0.65	33.0	4.32	0.98
	45.0	36.3	7.15	0.66	33.7	4.24	0.68
	60.0	36.0	7.21	0.60	36.0	4.19	0.52
130	0.0	36.3	14.95	1.60	34.0	11.60	3.40
	10.0	35.7	4.99	0.39	31.7	3.40	0.68
	20.0	36.0	0.38	0.19	32.0	0.31	0.19
	30.0	36.7	0.16	0.14	31.7	0.23	0.19

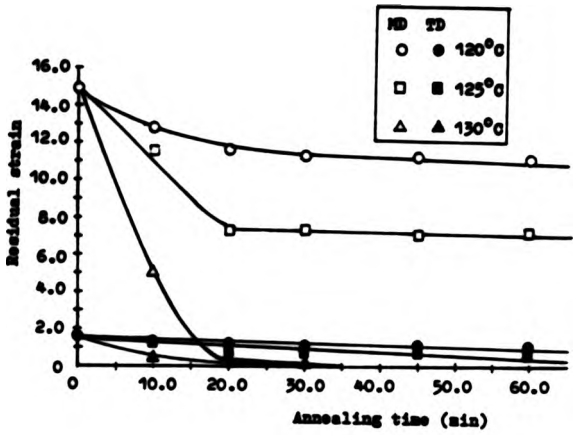

(a) Sample 4A

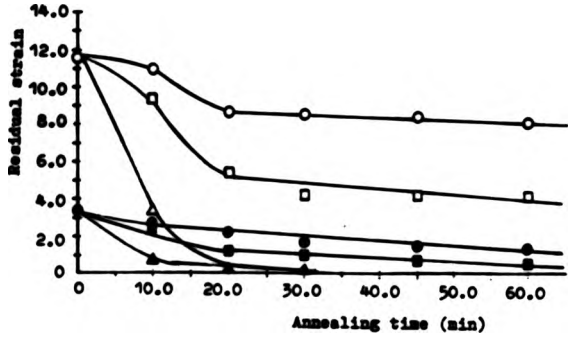

(b) Sample 4B

Figure 4.3. Residual strain of 25% LDPE/75% LLDPE blend films as a function of annealing temperature and time. The plots are for: (a) sample 4A; and (b) sample 4B.

4.4 Effect of Annealing Temperature and Time on the Residual Strains of Linear Low Density Polyethylene Films

The films were produced by changing the processing conditions and the thickness was kept constant at 35.0 ± 5 micron. The processing conditions used to produce LLDPE films are shown in Table 4.7.

Table 4.7. The processing conditions used to produce LLDPE films.

Die diameter	(10^{-3} m)	37.0
Die gap	(10^{-3} m)	2.0
FLH	(10^{-3} m)	100.0
SS	(rpm)	15.0
Output rate	(kg/hr/m die cir.)	44.6
Melt temperature	(^{o}C)	157.0

Sample	Haul-off speed (10^{-3}m/s)	Blow-up ratio
5A	167.0	1.7
5B	146.0	3.3

The films were annealed at annealing temperatures of 120^{o}C, 125^{o}C and 130^{o}C. At each annealing temperature, except at 130^{o}C, the annealing time range was 0 - 60 minutes. At 130^{o}C the annealing was up to 30.0 minutes because by that time the residual strain of the films seems to have relaxed completely. The results of annealing on the residual strain of LLDPE films are shown in Table

4.8 and plotted in Figure 4.4.

The plot of residual strain against annealing temperature and time of LLDPE films, Figure 4.4, showed the same behaviour as observed with other films.

Table 4.8. Residual strain of LLDPE films as a function of annealing temperature and time.

Annealing temperature (^{o}C)	Annealing time (min)	Sample 5A			Sample 5B		
		Average thickness (10^{-6}m)	Residual strain		Average thickness (10^{-6}m)	Residual strain	
			MD	TD		MD	TD
120	0.0	38.0	9.34	1.23	33.7	7.52	1.80
	10.0	35.0	8.21	0.99	34.0	6.63	1.48
	20.0	37.3	8.34	1.04	36.3	6.84	1.76
	30.0	36.7	7.85	1.05	36.0	6.21	1.39
	45.0	35.3	7.70	1.04	31.7	6.08	1.53
	60.0	36.3	7.64	1.03	31.7	5.90	1.47
125	0.0	38.0	9.34	1.23	33.7	7.52	1.80
	10.0	34.7	7.41	0.85	34.0	6.31	1.42
	20.0	37.3	6.28	0.73	33.7	4.97	1.10
	30.0	36.7	6.34	0.68	33.0	4.36	0.89
	45.0	36.3	5.43	0.65	35.0	4.51	0.98
	60.0	35.7	5.55	0.54	34.3	4.49	0.94
130	0.0	38.0	9.34	1.23	33.7	7.52	1.80
	10.0	34.7	6.23	0.83	34.3	5.14	1.13
	20.0	36.3	0.55	0.13	35.0	0.46	0.22
	30.0	35.3	0.06	0.10	35.3	0.18	0.19

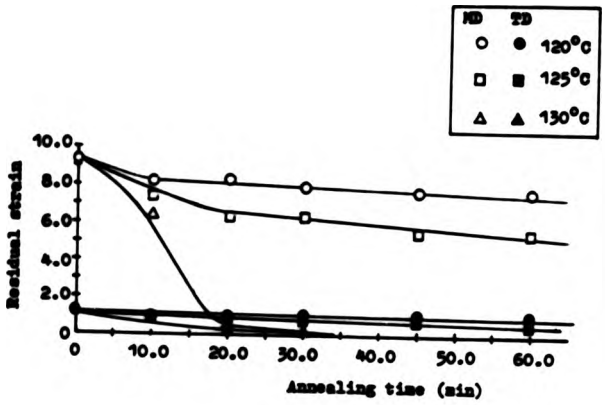

(a) Sample 5A

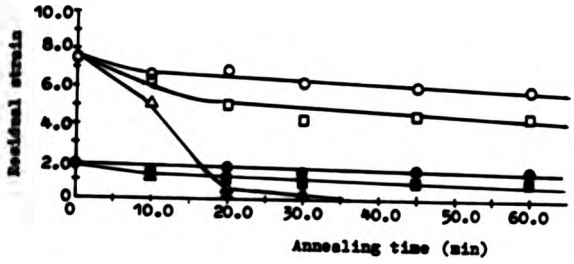

(b) Sample 5B

Figure 4.4. Residual strain of LLDPE films as a function annealing temperature and time. The plots are for: (a) sample 5A; and (b) sample 5B.

4.5 Discussion

Lamellae thickening takes place during annealing of the films *(120)*. This process involves melting the least stable part of the lamellae and recrystallising them at a higher thickness around the nuclei provided by the remainder of the lamellae.

The process of melting the unstable lamellae is greater at the beginning of the annealing process because there are more unstable lamellae in the film. As annealing process progresses, however, there are less unstable lamellae present in the sample. This results in reduced melting of the lamellae.

The melting of the unstable lamellae part results in the release of some of the residual strain of the film which had been held there because molecules were trapped in the lamellae. The rate of relaxation of residual strain depends on the rate of melting of the lamellae. The greater the rate of melting the greater will be the relaxation of the residual strain of the sample. This is reflected by the annealing curves of the films shown previously.

As the annealing temperature is increased above the melting point of the polymer, 130^{o}C, all the lamellae are melted. This results in complete relaxation of the residual strain.

CHAPTER 5.0

ORIGIN OF RESIDUAL STRAINS IN THE FILMS

5.1 Introduction

In this chapter the relationship between the residual strain and the stretching ratio in the bubble during blowing is shown. From this relationship the mechanism that gave rise to residual strain is suggested.

In the later part of this chapter the distribution of the residual strain around the *MD* is considered and this distribution is then linked to the distribution of the stretched molecules in the sample. Also from this distribution the proportion of molecules oriented along the *MD* and the *TD* can be estimated.

5.2 Relationship Between Residual Strains and the Stretching Ratios in the Film Bubble During Blowing

It has been established that the structure of blown PE films consists of alternating layers of crystalline and amorphous regions *(41,46,61,66,67)*. During film blowing the polymer molecules are stretched. In the region before the freeze line crystallisation and molecular relaxation will take place. As a result of molecular relaxation, some of the stretched molecules will relax before reaching the freeze line. Above the freeze line, the crystalline

regions in the solidified film will prevent the relaxation of some of the stretched molecules, i.e. those connecting the crystalline regions together. These molecules are called the tie molecules. The stretched molecules are strained compared to their most probable shape and this strain is the residual strain. As the name implies, the residual strain is the strain that is left in the sample after some of the stretched molecules have relaxed before reaching the freeze line.

When the film sample is heated at its melting point the crystals (lamellae) will melt and thus the stretched tie molecules will relax. The relaxation of these molecules resulted in the shrinkage of the film. The amount of shrinkage depends on the amount of stretching of the tie molecules. The greater the stretching the greater will be the shrinkage and thus the greater will be the residual strain.

The above simplified picture ignores any orientation of the crystal lamellae.

If the amount of residual strain depends on the stretching of the molecules then the ratio of the residual strain in the *MD* and the *TD* will be related to the stretching of the bubble in the *MD* and the *TD* during blowing. The amount of stretching of the bubble in the *MD* is proportional to the ratio of the velocity of the solid film at the freeze line to the velocity of the melt at the die lip, i.e. HOS/V_o. The value of V_o was calculated from

the output rate of the extruder and the dimensions of the die as well as the density of the melt at the temperature used in film blowing. The evaluation of V_o is shown in Appendix 3.0. The amount of stretching in the *TD* is related to the *BUR* of the bubble.

The ratio of the *MD/TD* stretching is given by the $(HOS/V_o)/BUR$ ratio. If the residual strain is related to the stretching of the bubble then the ratio of the *MD/TD* residual strain should be related to the ratio of $(HOS/V_o)/BUR$. This comparison is shown in Table 5.1 and plotted in Figure 5.1.

Table 5.1. The stretching and residual strain ratios of LDPE, LLDPE and blends of LDPE and LLDPE films.

Film	Melt temperature (°C)	Haul-off speed (HOS) (10^{-3} m/s)	V_o (10^{-3} m/s)	Blow-up ratio (BUR)	Stretching ratio $\frac{(HOS/V_o)}{(BUR)}$	Residual strain		Residual strain ratio (MD/TD)
						MD	TD	
LDPE	163	375.0	10.80	0.9	38.58	20.33	1.89	10.76
		250.0		1.3	17.81	19.59	2.60	7.53
		167.0		2.5	6.18	19.15	5.66	3.38
		125.0		3.8	3.04	18.25	5.79	3.15
		96.0		5.7	1.56	13.06	7.38	1.77
75% LDPE/ 25% LLDPE	155	146.0	6.65	1.6	13.72	18.51	1.91	9.69
		125.0		3.4	5.53	14.55	3.26	4.46
25% LDPE/ 75% LLDPE	157	167.0	8.04	1.8	11.54	14.95	1.60	9.34
		125.0		3.3	4.71	11.60	3.40	3.41
LLDPE	157	167.0	8.04	1.7	12.22	9.34	1.23	7.59
		146.0		3.3	5.50	7.52	1.80	4.18

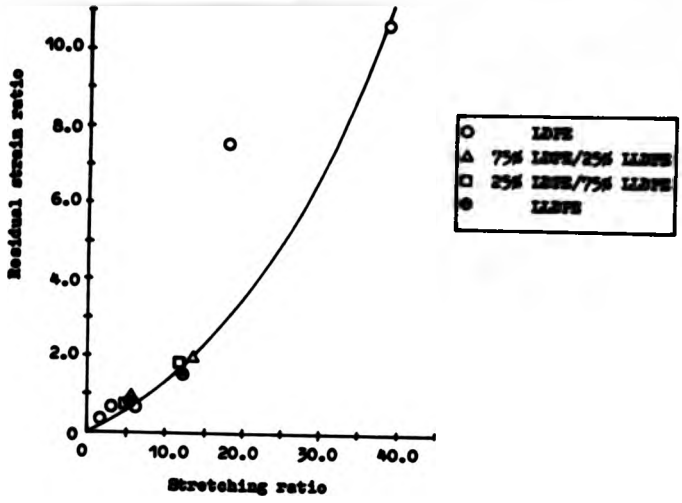

Figure 5.1. Plot of MD/TD residual strain ratio against MD/TD stretching ratio of the bubble, $(HOS/V_o)/(BUR)$, of LDPE, LLDPE and blends of LDPE and LLDPE films.

It can be seen that the residual strain ratio is related to the ratio of stretching in the bubble during blowing. This shows that the residual strain in the sample is due to the stretching of the molecules in the melt during bubble blowing.

The residual strain ratios are less than the corresponding stretching ratios. This can be ascribed to relaxation occuring below the freeze line in the film bubble.

5.3 Distribution of Strained Molecules in the Film

To understand the effect of residual strain in each

direction on the mechanical properties of the film, we need to understand the distribution of the strained molecules in the film. This is done by considering the two types of orientation. These are

a) uniaxial orientation; and
b) equibiaxial orientation.

As pointed out before in Chapter 1.0, in uniaxial orientation the strained molecules are oriented in one direction and in equibiaxial orientation the strained molecules are oriented equally in both directions. The possible distribution of strained molecules in these two types of orientation is shown in Figure 5.2.

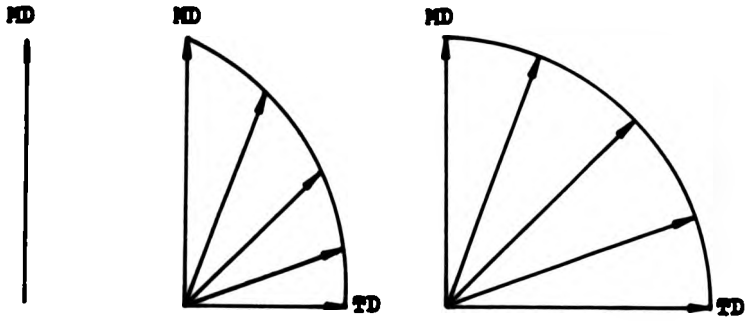

Figure 5.2. Distribution of strained molecules in (a) uniaxial orientation, (b) intermediate orientation and (c) equibiaxial orientation. Note the length of the line is indicative of the number of strained molecules oriented in the direction in which it is pointing.

The orientation encountered with the film samples prepared for this project, however, is in between the two types of orientation mentioned above. This is in line with orientations in commercial films and typical for films produced by the blown film process. Uniaxial films would be produced under unusual conditions, e.g. with the *BUR* less than 1.0, and equibiaxially oriented films are usually achieved in the industry by post extrusion stretching process. Therefore the possible distribution of strained molecules of the films produced in this project is in between the uniaxial and equibiaxial orientation, as shown in Figure 5.2(b). This type of orientation I have called intermediate orientation.

A simple shrinkage experiment was done to show that the intermediate orientation is observed in the films made in this project. The sample chosen for this experiment was sample 1*E*, that is LDPE film made with the processing conditions shown in Chapter 4.0. The residual strain of this sample was evaluated from the shrinkage results of several test pieces cut at different angles to the *MD*. The results of this test are shown in Table 5.2 and plotted in Figure 5.3. It can be seen from Figure 5.3 that the shape of the curve is the same as that shown in Figure 5.2(b), that is a quadrant of an ellipse. This confirms that the distribution of the strained molecules in the films produced in this project is the intermediate orientation.

Table 5.2. The variation of residual strain of LDPE film (sample ZE) with the direction of test from MD.

Direction of test relative to MD	Average thick-ness (10^{-6}m)	Residual strain
0°	35.7	13.06
10°	34.7	12.27
20°	33.3	11.10
30°	31.0	10.21
45°	31.3	8.50
60°	31.0	7.54
70°	33.3	7.58
80°	34.7	7.51
90°	35.7	7.38

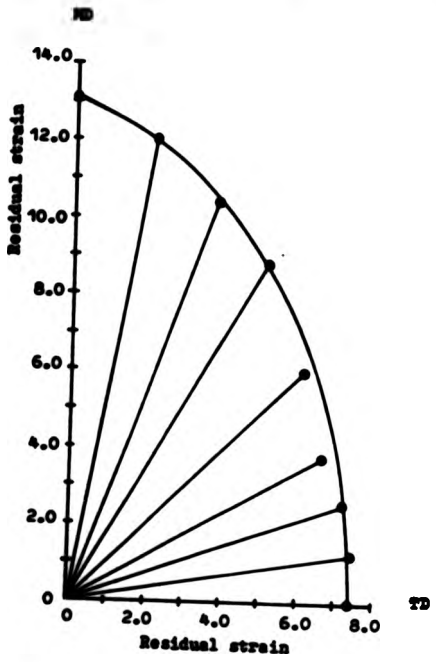

Figure 5.3. The distribution of strained molecules of LDPE film (sample ZE) at several angles to MD.

The proportion of strained molecules oriented along the *MD* or the *TD* is determined by the *MD/TD* residual strain ratio. If the ratio is 3:1, for example, then there are three times as many strained molecules oriented along the *MD* compared to the *TD*. The strain in the molecules oriented along any direction, however, is given by the value of residual strain in that direction.

To support the above argument, consider the residual strain values of the films produced by changing either the *HOS* or the *BUR*, keeping other processing conditions the same. These results were reported in the preliminary work of this project and are shown in Table 5.3. It can be seen that increasing the *HOS* increases the *MD/TD* residual strain ratio despite the fact that the residual strain in both directions increases with increasing *HOS*. Increasing the *HOS* results in the increase in the deformation along the *MD* of the film bubble. This will increase the amount of molecules oriented along the *MD*. The increase in the proportion of oriented molecules along the *MD* is shown by the increase in the *MD/TD* residual strain ratio.

From Table 5.3 it is observed that for a small increase in *HOS*, from 60.0 to 80.0 x 10^{-2} m/s, there is a big increase in the residual strain values. The big increase in the residual strain is due to the fact that the thickness of the film decreases with increasing *HOS*. The decrease in thickness results in the increase in residual strain, as explained in Chapter 3.0 previously.

The effect of increasing *BUR* on the *TD/MD* residual strain ratio can be explained using the same argument used for *HOS*. This time the orientation in *TD* increases with increasing *BUR* which results in the increase in *TD/MD* residual strain ratio.

Table 5.3. Residual strain as a function of (a) HOS and (b) BUR of LDPE films.

(a)

Haul-off speed (10^{-3}m/s)	Residual strain		Residual strain ratio (MD/TD)
	MD	TD	
60.0	1.05	0.97	1.08
75.0	2.69	1.52	1.77
80.0	6.20	2.44	2.54

(b)

Blow-up ratio	Residual strain		Residual strain ratio (TD/MD)
	MD	TD	
1.4	5.58	0.76	0.14
3.0	6.71	1.92	0.29
4.5	6.53	2.78	0.42

5.4 Discussion

The stretching that takes place in the bubble during film blowing gives rise to the residual strain in the film. The residual strain is the measure of the strain of the molecules frozen in the film and the value in each direction indicates the strain of the molecules oriented in that direction. The strain in the molecules is released when the film is heated at the melt temperature, as encountered in the shrinkage test. The release of the strain results in the shrinkage of the film.

The films produced for this project have the intermediate orientation. The proportion of molecules oriented along any direction is given the residual strain ratio in that direction. The greater the ratio the greater is the amount of molecules oriented in that direction.

CHAPTER 6.0

ANNEALING CONDITIONS USED TO PRODUCE FILM SAMPLES OF CONSTANT RESIDUAL STRAIN IN ONE DIRECTION

6.1 Introduction

To study the effect of residual strain on the mechanical properties of the films, samples of constant residual strain in one direction are needed. In this chapter the annealing conditions used to produce the samples are given.

6.2 General Method

The conditions used to make the film samples of constant *MD* or *TD* residual strain were chosen by drawing a line through the annealing curves as shown in Figure 6.1 and noting the annealing temperature and time for each chosen sample.

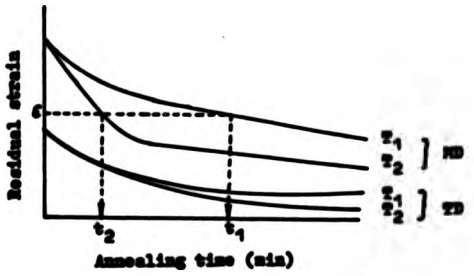

Figure 6.1. Selection of annealing time and temperature to produce sample of residual strain ε in the MD.

6.3 Annealing Conditions Used to Produce Low Density Polyethylene Films of Constant Residual Strain in One Direction

LDPE films of approximately constant MD residual strain of 7.0, 13.0 and 16.0 but varying TD residual strain were produced by using the annealing conditions shown in Table 6.1.

Table 6.1. Annealing conditions used to produce LDPE films of approximately constant MD residual strain of 7.0, 13.0 and 16.0 and constant film thickness of $35.0 \pm 5.0 \times 10^{-6}$ m (within experimental error).

Sample	Blow-up ratio	Haul-off speed (10^{-3} m/s)	Annealing temperature (^{o}C)	Annealing time (min)	Average thickness (10^{-6}m)	Residual strain	
						MD	TD
6A	1.3	250.0	115	17.0	31.0	7.82	0.70
6B	2.5	167.0	115	17.0	32.0	7.24	1.27
6C	3.8	125.0	115	15.0	32.3	6.68	1.41
6D	5.7	96.0	115	12.0	35.0	6.87	3.67
6E	1.3	250.0	115	10.0	37.7	12.84	1.19
6F	1.3	250.0	110	30.0	38.3	12.23	1.38
6G	2.5	167.0	110	30.0	31.3	13.04	3.10
6H	3.8	125.0	115	10.0	33.0	12.93	3.66
6I	5.7	96.0	n.a.	0.0	35.7	13.06	7.38
6J	0.9	375.0	110	17.0	33.3	16.05	1.37
6K	1.3	250.0	110	17.0	31.7	16.27	1.84
6L	2.5	167.0	110	14.0	32.3	16.19	4.20
6M	3.8	125.0	110	14.0	33.7	15.47	4.68

Table 6.2 shows the annealing conditions used to produce LDPE films of approximately constant TD residual strain of 0.5, 1.5 and 4.3.

Table 6.2. Annealing conditions used to produce LDPE films of approximately constant TD residual strain of 0.5, 1.5 and 4.3 and constant film thickness of $35.0 \pm 5.0 \times 10^{-6}$ m (within experimental error).

Sample	Blow-up ratio	Haul-off speed (10^{-3} m/s)	Annealing temperature (°C)	Annealing time (min)	Average thickness (10^{-6} m)	Residual strain	
						MD	TD
7A	5.7	96.0	115	60.0	39.0	1.75	0.68
7B	2.5	167.0	115	30.0	30.7	4.17	0.51
7C	3.8	125.0	115	30.0	33.0	4.83	0.72
7D	1.3	250.0	115	30.0	40.0	5.94	0.33
7E	5.7	96.0	115	17.0	37.3	3.52	1.40
7F	2.5	167.0	115	15.0	31.0	6.49	1.48
7G	3.8	125.0	115	15.0	31.0	6.68	1.41
7H	1.3	250.0	110	17.0	31.7	16.27	1.84
7I	0.9	375.0	n.a.	0.0	36.7	20.33	1.89
7J	5.7	96.0	115	12.0	31.7	7.05	3.82
7K	5.7	96.0	110	24.0	31.3	9.33	4.71
7L	3.8	125.0	115	7.5	34.7	15.07	4.34
7M	2.5	167.0	115	10.0	31.0	15.49	3.90

6.4 Annealing Conditions Used to Produce Blended Films of Constant Residual Strain in One Direction

The annealing conditions used to produce 75% LDPE/25% LLDPE blend films of approximately constant *MD* residual strain of 9.5 are shown in Table 6.3.

Table 6.3. Annealing conditions used to produce 75% LDPE/25% LLDPE blend films of approximately constant MD residual strain of 9.5 and constant film thickness of 35.0 ± 5.0 x 10^{-6} m (within experimental error).

Sample	Blow-up ratio	Haul-off speed (10^{-3} m/s)	Annealing temperature (°)	Annealing time (min)	Average thickness (10^{-6} m)	Residual strain	
						MD	TD
8A	1.6	146.0	125	10.0	35.3	9.38	0.60
8B	1.6	146.0	120	16.0	34.3	9.65	0.69
8C	3.4	125.0	125	6.0	35.0	9.42	1.62
8D	3.4	125.0	115	45.0	32.0	9.65	2.07
8E	3.4	125.0	120	10.0	31.0	9.83	2.18

75% LDPE/25% LLDPE blend films of constant *TD* residual strain of about 1.0 were made by using the annealing conditions shown in Table 6.4.

Table 6.4. Annealing conditions used to produce 75% LDPE/ 25% LLDPE blend films of approximately constant TD residual strain of 1.0 and constant film thickness of 35.0 ± 5.0 x 10^{-6} m (within experimental error).

Sample	Blow-up ratio	Haul-off speed (10^{-3}m/s)	Annealing temperature (°C)	Annealing time (min)	Average thickness (10^{-6}m)	Residual strain	
						MD	TD
9A	3.4	125.0	125	9.0	34.7	5.98	0.92
9B	3.4	125.0	120	12.0	36.0	6.31	1.09
9C	1.6	146.0	125	7.0	36.3	11.49	0.89
9D	1.6	146.0	120	10.0	37.0	12.61	1.06
9E	1.6	146.0	115	40.0	34.3	12.77	1.08

The annealing conditions used to produce 25% LDPE/75% LLDPE blend films of approximately constant *MD* residual strain of 9.0 are shown in Table 6.5.

Table 6.5. Annealing conditions used to produce 25% LDPE/ 75% LLDPE blend films of approximately constant MD residual strain of 9.0 and constant film thickness of 35.0 ± 5.0 x 10^{-6} m (within experimental error).

Sample	Blow-up ratio	Haul-off speed (10^{-3}m/s)	Annealing temperature (°C)	Annealing time (min)	Average thickness (10^{-6}m)	Residual strain	
						MD	TD
10A	1.8	167.0	130	9.0	37.3	8.95	0.80
10B	3.3	125.0	130	6.0	34.7	9.05	2.01
10C	3.3	125.0	120	20.0	30.3	8.76	2.20
10D	3.3	125.0	125	10.0	33.3	9.40	2.30

Table 6.6 shows the annealing conditions used to produce 25% LDPE/75% LLDPE blend films of approximately constant TD residual strain of 1.0.

Table 6.6. Annealing conditions used to produce 25% LDPE/75% LLDPE blend films of approximately constant TD residual strain of 1.0 and constant film thickness of 35.0 ± 5.0 x 10^{-6} m (within experimental error).

Sample	Blow-up ratio	Haul-off speed (10^{-3} m/s)	Annealing temperature (°C)	Annealing time (min)	Average thickness (10^{-6} m)	Residual strain	
						MD	TD
11A	3.3	125.0	125	30.0	33.0	4.32	0.98
11B	1.8	167.0	125	16.0	37.3	7.52	0.94
11C	1.8	167.0	130	7.0	38.0	10.47	1.05
11D	1.8	167.0	120	30.0	37.7	11.26	1.16

6.5 Annealing Conditions Used to Produce Linear Low Density Polyethylene Films of Constant Residual Strain in One Direction

LLDPE films of constant MD residual strain of about 6.5 were produced by using the annealing conditions shown in Table 6.7.

The annealing conditions used to make LLDPE films of approximately constant TD residual strain of 1.0 are shown in Table 6.8.

Table 6.7. Annealing conditions used to produce LLDPE films of approximately constant MD residual strain of 6.5 and constant film thickness of 35.0 ± 5.0 x 10^{-6} m (within experimental error).

Sample	Blow-up ratio	Haul-off speed (10^{-3}m/s)	Annealing temperature (°C)	Annealing time (min)	Average thickness (10^{-6}m)	Residual strain	
						MD	TD
12A	1.7	167.0	125	30.0	36.7	6.34	0.68
12B	1.7	167.0	130	10.0	34.7	6.23	0.83
12C	3.3	146.0	125	10.0	34.0	6.31	1.42
12D	3.3	146.0	120	40.0	32.7	6.54	1.47
12E	3.3	146.0	130	5.0	32.7	6.63	1.59

Table 6.8. Annealing conditions used to produce LLDPE films of approximately constant TD residual strain of 1.0 and constant film thickness of 35.0 ± 5.0 x 10^{-6} m (within experimental error).

Sample	Blow-up ratio	Haul-off speed (10^{-3}m/s)	Annealing temperature (°C)	Annealing time (min)	Average thickness (10^{-6}m)	Residual strain	
						MD	TD
13A	3.3	146.0	125	35.0	32.7	5.01	1.04
13B	3.3	146.0	130	10.0	34.3	5.14	1.13
13C	1.7	167.0	125	10.0	34.7	7.41	0.85
13D	1.7	167.0	120	30.0	36.7	7.85	1.05

CHAPTER 7.0

EFFECT OF RESIDUAL STRAINS ON THE ELONGATION AT BREAK OF POLYETHYLENE FILMS

7.1 Introduction

This chapter discussed the effect of the residual strains, ϵ_{MD} in the *MD* and ϵ_{TD} in the *TD*, on the elongation at break, *Eb*, of films made from LDPE, LLDPE and blends of the two. The annealing conditions to produce these films are shown in Chapter 6.0.

7.2 Effect of Residual Strains on the Elongation at Break of Low Density Polyethylene Films

The results of increasing ϵ_{TD} (at various levels of ϵ_{MD}) on the *Eb* of LDPE films are shown in Table 7.1 and Figure 7.1. From the plot in Figure 7.1 it can be seen that increasing ϵ_{TD} decreases the elongation at break in *TD*, Eb_{TD}. The elongation at break in *MD*, Eb_{MD}, however, increases with increasing ϵ_{TD}.

The effect of increasing ϵ_{MD} on the *Eb* of LDPE films is shown in Table 7.2 and plotted in Figure 7.2. The results show that Eb_{MD} decreases with increasing ϵ_{MD} and Eb_{TD} increases with increasing ϵ_{MD}.

Table 7.1. Effect of TD residual strain on the elongation at break of LDPE films. The MD residual strain and film thickness were held constant to within the experimental error.

Sample	Residual strain		MD		TD	
	MD	TD	Thickness (10^{-6}m)	Eb (%)	Thickness (10^{-6}m)	Eb (%)
6A	7.82	0.70	33.7	68	36.3	675
6B	7.24	1.27	34.6	114	34.3	654
6C	6.68	1.41	33.3	159	33.3	628
6D	6.87	3.67	32.3	291	30.7	463
6E	12.84	1.19	32.3	78	33.3	674
6F	12.23	1.38	31.7	63	33.3	733
6G	13.04	3.10	31.7	150	31.7	575
6H	12.93	3.66	31.3	167	32.3	611
6I	13.06	7.38	37.3	393	37.7	495
6J	16.05	1.37	37.0	67	35.3	679
6K	16.27	1.84	35.0	78	36.7	666
6L	16.19	4.20	32.3	131	34.0	640
6M	15.47	4.68	33.0	151	33.3	618

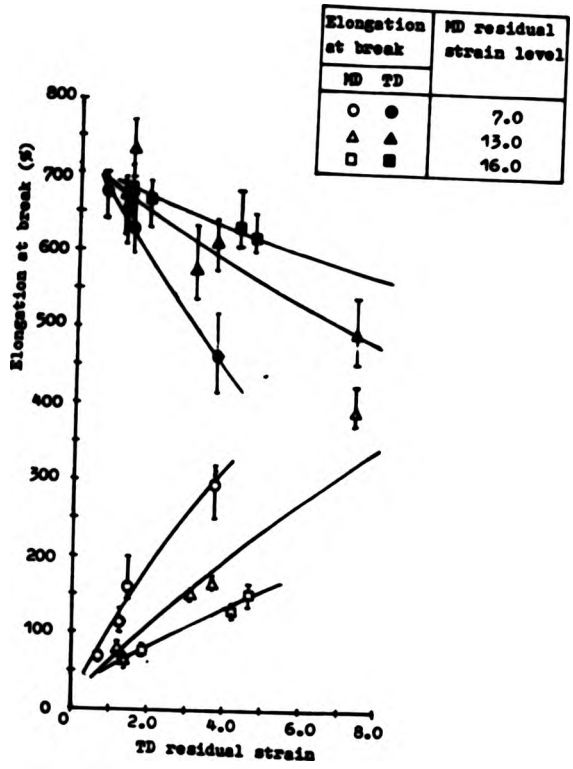

Figure 7.1. Effect of TD residual strain (at constant MD residual strain and thickness) on the elongation at break of LDPE films.

Table 7.2. Elongation at break as a function of MD residual strain of LDPE films. The TD residual strain and film thickness were held constant to within the experimental error.

Sample	Residual strain		MD		TD	
			Thickness	Eb	Thickness	Eb
	MD	TD	(10^{-6}m)	(%)	(10^{-6}m)	(%)
7A	1.75	0.68	36.3	424	35.0	524
7B	4.17	0.51	33.0	200	31.3	672
7C	4.83	0.72	34.0	230	34.7	620
7D	5.94	0.33	34.3	94	34.0	675
7E	3.52	1.40	35.0	423	36.7	535
7F	6.49	1.48	33.3	164	31.7	629
7G	6.68	1.41	33.3	159	33.3	628
7H	16.27	1.84	35.0	78	36.7	666
7I	20.33	1.89	34.0	69	35.0	648
7J	7.05	3.82	32.3	291	30.7	463
7K	9.33	4.71	32.7	312	32.3	445
7L	15.07	4.34	33.7	170	32.3	490
7M	15.49	3.90	31.3	114	31.7	496

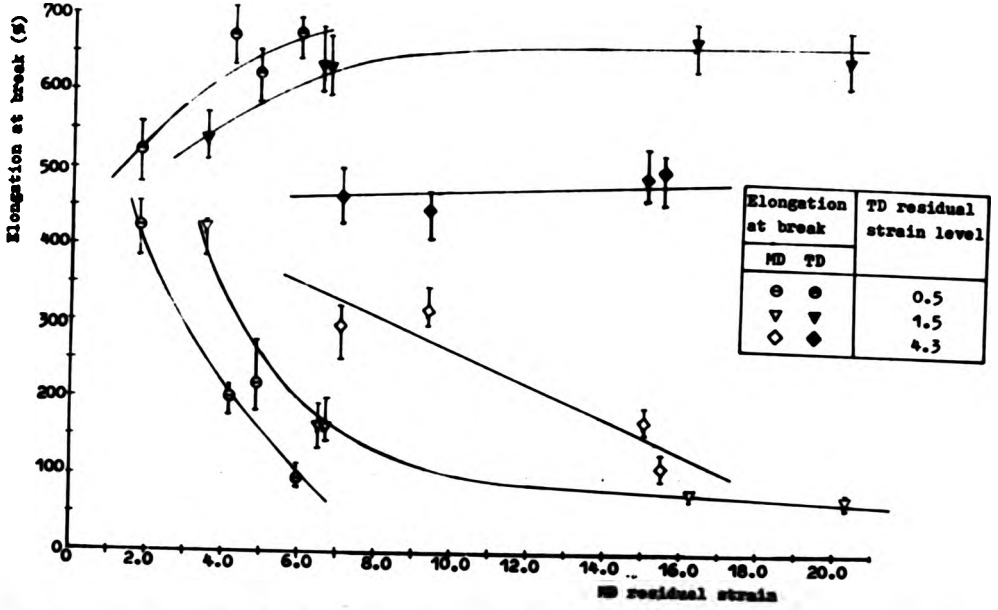

Figure 7.2. Effect of MD residual strain (at constant TD residual strain and thickness) on the elongation at break of LDPE films.

From the plots in Figures 7.1 and 7.2 it could be seen that there is some scatter in the data. This scattering is due to the fact that the thickness of the films varies in the range of 35.0 ± 5 x 10^{6} m. Also the supposed constant level of residual strain value is not exactly constant but varies within 20% of the stated values. The variation in thickness and residual strain results in the variation of the measured *Eb* values.

The *Eb* at the crossover points appears to be in the range of 450-500% in each case. This implies that in a balanced biaxial film the *Eb* is not strongly dependent on the residual strain value at least over the range from 0.5 to 4.3. This is a somewhat surprising observation. More work is needed to explain this.

7.3 Effect of Residual Strains on the Elongation at Break of Blended and Linear Low Density Polyethylene Films

The results of increasing ϵ_{MD} and ϵ_{TD} on the *Eb* of 75% LDPE/25% LLDPE, 25% LDPE/75% LLDPE blend films and LLDPE films are shown in Tables 7.3 to 7.8. These results are plotted in Figures 7.3 to 7.8.

The results show the same trend as observed with LDPE films. The general conclusion that can be drawn from these series of graphs is that:

a) increasing ϵ_{MD} leads to an increase in Eb_{TD} and a

reduction in EB_{MD};

b) increasing ε_{TD} leads to an increase in EB_{MD} and a reduction in EB_{TD}; and

c) increasing LLDPE composition in the blends increases Eb of the films.

Table 7.3. Effect of TD residual strain on the elongation at break of 75% LDPE/25% LLDPE blend films. The MD residual strain and film thickness were kept constant (within experimental error).

Sample	Residual strain		MD		TD	
	MD	TD	Thickness (10^{-6}m)	Eb (%)	Thickness (10^{-6}m)	Eb (%)
8A	9.38	0.60	36.3	112	36.0	854
8B	9.65	0.69	38.7	98	37.0	914
8C	9.42	1.62	35.3	176	38.0	767
8D	9.65	2.07	36.0	182	35.7	750
8E	9.83	2.18	34.7	195	35.0	694

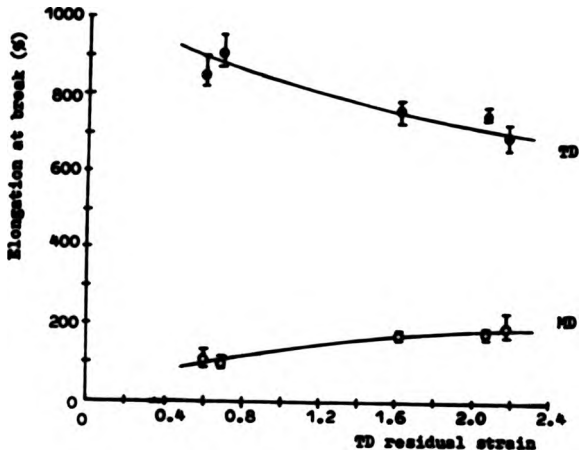

Figure 7.3. Effect of TD residual strain (at constant MD residual strain and thickness) on the elongation at break of 75% LDPE/25% LLDPE blend films.

Table 7.4. Elongation at break as a function of MD residual strain of 75% LDPE/25% LLDPE blend films. The TD residual strain and film thickness were held constant (within experimental error).

Sample	Residual strain		MD		TD	
	MD	TD	Thickness (10^{-6}m)	Eb (%)	Thickness (10^{-6}m)	Eb (%)
9A	5.98	0.92	36.7	312	36.7	754
9B	6.31	1.09	37.0	249	36.3	816
9C	11.49	0.89	37.3	83	38.3	855
9D	12.61	1.06	36.3	70	38.3	885
9E	12.77	1.08	37.3	73	37.0	850

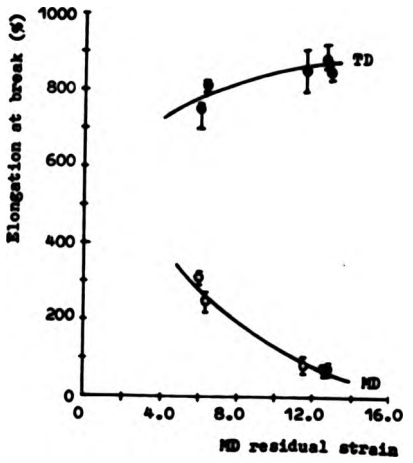

Figure 7.4. Effect of MD residual strain (at constant TD residual strain and thickness) on the elongation at break of 75% LDPE/25% LLDPE blend films.

Table 7.5. Effect of TD residual strain on the elongation at break of 25% LDPE/75% LLDPE blend films. The MD residual strain and film thickness were held constant (within experimental error).

Sample	Residual strain		MD		TD	
	MD	TD	Thickness (10^{-6}m)	Eb (%)	Thickness (10^{-6}m)	Eb (%)
10A	8.95	0.80	37.3	415	37.7	970
10B	9.05	2.01	34.3	615	35.0	930
10C	8.76	2.20	35.7	542	36.3	867
10D	9.40	2.30	34.7	606	33.7	894

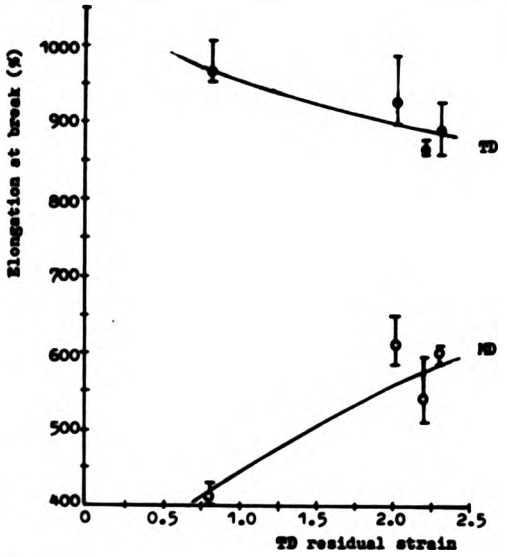

Figure 7.5. Effect of TD residual strain (at constant MD residual strain and thickness) on the elongation at break of 25% LDPE/75% LLDPE blend films.

Table 7.6. Elongation at break as a function of MD residual strain of 25% LDPE/75% LLDPE blend films. The TD residual strain and film thickness were held constant (within experimental error).

Sample	Residual strain		MD		TD	
	MD	TD	Thickness (10^{-6}m)	Eb (%)	Thickness (10^{-6}m)	Eb (%)
11A	4.32	0.98	34.3	656	35.0	867
11B	7.52	0.94	37.3	449	36.3	927
11C	10.47	1.05	37.7	397	38.0	1013
11D	11.26	1.16	37.3	321	37.7	978

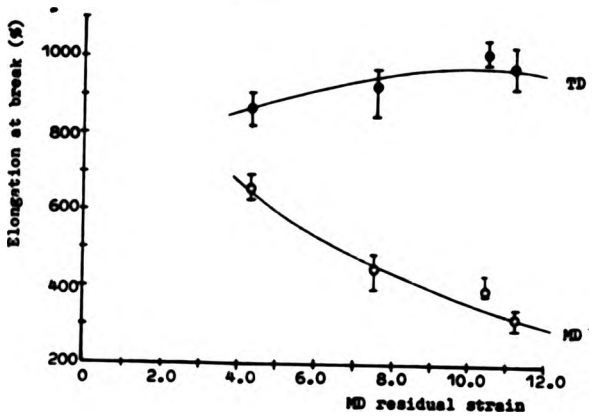

Figure 7.6. Effect of MD residual strain (at constant TD residual strain and thickness) on the elongation at break of 25% LDPE/75% LLDPE blend films.

Table 7.7. Elongation at break as a function of TD residual strain of LLDPE films. The MD residual strain and film thickness were held constant (within experimental error).

Sample	Residual strain		MD		TD	
	MD	TD	Thickness (10^{-6}m)	Eb (%)	Thickness (10^{-6}m)	Eb (%)
12A	6.34	0.68	35.7	542	35.0	988
12B	6.23	0.83	33.7	551	34.0	960
12C	6.31	1.42	34.0	630	35.7	940
12D	6.54	1.47	34.3	592	34.7	923
12E	6.63	1.59	35.7	620	35.3	907

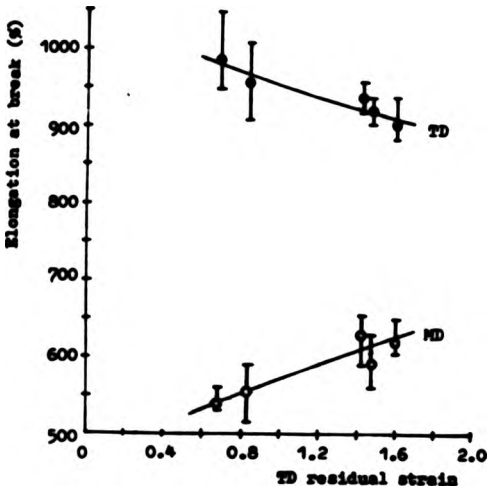

Figure 7.7. Effect of TD residual strain (at constant MD residual strain and thickness) on the elongation at break of LLDPE films.

Table 7.8. Effect of MD residual strain on the elongation at break of LLDPE films. The TD residual strain and film thickness were held constant (within experimental error).

Sample	Residual strain		MD		TD	
	MD	TD	Thickness (10^{-6}m)	Eb (%)	Thickness (10^{-6}m)	Eb (%)
13A	5.01	1.04	33.0	687	33.7	924
13B	5.14	1.13	31.3	691	37.3	956
13C	7.41	0.85	36.0	506	37.0	945
13D	7.85	1.05	36.0	457	38.3	967

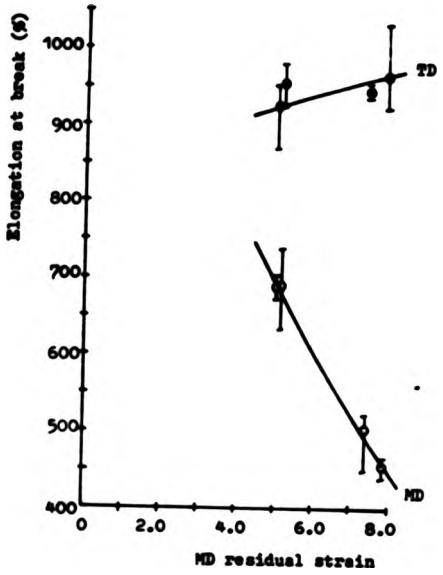

Figure 7.8. Effect of MD residual strain (at constant TD residual strain and thickness) on the elongation at break of LLDPE films.

7.4 Mathematical Model of the Dependance of Elongation at Break on Residual Strains

The results in Tables 7.1 and 7.2, for LDPE films, can be viewed from the perspective of whether the residual strain varies in the direction of the tensile test or at right angles to it.

In Figure 7.9, results from *MD* and *TD* tensile tests are plotted on the same graph, showing the dependence of Eb on the residual strain in the test direction, ϵ_t, for various levels of residual strain in the direction perpendicular to the test direction, ϵ_p.

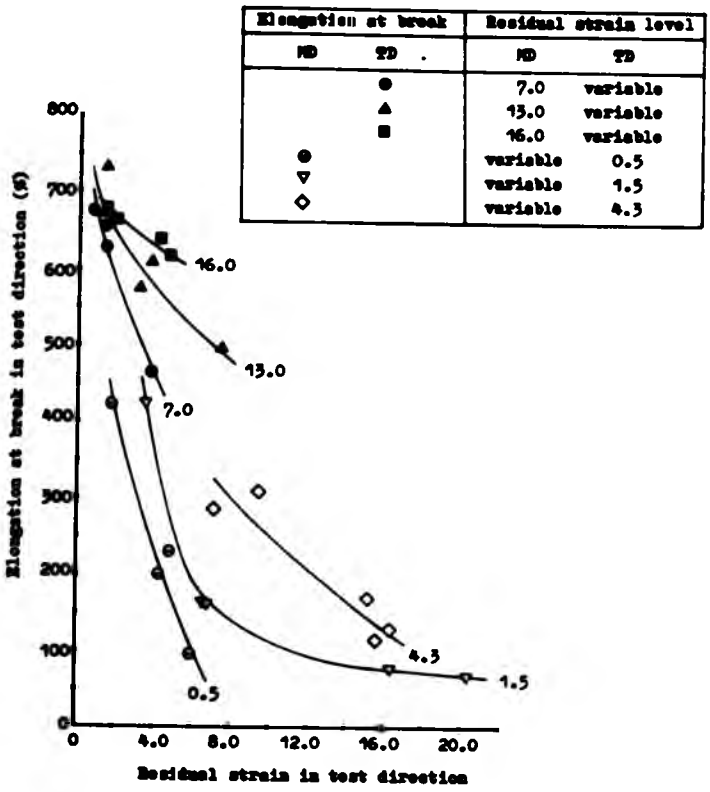

Figure 7.9. Plot of elongation at break against the residual strain in the test direction at various levels of residual strain in the perpendicular direction of LDPE films.

Figure 7.9 shows that the Eb in the test direction, Eb_t, is inversely related to ε_t and is related to ε_p, i.e. the value of Eb_t is a function of $\varepsilon_p/\varepsilon_t$. This is summarised below:

$$Eb_t = \frac{F(\varepsilon_p)}{F(\varepsilon_t)} \qquad (7.1)$$

where $F(\varepsilon)$ is a function of ε which increases with ε.

Assuming, at this stage, that Eb is a function of $\varepsilon_p/\varepsilon_t$ the results in Figures 7.1 and 7.2 can be transformed to give those shown in Table 7.9 and plotted in Figure 7.10. It can be seen that the Eb of all LDPE films falls on one curve and increases with increasing $\varepsilon_p/\varepsilon_t$. The Eb of LDPE films seems to reach a maximum value at around 700%.

Similar results were obtained for the blends of LDPE and LLDPE and for LLDPE films. These results are shown in Figures 7.11 to 7.13.

Table 7.9. Elongation at break as a function of ϵ_p/ϵ_t of LDPE films.

Sample	Residual strain		MD		TD	
	MD	TD	$\epsilon_{TD}/\epsilon_{MD}$	Eb (%)	$\epsilon_{MD}/\epsilon_{TD}$	Eb (%)
6A	7.82	0.70	0.09	68	11.17	675
6B	7.24	1.27	0.17	114	5.70	654
6C	6.68	1.41	0.21	159	4.74	628
6D	6.87	3.67	0.53	291	1.87	463
6E	12.84	1.19	0.09	78	10.79	674
6F	12.23	1.38	0.11	63	8.86	733
6G	13.04	3.10	0.24	150	4.21	575
6H	12.93	3.66	0.28	167	3.54	611
6I	13.06	7.38	0.56	393	1.77	495
6J	16.05	1.37	0.08	67	11.71	679
6K	16.27	1.84	0.11	78	8.84	666
6L	16.19	4.20	0.26	131	3.85	640
6M	15.47	4.68	0.30	151	3.30	618
7A	1.75	0.68	0.39	424	2.57	524
7B	4.17	0.51	0.12	200	8.18	672
7C	4.83	0.72	0.15	230	6.71	620
7D	5.94	0.33	0.05	94	18.00	675
7E	3.52	1.40	0.40	423	2.51	535
7F	6.49	1.48	0.23	164	4.38	629
7G	6.68	1.41	0.21	159	4.74	628
7H	16.27	1.84	0.11	78	8.84	666
7I	20.33	1.89	0.09	69	10.76	648
7J	7.05	3.82	0.54	291	1.84	463
7K	9.33	4.71	0.50	312	1.98	445
7L	15.07	4.34	0.29	170	3.47	490
7M	15.49	3.90	0.25	114	3.97	496

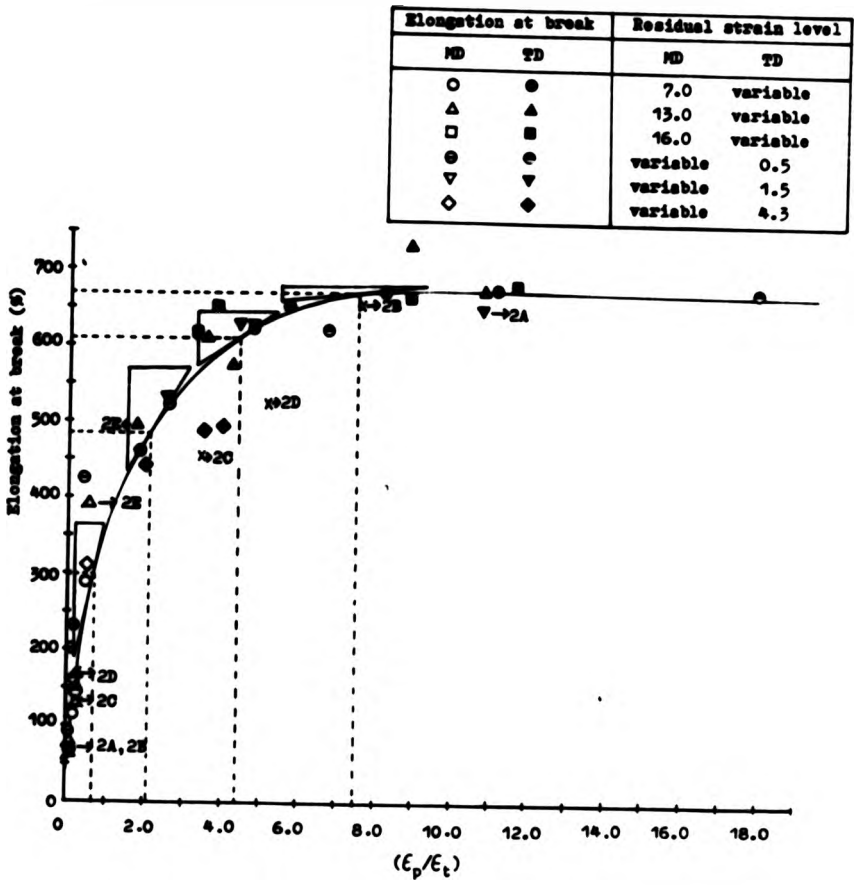

Figure 7.10. Elongation at break as a function of ϵ_p/ϵ_t of LDPE films.

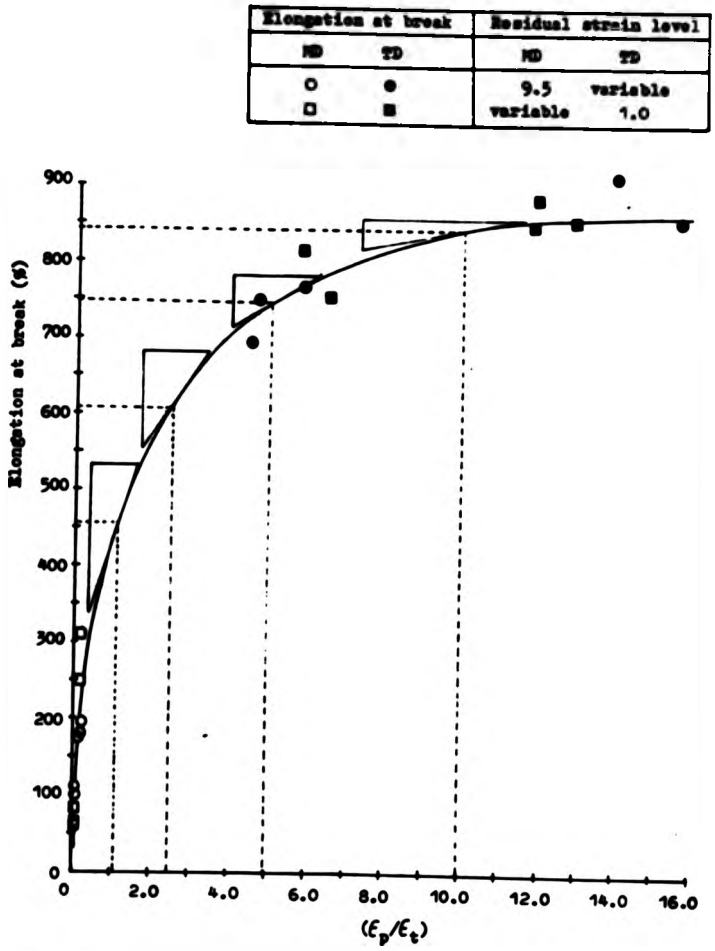

Figure 7.11. Elongation at break as a function of $\varepsilon_p/\varepsilon_t$ of 75% LDPE/25% LLDPE blend films.

Elongation at break		Residual strain level	
MD	TD	MD	TD
○	●	9.0	variable
□	■	variable	1.0

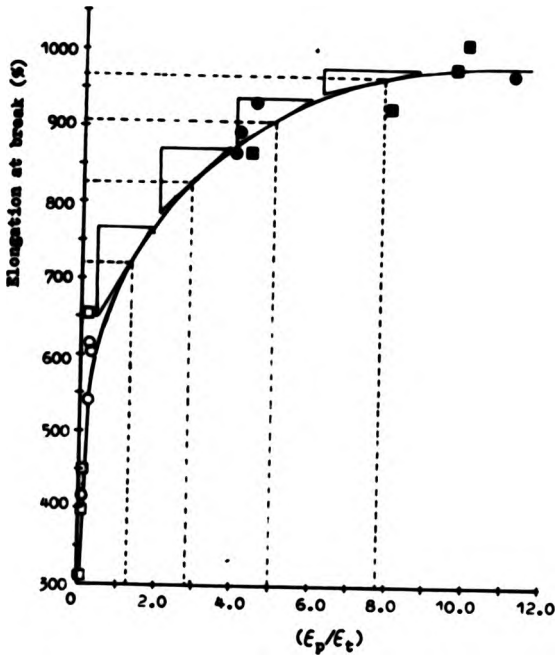

Figure 7.12. Elongation at break as a function of ϵ_p/ϵ_t of 25% LDPE/75% LLDPE blend films.

Elongation at break		Residual strain level	
MD	TD	MD	TD
○	●	6.5	variable
□	■	variable	1.0

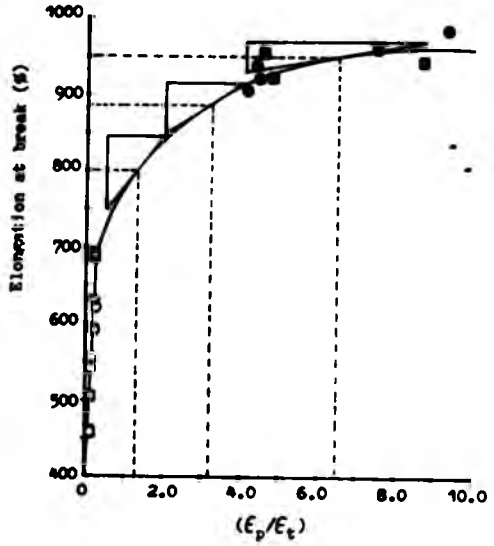

Figure 7.13. Elongation at break as a function of ϵ_p/ϵ_t of LLDPE films.

Curves of the shape shown in Figures 7.10 to 7.13 which appear to approach a limiting value asymptotically can have the form

$$y = a - be^{-kx} \qquad (7.2)$$

Assuming this to be the case here, then:

$$Eb_t = a - be^{-k(\varepsilon_p/\varepsilon_t)}$$

or (7.3)

$$\ln(a - Eb_t) = \ln(b) - k(\varepsilon_p/\varepsilon_t)$$

where a is the maximum value of Eb, Eb_{max}; b is (Eb_{max} - Eb_o) and k is a constant.

The value of Eb_{max} is the Eb value when the curves in Figures 7.10 to 7.13 level off. This value is difficult to estimate accurately from the plots due to scattering. However, it can be more easily estimated by plotting Eb against the slope of several selected points on the curves in Figures 7.10 to 7.13. Plotting Eb against the slope and extrapolating to zero slope will give Eb_{max}.

The results of Eb as a function of the slope of the tangent of all the films investigated in this project are shown in Table 7.10 and plotted in Figure 7.14.

Table 7.10. Elongation at break as a function of the slope of the tangent of LDPE, 75% LDPE/25% LLDPE, 25% LDPE/75% LLDPE and LLDPE films.

Film sample	Elongation at break (%)	Slope (%)
LDPE	305	187
	485	87
	615	36
	670	5
75% LDPE/ 25% LLDPE	455	162
	615	81
	745	35
	840	9
25% LDPE/ 75% LLDPE	720	82
	825	53
	905	28
	965	10
LLDPE	800	63
	890	31
	950	9

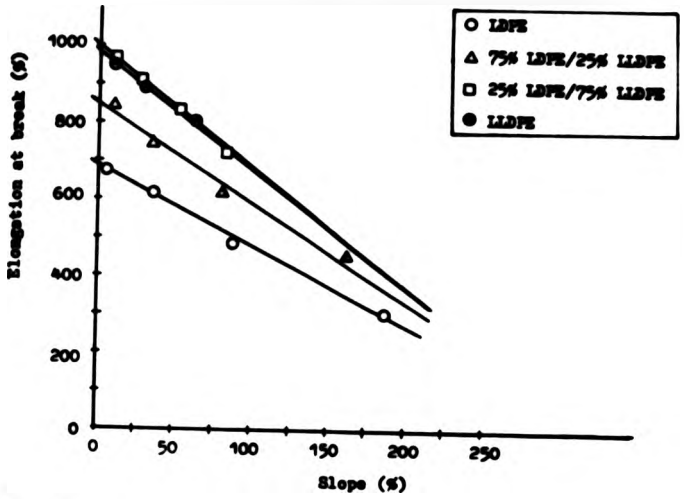

Figure 7.14. Elongation at break as a function of the slope of the tangent of LDPE, LLDPE and blends of LDPE and LLDPE films.

The values of Eb_{max} of all the films are estimated from Figure 7.14 using the linear regression method. These values are tabulated in Table 7.11.

Table 7.11. The values of Eb_{max} of LDPE, 75% LDPE/25% LLDPE, 25% LDPE/75% LLDPE and LLDPE films.

Film sample	Eb_{max} (%)
LDPE	679
75% LDPE/ 25% LLDPE	840
25% LDPE/ 75% LLDPE	1000
LLDPE	975

Using the Eb_{max} values, the values of $\ln(Eb_{max} - Eb_t)$ can be calculated. The values of $\ln(Eb_{max} - Eb_t)$ against ϵ_p/ϵ_t of LDPE films are plotted in Figure 7.15. The results, though scattered, appear to give a linear plot.

The plots of $\ln(Eb_{max} - Eb_t)$ against ϵ_p/ϵ_t for the blend of LDPE and LLDPE and LLDPE films are shown in Figure 7.16 to Figure 7.18. As observed with LDPE films, these films also produce linear plots.

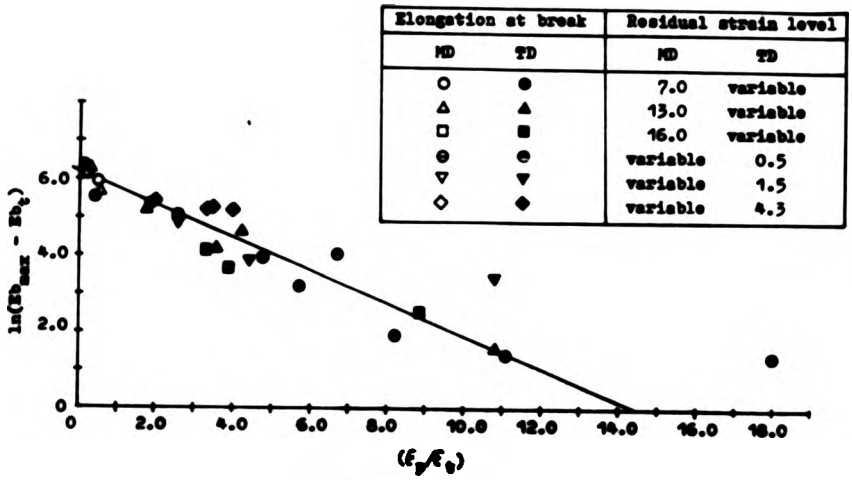

Figure 7.15. Plot of $\ln(Eb_{max} - Eb_t)$ as a function of ϵ_p/ϵ_t of LDPE films.

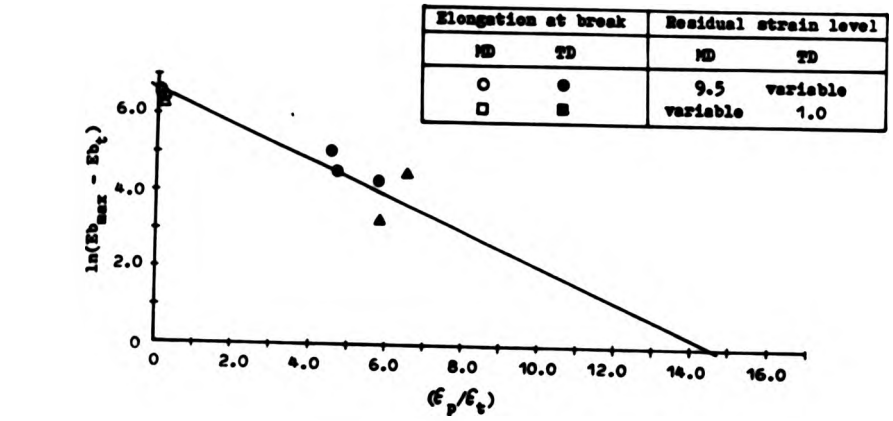

Figure 7.16. Plot of $\ln(Eb_{max} - Eb_t)$ as a function of ϵ_p/ϵ_t of 75% LDPE/25% LLDPE blend films.

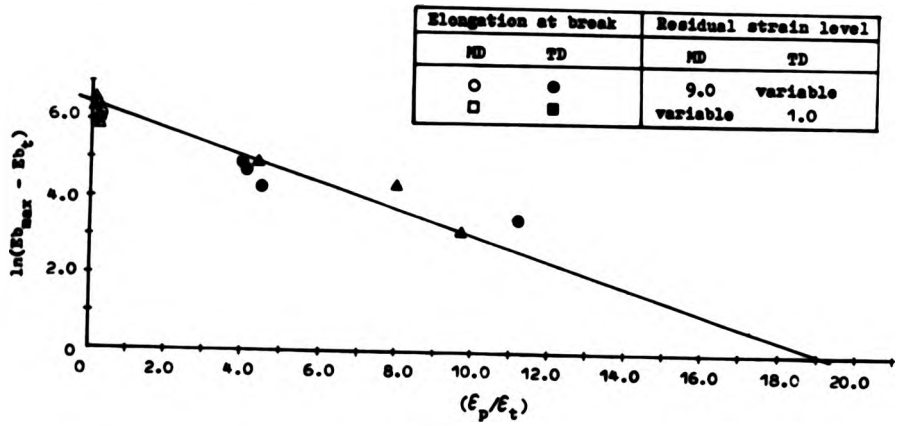

Figure 7.17. Plot of $\ln(Eb_{max} - Eb_t)$ as a function of ϵ_p/ϵ_t of 25% LDPE/75% LLDPE blend films.

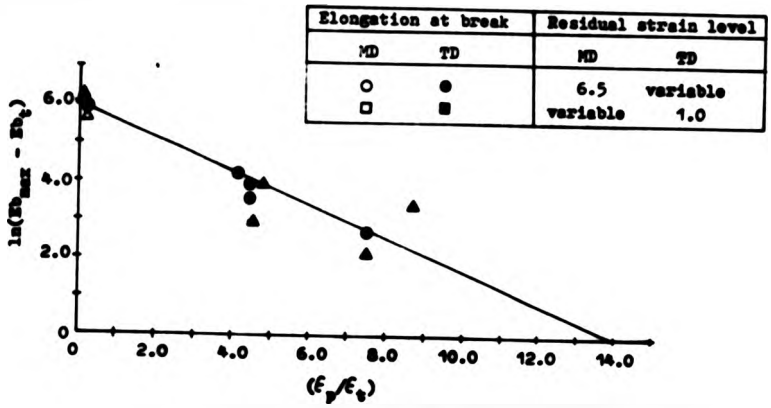

Figure 7.18. Plot of $\ln(Eb_{max} - Eb_t)$ as a function of $\varepsilon_p/\varepsilon_t$ of LLDPE films.

7.5 Test of Model

The values of k and b are evaluated from the logarithmic plot using the linear regression method. The values of Eb_{max}, b, Eb_o and k of all the PE films studied are tabulated in Table 7.12.

Table 7.12. The values of Eb_{max}, b, Eb_o and k of LDPE, LLDPE and blends of LDPE and LLDPE films.

Film sample	Eb_{max} (%)	b (%)	Eb_o (%)	k
LDPE	679	478	201	0.40
75% LDPE/ 25% LLDPE	840	757	83	0.48
25% LDPE/ 75% LLDPE	1000	518	482	0.37
LLDPE	975	564	411	0.49

Using the values of Eb_{max}, b and k shown in Table 7.12, the Eb of several unannealed PE films could be estimated using equation 7.3. The estimated values of Eb of these films are then compared with the measured values of Eb. This comparison is illustrated in Table 7.13 and plotted in Figure 7.19.

Table 7.13. The estimated and measured values of elongation at break of LDPE, LLDPE and blends of LDPE and LLDPE films using the values of Eb_o tabulated in Table 7.12.

Film	Sample	Residual strain		MD		TD	
		MD	TD	Estimated elongation at break (%)	Measured elongation at break (%)	Estimated elongation at break (%)	Measured elongation at break (%)
LDPE	2A	20.33	1.89	218	69	672	648
	2B	19.59	2.60	226	74	655	656
	2C	19.15	5.66	254	129	555	455
	2D	18.25	5.79	258	171	543	525
	2E	13.06	7.38	298	393	443	495
75% LDPE/ 25% LLDPE	3A	18.51	1.91	119	93	833	880
	3B	14.55	3.26	160	204	751	732
25% LDPE/ 75% LLDPE	4A	14.95	1.60	502	332	984	996
	4B	11.60	3.40	535	541	853	897
LLDPE	5A	9.34	1.23	446	468	961	981
	5B	7.52	1.80	473	600	902	876

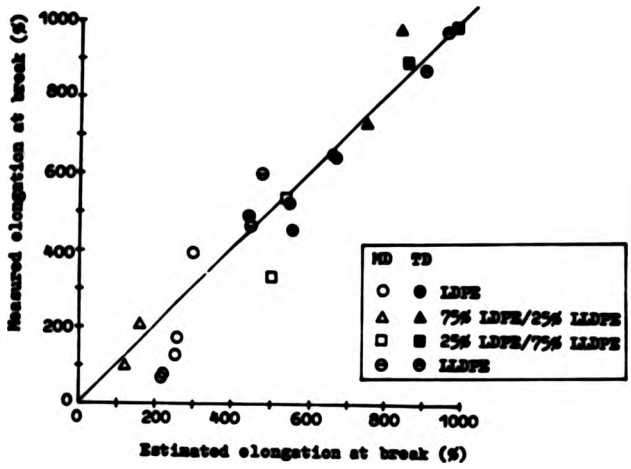

Figure 7.19. Plot of measured elongation at break against the elongation at break estimated using Eb_o values from Table 7.12.

It can be seen from Figure 7.19 that the points are scattered about the 45° line. This means that the estimated values of *Eb* are different from the measured values. The reason for this is due to the unreasonable values of Eb_o.

The values of Eb_o were estimated using the values of Eb_{max}, by the linear regression method. There is error in the values of Eb_{max} which were estimated from the curves that were drawn by a "by eye" method. The error in the estimated values of Eb_{max} is transferred to the estimated values of Eb_o. This results in the higher values of estimated Eb_o.

The value of Eb of the films can be estimated accurately using the values of Eb_o obtained directly from Figures 7.10 to 7.13. The values of Eb_o obtained from Figures 7.10 to 7.13 are shown in Table 7.14.

Table 7.14. The values of Eb_o evaluated from Figures 7.10 to 7.13.

Film sample	Eb_o (%)
LDPE	50
75% LDPE/ 25% LLDPE	50
25% LDPE/ 75% LLDPE	300
LLDPE	450

Table 7.15 and Figure 7.20 show the values of measured Eb and the values of Eb estimated using the values of Eb_{max} and k from Table 7.12 and Eb_o from Table 7.14. It can be seen that the points are less scattered.

Table 7.15. The estimated and measured values of elongation at break of LDPE, LLDPE and blends of LDPE and LLDPE films using the values of Eb_o evaluated from Figures 7.9 to 7.12.

Film	Sample	Residual strain		MD		TD	
		MD	TD	Estimated elongation at break (%)	Measured elongation at break (%)	Estimated elongation at break (%)	Measured elongation at break (%)
LDPE	2A	20.33	1.89	73	69	670	648
	2B	19.59	2.60	82	74	648	656
	2C	19.15	5.66	120	129	516	455
	2D	18.25	5.79	125	171	501	525
	2E	13.06	7.38	177	393	369	495
75% LDPE/ 25% LLDPE	3A	18.51	1.91	88	93	832	880
	3B	14.55	3.26	130	204	747	732
25% LDPE/ 75% LLDPE	4A	14.95	1.60	327	332	978	996
	4B	11.60	3.40	372	541	802	897
LLDPE	5A	9.34	1.23	483	468	962	981
	5B	7.52	1.80	508	600	907	876

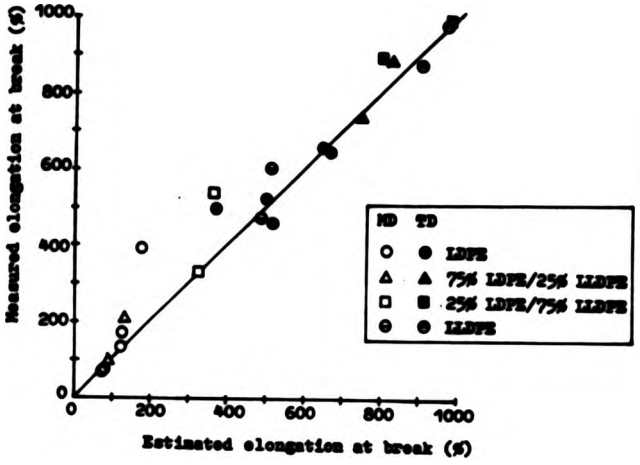

Figure 7.20. Plot of measured elongation at break against the elongation at break estimated using Eb_o values from Table 7.14.

Taking the values of Eb_{max} and k from Table 7.12 and the value of Eb_o from Table 7.14 and equation 7.3, predicted Eb against residual strain curves for LDPE films were drawn. The results are shown in Figures 7.21 and 7.22. From these plots it could be seen that the predicted curves are of the same shape as the measured curves. However, at low residual strain values the predicted curves are lower than the measured curves. The reason for this is not clear, possibly it is due to the inaccuracy in estimating the values of Eb_{max} and k. It could also be seen from Figures 7.21 and 7.22 that the predicted curves

meet at the points corresponding to the same residual strain in both directions. This is expected because at this point Eb_{MD} is equal to Eb_{TD}. However, as mentioned before in section 7.2, the values of Eb at the cross-over points are in the same range eventhough the levels of residual strain are different.

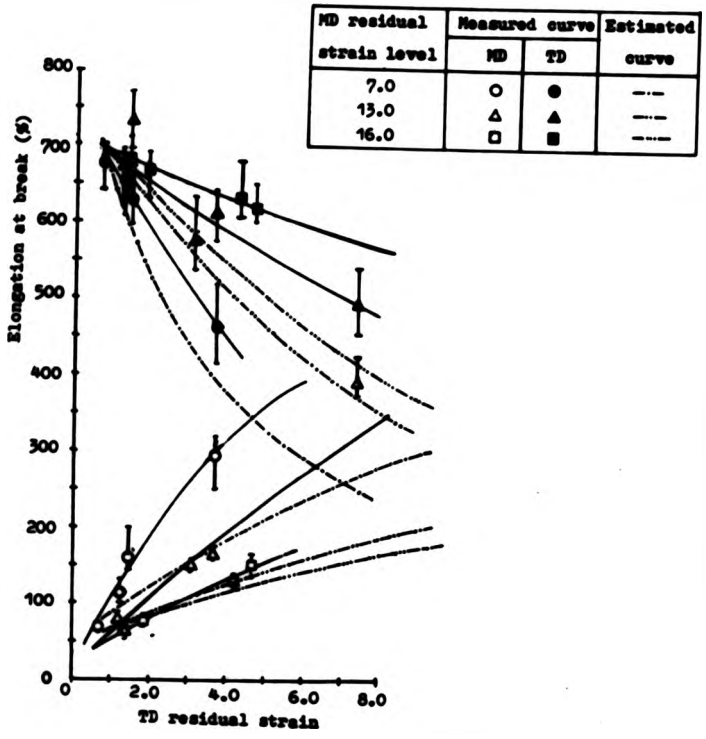

Figure 7.21. Measured and predicted curves of the effect of TD residual strain (at constant MD residual strain and thickness) on the elongation at break of LDPE films.

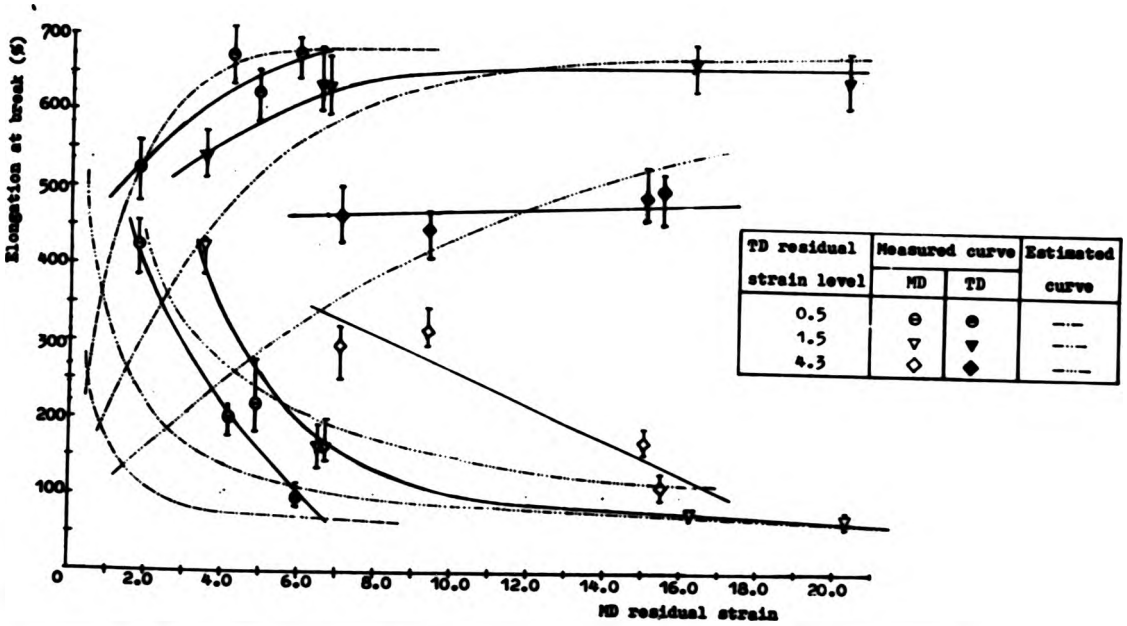

Figure 7.22. Measured and predicted curves of the effect of MD residual strain (at constant TD residual strain and thickness) on the elongation at break of LDPE films.

Using equation 7.3, the effect of changing the values of Eb_{max}, Eb_o and k on the Eb for a range of values of ε_t and ε_p can be studied. This is done by choosing theoretical values of the parameters.

The effect of changing Eb_{max} at constant values of Eb_o and k for a range of values of ε_t and ε_p is shown in Figure 7.23. It can be seen that increasing Eb_{max} shifts the curves vertically.

The effect of increasing Eb_o at constant values of Eb_{max} and k for a range of values of ε_t and ε_p is shown in Figure 7.24. It can be seen that increasing Eb_o for a range of values of ε_t shifts the curve vertically. However, increasing Eb_o for a range of values of ε_p, only increases the initial part of the curves a little.

Increasing the values of k at constant Eb_{max} and Eb_o for a range of values of ε_t and ε_p, shifts the curves vertically. This is shown in Figure 7.25.

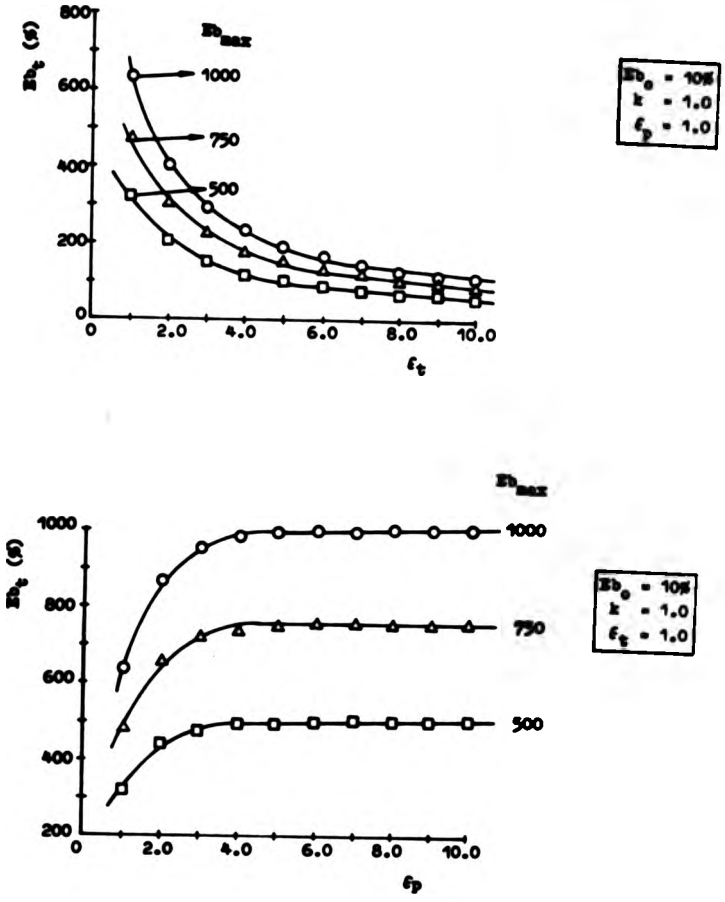

Figure 7.23. Effect of changing Eb_{max} on the Eb_t at constant values of Eb_o and k for a range of values of: (a) ϵ_t and (b) ϵ_p.

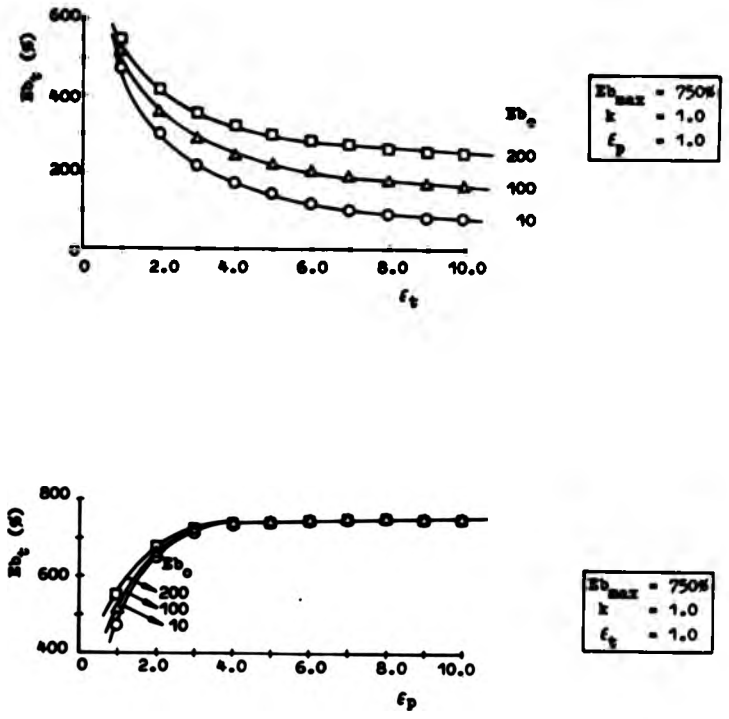

Figure 7.24. Effect of increasing Eb_o on the Eb_t at constant values of Eb_{max} and k for a range of values of: (a) ε_t and (b) ε_p.

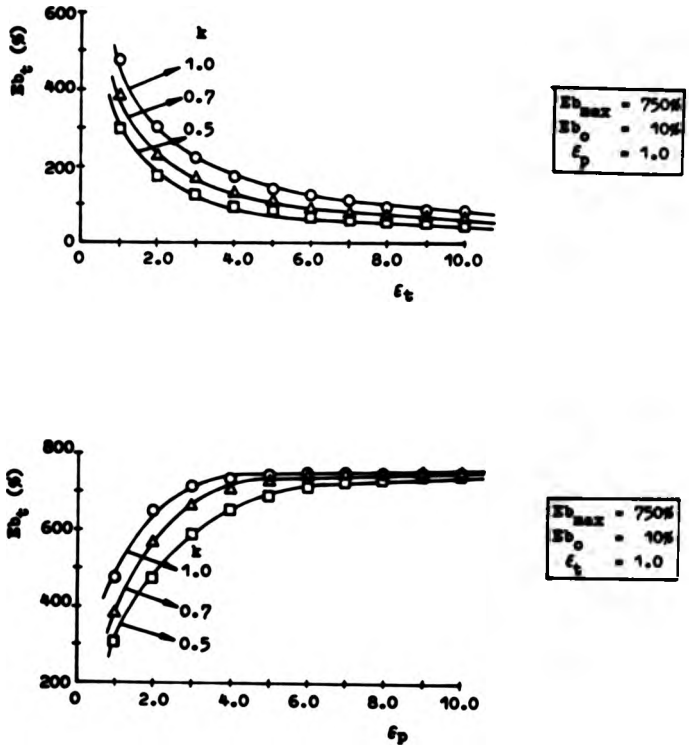

Figure 7.25. Effect of increasing k on the Eb_t at constant values of Eb_{max} and Eb_o for a range of values of: (a) ϵ_t and (b) ϵ_p.

7.6 Discussion

To explain the relationship between E_b and residual strains, we need to understand the stretching process that takes place when the film sample is stretched during tensile testing.

When the film sample is stretched along the direction of orientation during tensile testing, the molecules in the amorphous region will be stretched. When these molecules are fully stretched, lamellae tilting will take place. Unfolding of the folded molecules in the lamellae will follow and these molecules will be incorporated into the amorphous region to form the fibrillar structure. Further stretching of the fibrillar structure will result in the breaking of the molecules and consequently the sample will fail.

The reduction in E_{b_t} with increasing ε_t can be visualised in terms of a simple model of the tie molecules as shown in Figure 7.26. There is more potential for stretching an unstrained tie molecule (low ε_t) than a strained tie molecule (high ε_t). Once the molecules are fully stretched, some additional stretching may occur due to unfolding of the lamellae. However, a component of the total stretching before break will depend on the strain in the tie molecules.

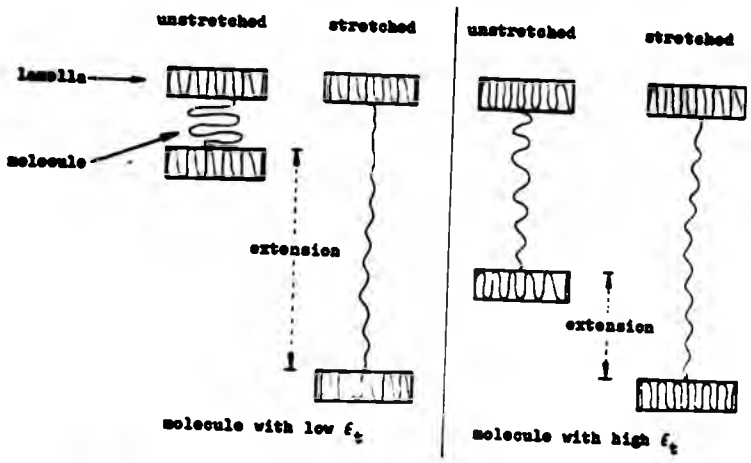

Figure 7.26. Comparison of extension between molecule of low ϵ_t and molecule of high ϵ_t.

The above explanation does not fully explain the relationship between Eb_t and ϵ_p. The dependence of Eb_t on ϵ_p can be explained by considering the orientation of the lamellae in the sample and the mode of deformation associated with a given lamellae orientation during stretching.

The lamellae of the sample with high ϵ_t and very low ϵ_p are oriented in a plane perpendicular to the stretching direction, as shown in Figure 7.27(a). When the sample is stretched, the sample will undergo the same process as explained earlier. However, since the lamellae are oriented in the same direction, they are closer together.

Therefore tilting of lamellae will not be easy and only some of the lamellae will be tilted. The sample will fail due to the breaking of the chains in the amorphous region. Therefore the Eb will be lower.

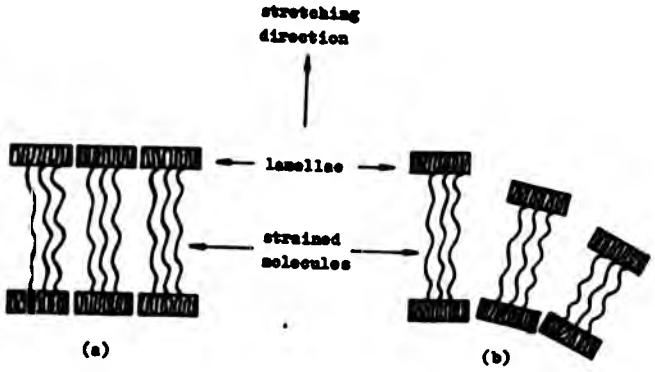

Figure 7.27. Orientation of lamellae in: (a) sample with very low ε_p and (b) sample with some ε_p.

Samples that have some ε_p will have an intermediate orientation. Some of the lamellae of these samples will be oriented at some angle to the stretching direction, Figure 7.27(b). Therefore the lamellae can be tilted easily and unfolding of the folded molecules in the lamellae will take place and thus the samples will have greater Eb.

The above argument also explains why Eb_{TD} is always greater than Eb_{MD}.

Since the Eb of the films also depends on the

crystalline region, the observed relationship between Eb and residual strains may also be due to the different morphology in the films. This is because the samples of various residual strain values were obtained by annealing. The crystallisation conditions that takes place in annealing are different from that encountered in blowing process. The difference in the crystallising conditions could result in the formation of different morphology.

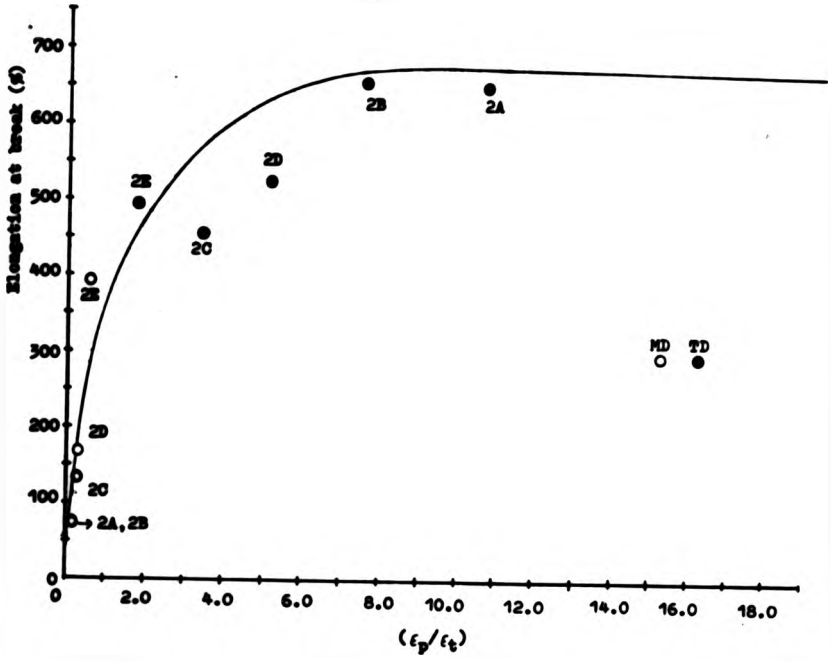

Figure 7.28. Elongation at break of unannealed LDPE films as a function of ϵ_p/ϵ_t.

To show that the relationship obtained is due to

residual strains alone, the Eb of several unannealed LDPE films shown in Table 7.13 is plotted in Figure 7.28 above, points 2A to 2E. The curve taken from Figure 7.10 is also included for comparison, representing the results from the annealed samples. The plot shows that the points are scattered along the curve. This means that the relationship is due to residual strains alone. Otherwise the points may group at some point on the curve because the unannealed films have the same morphology.

Thus the results based largely on annealed samples can also be applied to unannealed samples.

The increase in Eb with LLDPE composition in the blend is due to the linear structure of LLDPE. Linear structure will result in less entanglement between the tie molecules and therefore the molecules can slide over each other easily. LDPE resin has a long chain branched structure and therefore entanglements will take place. Entangled molecules will not be stretched evenly and some part will be stretched more that the other. Therefore the part that is being stretched more will break quicker and results in low Eb of the films.

The plots of Eb_t against $\varepsilon_p/\varepsilon_t$ of the films under investigation showed that the Eb reached a terminal value after certain $\varepsilon_p/\varepsilon_t$ value. This is because the residual strain has a limiting value after which it cannot increase anymore. At this limiting value of residual strain, the molecules could not be extended anymore and thus limits

the Eb of the films.

The values of Eb_{max} and Eb_o increased with increasing LLDPE composition in the film, Table 7.12. This is expected because LLDPE-rich films have greater Eb than LDPE-rich films.

The value of the constant k represents the rate at which Eb_o changes to Eb_{max}. The value seems not to be affected by blending. This means that the rate of change of Eb_o to Eb_{max} is also not affected by blending and the rate seems to be the same for all the films studied.

CHAPTER 8.0

EFFECT OF RESIDUAL STRAINS ON THE TENSILE STRENGTH OF POLYETHYLENE FILMS

8.1 Introduction

The effect of residual strain in the *MD*, ε_{MD}, and in the *TD*, ε_{TD}, on the tensile strength, *TS*, of LDPE, LLDPE and blends of LDPE and LLDPE films is discussed in this chapter.

8.2 Effect of Residual Strains on the Tensile Strength of Low Density Polyethylene Films

Table 8.1 shows the results of *TS* of LDPE films as a function of ε_{TD}. These results are plotted in Figure 8.1. It can be seen that the effect of increasing ε_{TD} is to increase the TS_{TD} of the LDPE films and to reduce the TS_{MD} of the films.

The effect of increasing ε_{MD} on the *TS* of LDPE film is shown in Table 8.2 and Figure 8.2. The effect of increasing ε_{MD} on the *TS* of LDPE films is to increase the TS_{MD} and to reduce TS_{TD} of the films.

Table 8.1. Tensile strength of LDPE films as a function of TD residual strain. The MD residual strain and film thickness were kept constant (within experimental error).

Sample	Residual strain		MD		TD	
	MD	TD	Thickness (10^{-6} m)	Tensile strength (10^6 N/m^2)	Thickness (10^{-6} m)	Tensile strength (10^6 N/m^2)
6A	7.82	0.70	33.7	48.73	36.3	10.40
6B	7.24	1.27	34.6	18.74	34.3	11.88
6C	6.68	1.41	33.3	18.56	33.3	14.62
6D	6.87	3.67	32.3	14.36	30.7	14.99
6E	12.84	1.19	32.3	51.38	33.3	12.62
6F	12.23	1.38	31.7	42.98	33.3	13.77
6G	13.04	3.10	31.7	32.12	31.7	18.70
6H	12.93	3.66	31.3	32.35	32.3	21.34
6I	13.06	7.38	37.3	24.14	37.7	24.45
6J	16.05	1.37	37.0	53.75	35.3	10.59
6K	16.27	1.84	35.0	50.13	36.7	13.48
6L	16.19	4.20	32.3	31.15	34.0	13.85
6M	15.47	4.68	33.0	32.28	33.3	19.03

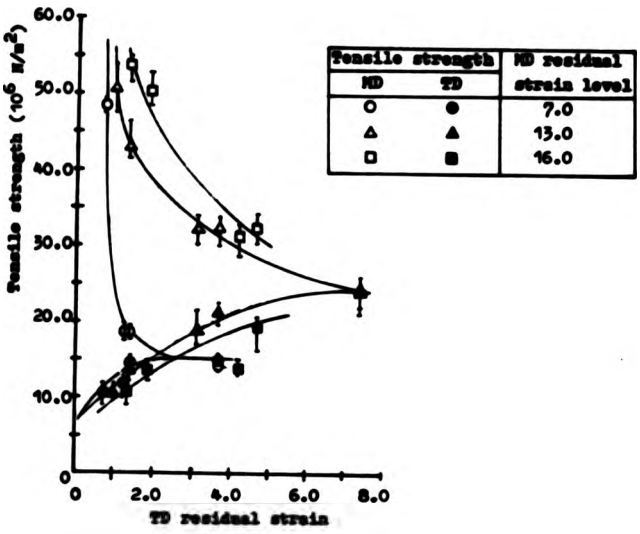

Figure 8.1. Effect of TD residual strain (at constant MD residual strain and thickness) on the tensile strength of LDPE films.

Table 8.2. Effect of MD residual strain on the tensile strength of LDPE films. The TD residual strain and film thickness were kept constant (within experimental error).

Sample	Residual strain		MD		TD	
	MD	TD	Thickness (10^{-6} m)	Tensile strength (10^6 N/m^2)	Thickness (10^{-6} m)	Tensile strength (10^6 N/m^2)
7A	1.75	0.68	36.3	17.36	35.0	13.61
7B	4.17	0.51	33.0	22.82	31.3	12.07
7C	4.83	0.72	34.0	25.00	34.7	12.13
7D	5.94	0.33	34.3	32.68	34.0	9.36
7E	3.52	1.40	35.0	15.16	36.7	13.13
7F	6.49	1.48	33.3	20.98	31.7	11.53
7G	6.68	1.41	33.3	18.56	33.3	14.62
7H	16.27	1.84	35.0	50.13	36.7	13.48
7I	20.33	1.89	34.0	52.99	35.0	11.95
7J	7.05	3.82	32.3	14.36	30.7	14.99
7K	9.33	4.71	32.7	20.14	32.3	16.97
7L	15.07	4.34	33.7	31.88	32.3	18.25
7M	15.49	3.90	31.3	31.28	31.7	16.62

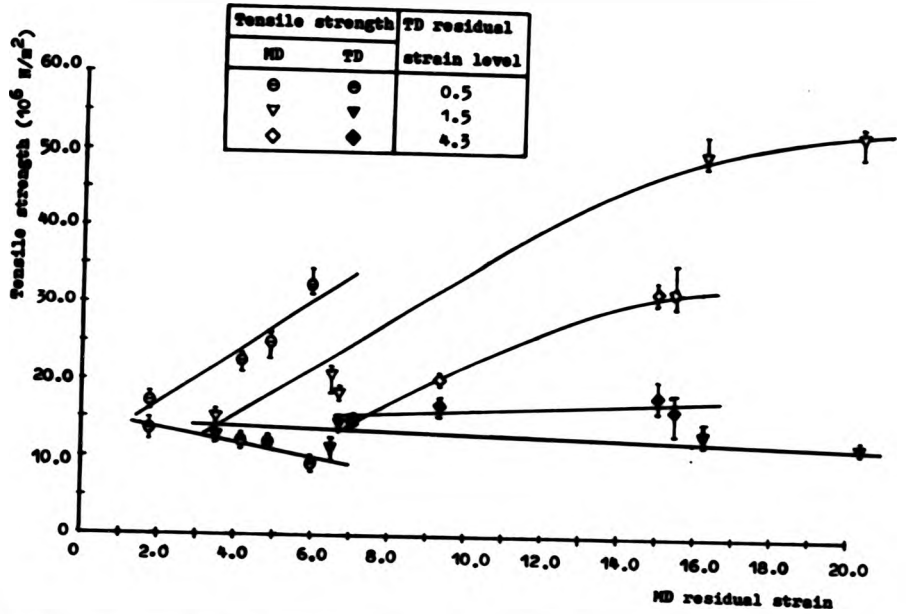

Figure 8.2. Effect of MD residual strain (at constant TD residual strain and thickness) on the tensile strength of LDPE films.

8.3 Effect of Residual Strains on the Tensile Strength of Blended Films and Linear Low Density Polyethylene Films

The results of increasing ε_{MD} and ε_{TD} on the tensile strength of 75% LDPE/25% LLDPE, 25% LDPE/75% LLDPE blend films and LLDPE films are shown in Tables 8.3 to 8.8. These results are plotted in Figures 8.3 to 8.8.

The results show the same trend as observed with LDPE films. Although there is some scatter, the general conclusion of this series of graphs is that:

a) increasing ε_{MD} leads to an increase in TS_{MD} and a slight reduction in TS_{TD};

b) increasing ε_{TD} leads to an increase in TS_{TD} and a reduction in TS_{MD}; and

c) increasing LLDPE composition in the blends increases TS of the films.

Table 8.3. Tensile strength of 75% LDPE/25% LLDPE blend films as a function of TD residual strain. The MD residual strain and film thickness were kept constant (within experimental limits).

Sample	Residual strain		MD		TD	
	MD	TD	Thickness (10^{-6} m)	Tensile strength (10^6 N/m^2)	Thickness (10^{-6} m)	Tensile strength (10^6 N/m^2)
8A	9.38	0.60	36.3	26.34	36.0	14.55
8B	9.65	0.69	38.7	33.15	37.0	15.12
8C	9.42	1.62	35.3	26.86	38.0	17.06
8D	9.65	2.07	36.0	30.32	35.7	17.95
8E	9.83	2.18	34.7	28.60	35.0	16.62

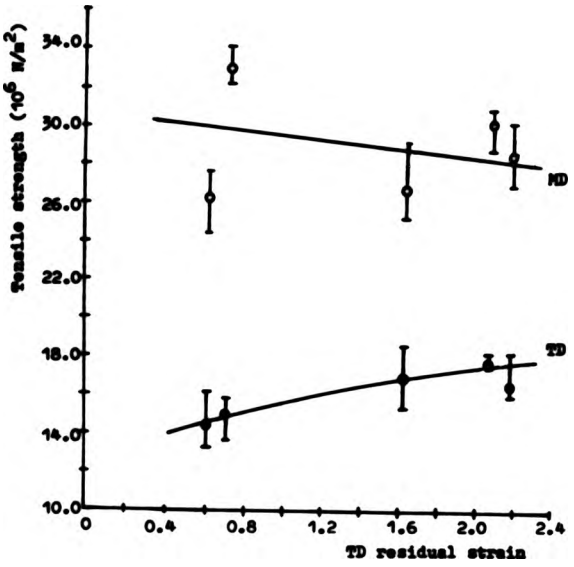

Figure 8.3. Effect of TD residual strain (at constant MD residual strain and thickness) on the tensile strength of 75% LDPE/25% LLDPE blend films.

Table 8.4. Effect of MD residual strain on the tensile strength of 75% LDPE/25% LLDPE blend films. The TD residual strain and film thickness were kept constant (within experimental limits).

Sample	Residual strain		MD		TD	
	MD	TD	Thickness (10^{-6} m)	Tensile strength (10^6 N/m^2)	Thickness (10^{-6} m)	Tensile strength (10^6 N/m^2)
9A	5.98	0.92	36.7	21.13	36.7	14.27
9B	6.31	1.09	37.0	22.50	36.3	17.33
9C	11.49	0.89	37.3	37.01	38.3	12.78
9D	12.61	1.06	36.3	40.06	38.3	13.95
9E	12.77	1.08	37.3	41.02	37.0	14.25

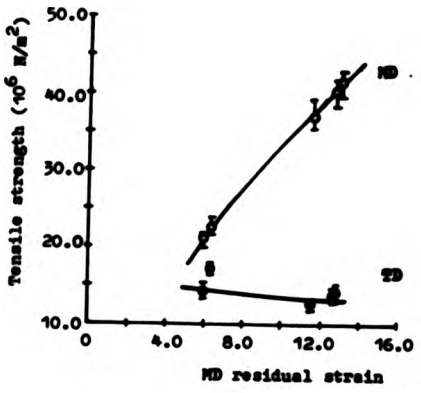

Figure 8.4. Effect of MD residual strain (at constant TD residual strain and thickness) on the tensile strength of 75% LDPE/25% LLDPE blend films.

Table 8.5. Tensile strength of 25% LDPE/75% LLDPE blend films as a function of TD residual strain. The MD residual strain and film thickness were kept constant (within experimental limits).

Sample	Residual strain		MD		TD	
	MD	TD	Thickness (10^{-6} m)	Tensile strength (10^6 N/m^2)	Thickness (10^{-6} m)	Tensile strength (10^6 N/m^2)
10A	8.95	0.80	37.3	41.67	37.7	26.01
10B	9.05	2.01	34.3	38.48	35.0	30.07
10C	8.76	2.20	35.7	37.47	36.3	33.19
10D	9.40	2.30	34.7	39.18	33.7	31.65

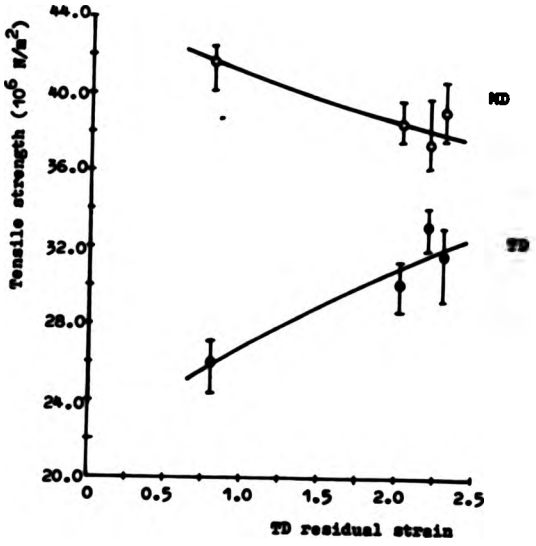

Figure 8.5. Effect of TD residual strain (at constant MD residual strain and thickness) on the tensile strength of 25% LDPE/75% LLDPE blend films.

Table 8.6. Tensile strength of 25% LDPE/75% LLDPE blend films as a function of MD residual strain. The TD residual strain and film thickness were kept constant (within experimental limits).

Sample	Residual strain		MD		TD	
	MD	TD	Thickness (10^{-6} m)	Tensile strength (10^6 N/m^2)	Thickness (10^{-6} m)	Tensile strength (10^6 N/m^2)
11A	4.32	0.98	34.3	34.01	35.0	25.59
11B	7.52	0.94	37.3	47.16	36.3	25.89
11C	10.47	1.05	37.7	50.08	38.0	25.65
11D	11.26	1.16	37.3	48.96	37.7	25.19

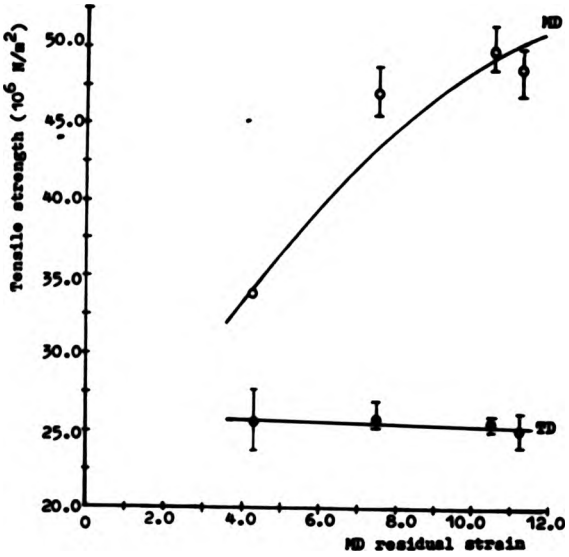

Figure 8.6. Effect of MD residual strain (at constant TD residual strain and thickness) on the tensile strength of 25% LDPE/75% LLDPE blend films.

Table 8.7. Tensile strength of LLDPE films as a function of TD residual strain. The MD residual strain and film thickness were kept constant (within experimental limits).

Sample	Residual strain		MD		TD	
	MD	TD	Thickness (10^{-6} m)	Tensile strength (10^6 N/m^2)	Thickness (10^{-6} m)	Tensile strength (10^6 N/m^2)
12A	6.34	0.68	35.7	51.79	35.0	34.64
12B	6.23	0.83	33.7	51.75	34.0	34.12
12C	6.31	1.42	34.0	50.35	35.7	38.18
12D	6.54	1.47	34.3	49.36	34.7	38.15
12E	6.63	1.59	35.7	48.97	35.3	38.66

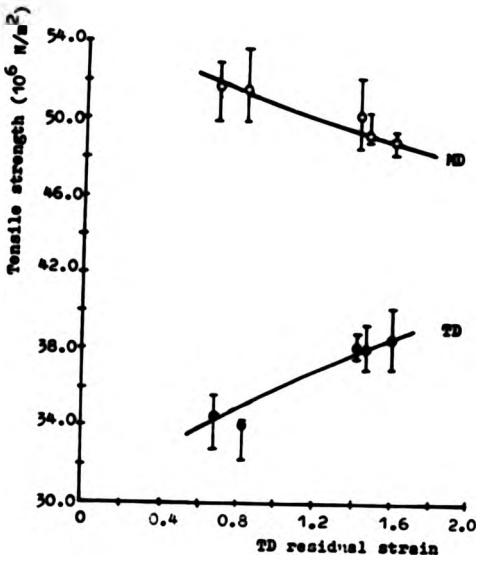

Figure 8.7. Effect of TD residual strain (at constant MD residual strain and thickness) on the tensile strength of LLDPE films.

Table 8.8. Tensile strength of LLDPE films as a function of MD residual strain. The TD residual strain and film thickness were kept constant (within experimental limits).

Sample	Residual strain		MD		TD	
	MD	TD	Thickness (10^{-6} m)	Tensile strength (10^6 N/m^2)	Thickness (10^{-6} m)	Tensile strength (10^6 N/m^2)
13A	5.01	1.04	33.0	45.76	33.7	35.15
13B	5.14	1.13	31.3	43.24	37.3	33.84
13C	7.41	0.85	36.0	49.85	37.0	32.91
13D	7.85	1.05	36.0	53.54	38.3	32.94

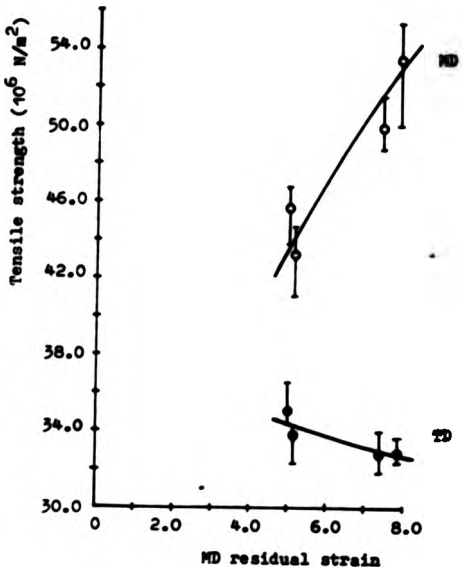

Figure 8.8. Effect of MD residual strain (at constant TD residual strain and thickness) on the tensile strength of LLDPE films.

8.4 Mathematical Model of the Dependance of Tensile Strength on the Residual Strains

The effect of residual strain on the tensile strength of the films can be clearly shown by plotting the tensile strength in the test direction, TS_t, against the residual strain in the test direction, ε_t, for several levels of residual strain in the perpendicular direction, ε_p. Figure 8.9 shows the above plot for LDPE films, from the results shown in Tables 8.1 and 8.2.

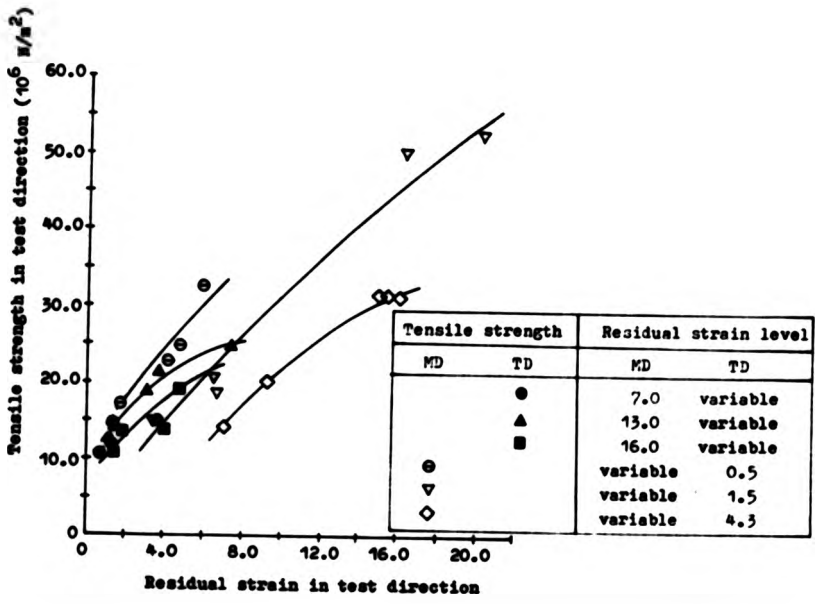

Figure 8.9. Plot of tensile strength in the test direction against residual strain in the test direction of LDPE films at several levels of residual strain in the perpendicular direction.

The general trend that is observed with the results is that TS_t increases with increasing ε_t but reduces with increasing ε_p. This is true for both *MD* and *TD* tests. However, the results in the two directions do not obviously tie in with each other even though they both exhibit the trend just described. However, an attempt is made to model their behaviour.

It can be stated that:

$$TS_t = \frac{F(\varepsilon_t)}{F(\varepsilon_p)} \qquad (8.1)$$

where $F(\varepsilon)$ indicates a function of ε that increases with ε.

As a first approximation it was assumed that TS_t depends on $(\varepsilon_t/\varepsilon_p)$. This was not satisfactory as TS_t is more strongly dependent on ε_t than ε_p. The following relationship was considered:

$$TS_t \text{ versus } (\varepsilon^2{}_t/\varepsilon_p) \qquad (8.2)$$

The TS_t as a function of $\varepsilon^2{}_t/\varepsilon_p$ of LDPE films is shown in Table 8.9 and plotted in Figure 8.10. It can be seen that the plot correlates all *MD* results reasonably well. It also correlates *TD* results but the *MD* and *TD* results do not correlate with each other. The TS_t seems to increase to a limiting value. This limiting value is

expected to correspond to the *TS* when the molecules in the test direction are fully stretched, i.e. uniaxially oriented sample.

The plot in Figure 8.10 shows that TS_{MD} and TS_{TD} do not appear to fall on the same curve. The curve for TS_{TD} is steeper than that for TS_{MD}. Therefore two separate curves are drawn for the *MD* and the *TD* data. This is shown in Figures 8.11 and 8.12.

Similar pairs of curves were obtained for LLDPE and blend films. These curves are shown in Figures 8.13 to 8.18.

Table 8.9. Tensile strength of LDPE films as a function of ϵ^2_t/ϵ_p .

Sample	Residual strain		MD		TD	
	MD	TD	$\epsilon^2_{MD}/\epsilon_{TD}$	Tensile strength (10^6 N/m^2)	$\epsilon^2_{TD}/\epsilon_{MD}$	Tensile strength (10^6 N/m^2)
6A	7.82	0.70	87.35	48.73	0.06	10.40
6B	7.24	1.27	41.27	18.74	0.21	11.88
6C	6.68	1.41	31.66	18.56	0.30	14.62
6D	6.87	3.67	12.85	14.36	1.94	14.99
6E	12.84	1.19	138.54	51.38	0.11	12.62
6F	12.23	1.38	108.36	42.98	0.15	13.77
6G	13.04	3.10	54.90	32.12	0.74	18.70
6H	12.93	3.66	45.68	32.35	1.04	21.34
6I	13.06	7.38	23.12	24.14	4.13	24.45
6J	16.05	1.37	187.94	53.75	0.11	10.59
6K	16.27	1.84	143.83	50.13	0.20	13.48
6L	16.19	4.20	62.33	31.15	1.09	13.85
6M	15.47	4.68	51.05	32.28	1.40	19.03
7A	1.75	0.68	4.50	17.36	0.26	13.61
7B	4.17	0.51	34.11	22.82	0.06	12.07
7C	4.83	0.72	32.41	25.00	0.11	12.13
7D	5.94	0.33	106.92	32.68	0.02	9.36
7E	3.52	1.40	8.83	15.16	0.56	13.13
7F	6.49	1.48	28.43	20.98	0.34	11.53
7G	6.68	1.41	31.66	18.56	0.30	14.62
7H	16.27	1.84	143.83	50.13	0.20	13.48
7I	20.33	1.89	218.68	52.99	0.17	11.95
7J	7.05	3.82	12.97	14.36	2.06	14.99
7K	9.33	4.71	18.47	20.14	2.35	16.97
7L	15.07	4.34	52.29	31.88	1.26	18.25
7M	15.49	3.90	61.49	31.28	0.97	16.62

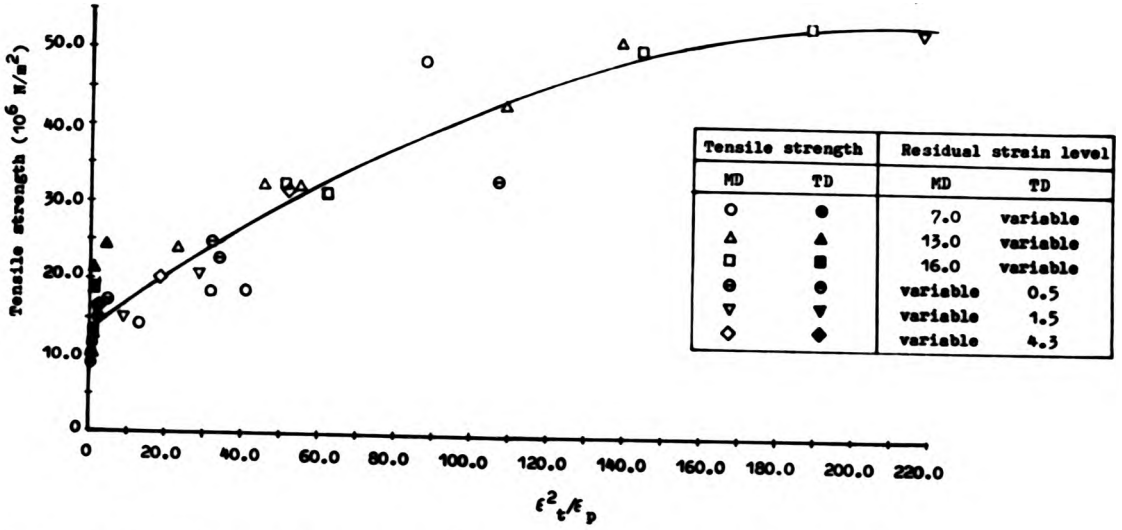

Figure 8.10. Tensile strength of LDPE films as a function of ϵ^2_t/ϵ_p .

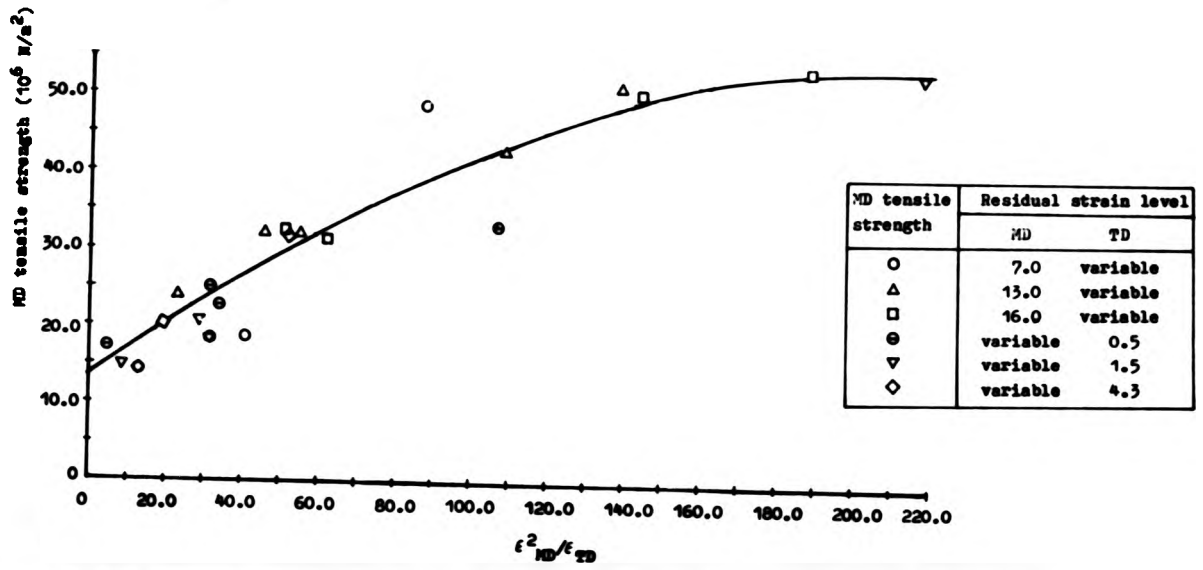

Figure 8.11. Tensile strength in MD of LDPE films as a function of $\epsilon^2_{MD}/\epsilon_{TD}$.

TD tensile strength	Residual strain level	
	MD	TD
●	7.0	variable
▲	13.0	variable
■	16.0	variable
●	variable	0.5
▼	variable	1.5
◆	variable	4.3

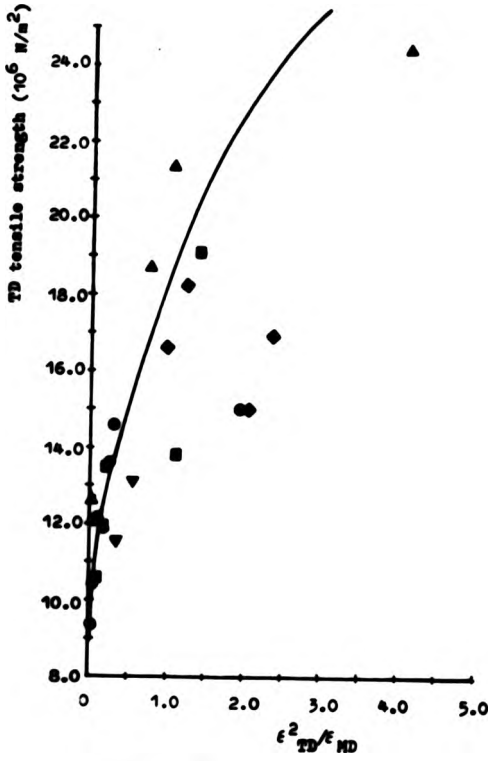

Figure 8.12. Tensile strength in TD of LDPE films as a function of $\epsilon^2_{TD}/\epsilon_{MD}$.

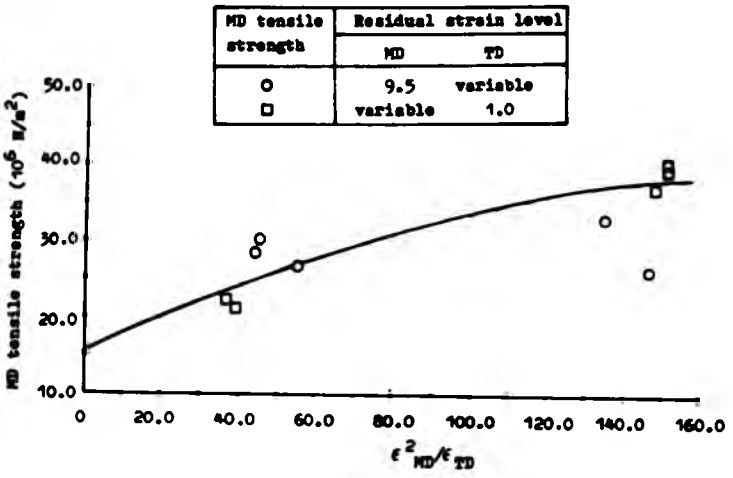

Figure 8.13. Tensile strength in MD of 75% LDPE/25% LLDPE blend films as a function of $\epsilon^2_{MD}/\epsilon_{TD}$.

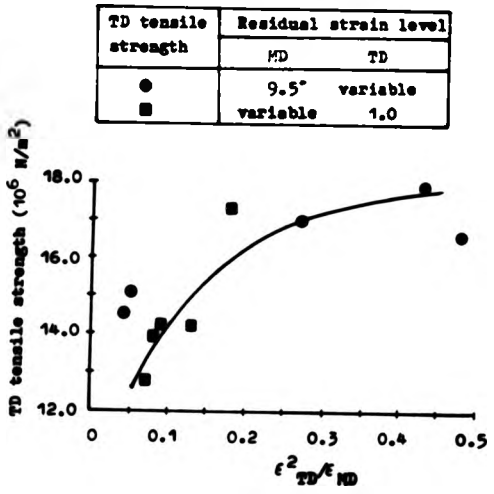

Figure 8.14. Tensile strength in TD of 75% LDPE/25% LLDPE blend films as a function of $\epsilon^2_{TD}/\epsilon_{MD}$.

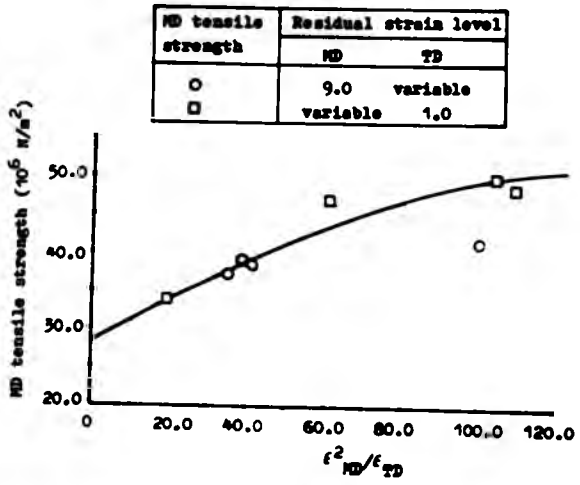

Figure 8.15. Tensile strength in MD of 25% LDPE/75% LLDPE blend films as a function of $\epsilon^2_{MD}/\epsilon_{TD}$.

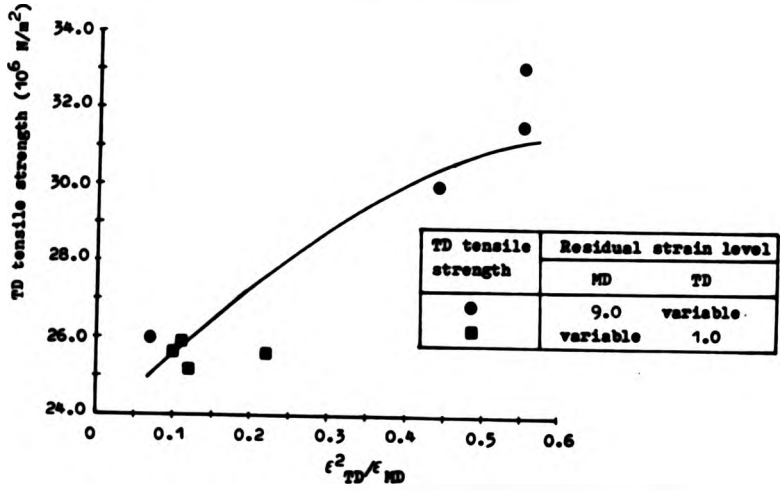

Figure 8.16. Tensile strength in TD of 25% LDPE/75% LLDPE blend films as a function of $\epsilon^2_{TD}/\epsilon_{MD}$.

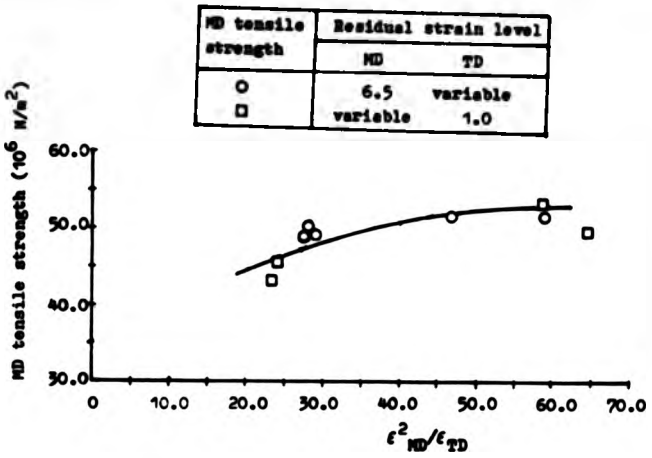

Figure 8.17. Tensile strength in MD of LLDPE films as a function of $\epsilon^2_{MD}/\epsilon_{TD}$.

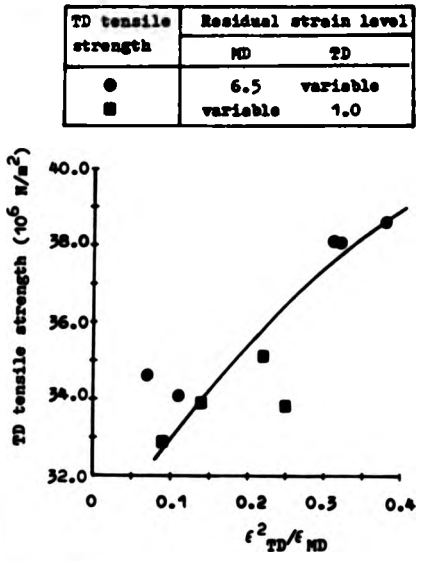

Figure 8.18. Tensile strength in TD of LLDPE films as a function of $\epsilon^2_{TD}/\epsilon_{MD}$.

It was thought that the curves obtained might have the following relationship; i.e. are similar to that found for the *Eb* results except that in this case the appropriate residual strain function is $x = \varepsilon^2_t/\varepsilon_p$.

$$TS_t = a - be^{-kx} \qquad (8.3)$$

where *a*, *b* and *k* are the constants.

Doing the same treatment as shown in Chapter 7.0 to equation 8.3 results in:

$$TS_t = TS_{max} - be^{-k(\varepsilon^2_t/\varepsilon_p)} \qquad (8.4)$$

Rearranging equation 8.4 and taking logarithms results in:

$$\ln(TS_{max} - TS_t) = \ln(b) - k(\varepsilon^2_t/\varepsilon_p) \qquad (8.5)$$

If equation 8.5 applies to the results obtained then the plot of $\ln(TS_{max} - TS_t)$ against $\varepsilon^2_t/\varepsilon_p$ will be linear.

Before this can be checked, a value for TS_{max} must be established. The value of TS_{max} is estimated from the slopes of the TS_t against $\varepsilon^2_t/\varepsilon_p$ curve in the same manner as used in Chapter 7.0 for *Eb* results. Only a single value of TS_{max} is evaluated for each film sample because the value of TS_{max} for the *MD* and the *TD* should be the same.

This is because TS_{max} is taken to represent the value of *TS* of a sample with very high residual strain in the test direction and very low residual strain in the perpendicular direction, i.e. uniaxially oriented in the test direction. Therefore the values of TS_{max} in the *MD* and the *TD* directions should be the same for the same film.

Incidentally, since the *TD* results refer to relatively low residual strains in the test direction any value of TS_{max} estimated from these curves would likely to be not very accurate.

The estimated values of TS_{max} of the films are shown in Table 8.10.

Table 8.10. The estimated values of TS_{max} of LDPE, LLDPE and blends of LDPE and LLDPE films.

Film sample	TS_{max} (10^6 N/m^2)
LDPE	57.50
75% LDPE/ 25% LLDPE	45.50
25% LDPE/ 75% LLDPE	62.00
LLDPE	57.00

Having found the values of TS_{max} it is now possible to plot $\ln(TS_{max} - TS_t)$ as a function of $\varepsilon^2_t/\varepsilon_p$. The values of $\ln(TS_{max} - TS_t)$ as a function of $\varepsilon^2_t/\varepsilon_p$ of LDPE films are plotted in Figures 8.19 and 8.20. It could be seen that the plots are linear.

The results for the other films were treated in a similar manner. These results are shown in Figures 8.21 to 8.26. These plots again show the model to be a reasonable representation of the data.

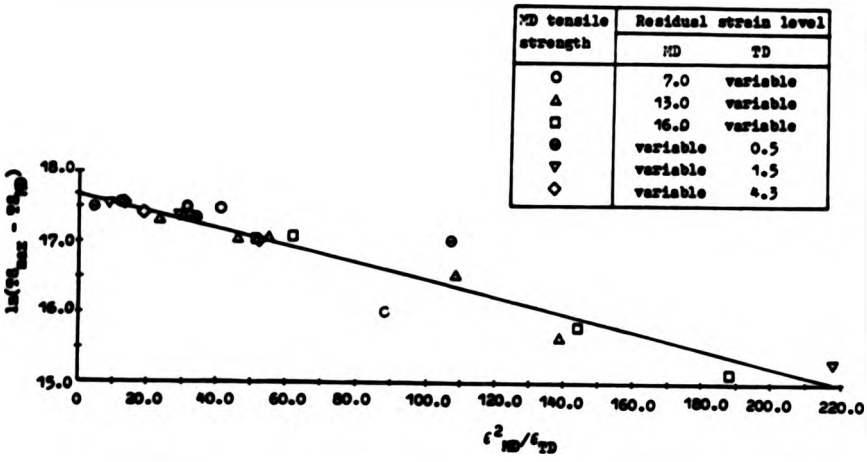

Figure 8.19. The values of $\ln(TS_{max} - TS_{MD})$ as a function of $\varepsilon^2_{MD}/\varepsilon_{TD}$ of LDPE films.

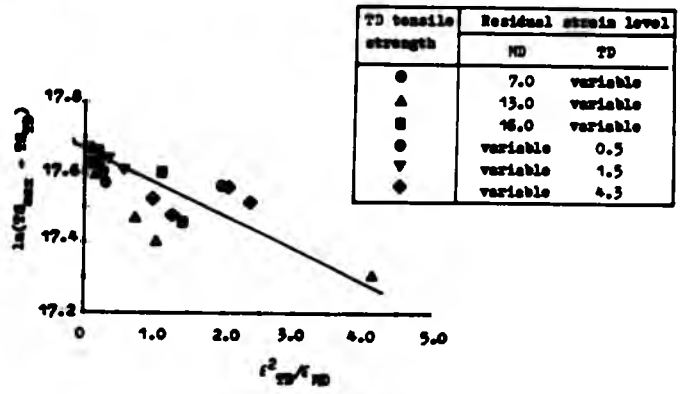

Figure 8.20. The values of $\ln(TS_{max} - TS_{TD})$ as a function of $\varepsilon^2_{TD}/\varepsilon_{MD}$ of LDPE films.

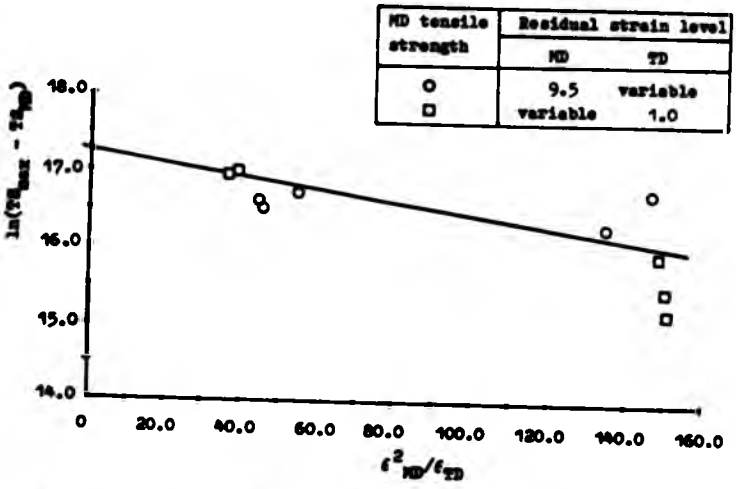

Figure 8.21. The values of $\ln(TS_{max} - TS_{MD})$ as a function of $\varepsilon^2_{MD}/\varepsilon_{TD}$ of 75% LDPE/25% LLDPE blend films.

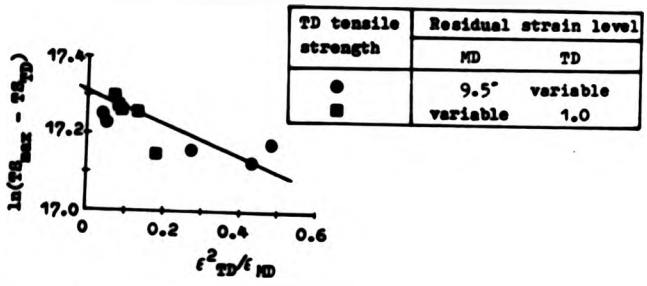

Figure 8.22. The values of $\ln(TS_{max} - TS_{TD})$ as a function of $\varepsilon^2_{TD}/\varepsilon_{MD}$ of 75% LDPE/25% LLDPE blend films.

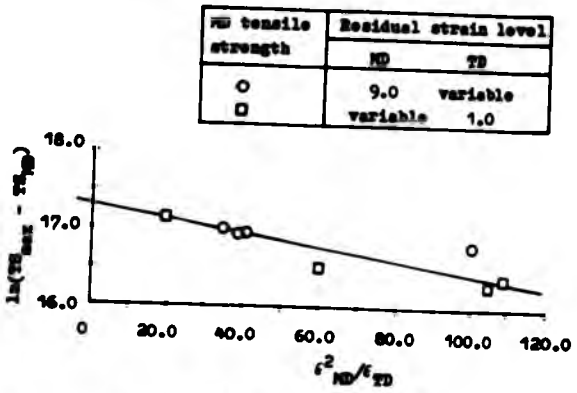

Figure 8.23. The values of $\ln(TS_{max} - TS_{MD})$ as a function of $\epsilon^2_{MD}/\epsilon_{TD}$ of 25% LDPE/75% LLDPE blend films.

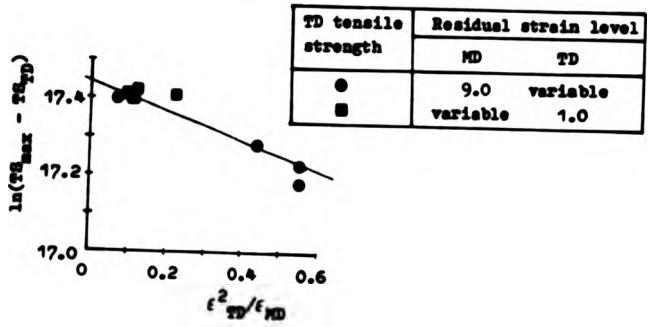

Figure 8.24. The values of $\ln(TS_{max} - TS_{TD})$ as a function of $\epsilon^2_{TD}/\epsilon_{MD}$ of 25% LDPE/75% LLDPE blend films.

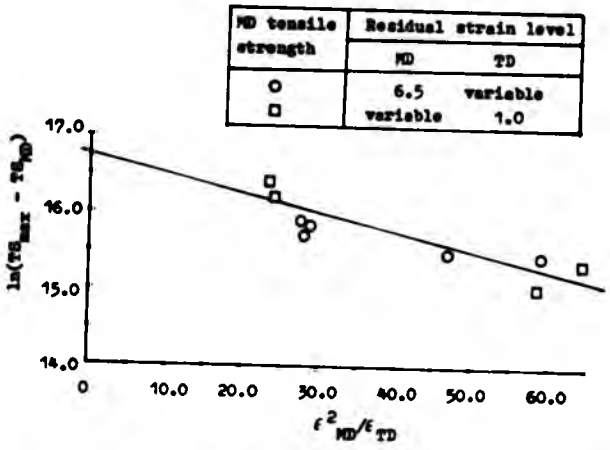

Figure 8.25. The values of $\ln(TS_{max} - TS_{MD})$ as a function of $\varepsilon^2_{MD}/\varepsilon_{TD}$ of LLDPE films.

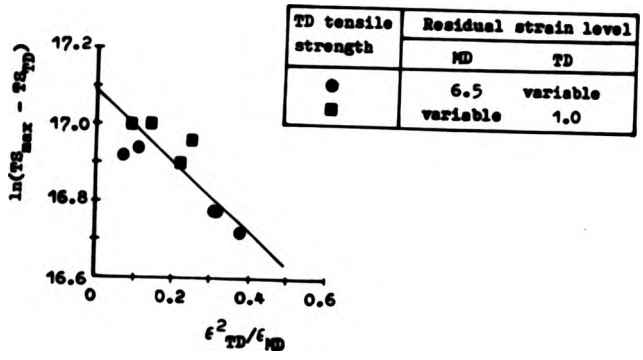

Figure 8.26. The values of $\ln(TS_{max} - TS_{TD})$ as a function of $\varepsilon^2_{TD}/\varepsilon_{MD}$ of LLDPE films.

8.5 Test of Model

The values of b and k of the films made from different materials were estimated from the log plots using the linear regression method. From the values of b, the values of TS_o were calculated. These values are tabulated, together with TS_{max} and k values, in Table 8.11.

Table 8.11. The values of TS_{max}, TS_o and k of LDPE, LLDPE and blended films.

Film sample	TS_{max} (10^6 N/m^2)	TS_o (10^6 N/m^2)		k (10^{-2})	
		MD	TD	MD	TD
LDPE	57.50	7.38	12.15	1.26	7.03
75% LDPE/ 25% LLDPE	45.50	27.61	14.17	0.34	29.82
25% LDPE/ 75% LLDPE	62.00	31.60	22.57	0.74	44.90
LLDPE	57.00	42.64	32.36	1.77	84.95

It can be seen from Table 8.11 that the values of TS_o in the *MD* and the *TD* are not the same. These values are expected to be equal because they are both the value of TS of a sample with zero residual strain in the test direction and some residual strain in the perpendicular

direction. The difference in the estimated value of TS_o is due to the scattering of the data and consequent uncertainty in determining TS_o. There is greater scatter in the TD data.

Using the values of TS_{max}, b and k tabulated in Table 8.11, TS of several unannealed PE films could be estimated. The estimated values of TS were then compared with the measured values, as shown in Table 8.12 and Figure 8.27. It can be seen that there is a good agreement between the estimated and measured values.

Table 8.12. The estimated and measured values of tensile strength of LDPE, LLDPE and blends of LDPE and LLDPE films.

Film	Sample	Residual strain		MD		TD	
		MD	TD	Estimated tensile strength ($10^6 N/m^2$)	Measured tensile strength ($10^6 N/m^2$)	Estimated tensile strength ($10^6 N/m^2$)	Measured tensile strength ($10^6 N/m^2$)
LDPE	2A	20.33	1.89	54.31	52.99	12.71	11.95
	2B	19.59	2.60	49.70	49.76	13.24	19.83
	2C	19.15	5.66	35.34	32.67	17.18	24.42
	2D	18.25	5.79	33.22	28.81	17.64	23.50
	2E	13.06	7.38	20.04	24.14	23.67	24.45
75% LDPE/ 25% LLDPE	3A	18.51	1.91	35.78	52.24	15.96	20.35
	3B	14.55	3.26	31.15	34.82	20.30	25.06
25% LDPE/ 75% LLDPE	4A	14.95	1.60	51.19	54.20	25.49	28.42
	4B	11.60	3.40	39.32	44.11	36.79	36.01
LLDPE	5A	9.34	1.23	52.91	57.27	35.53	35.28
	5B	7.52	1.80	48.76	52.16	39.91	46.09

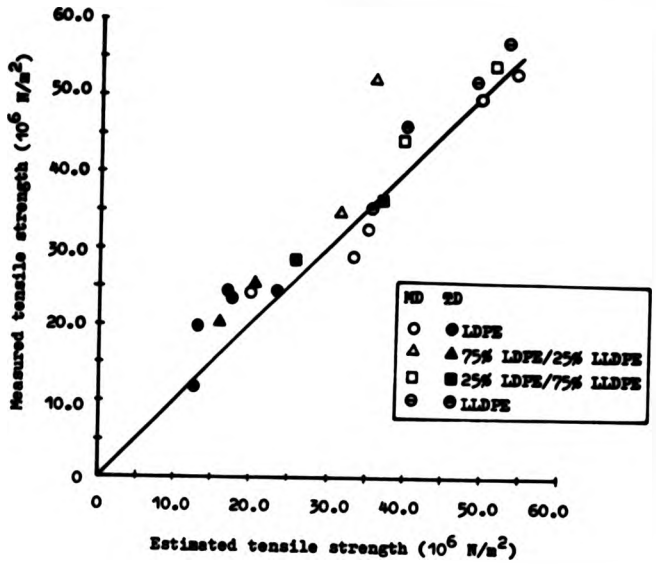

Figure 8.27. Plot of measured tensile strength against estimated tensile strength of LDPE, LLDPE and blended films.

The model can also be used to draw the estimated *TS* against residual strain curves of the films. The estimated curves for LDPE films are shown in Figures 8.28 and 8.29. It can be seen that the estimate curves have a similar shape to the measured curves.

From Figure 8.28 it can be seen that the *TD* estimated curves bend downwards, whilst the *TD* measured curves bend in the opposite way. The possible reason for this observation is the scattering of the *TD* data and defects in the mathematical model.

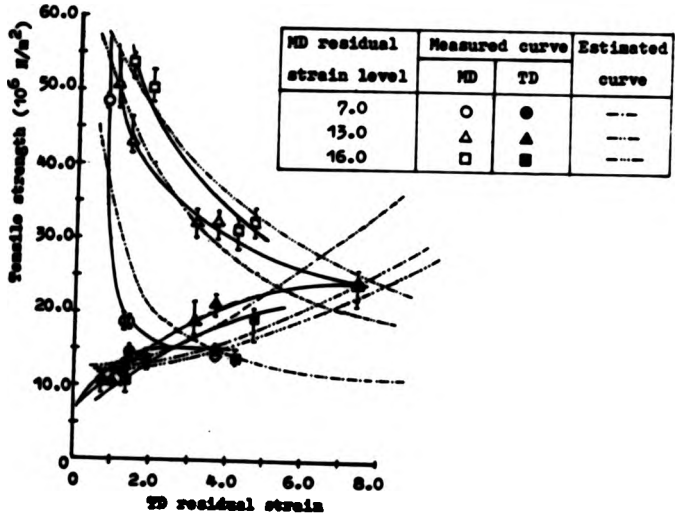

Figure 8.28. Estimated and measured curves of the effect of TD residual strain on the tensile strength of LDPE films.

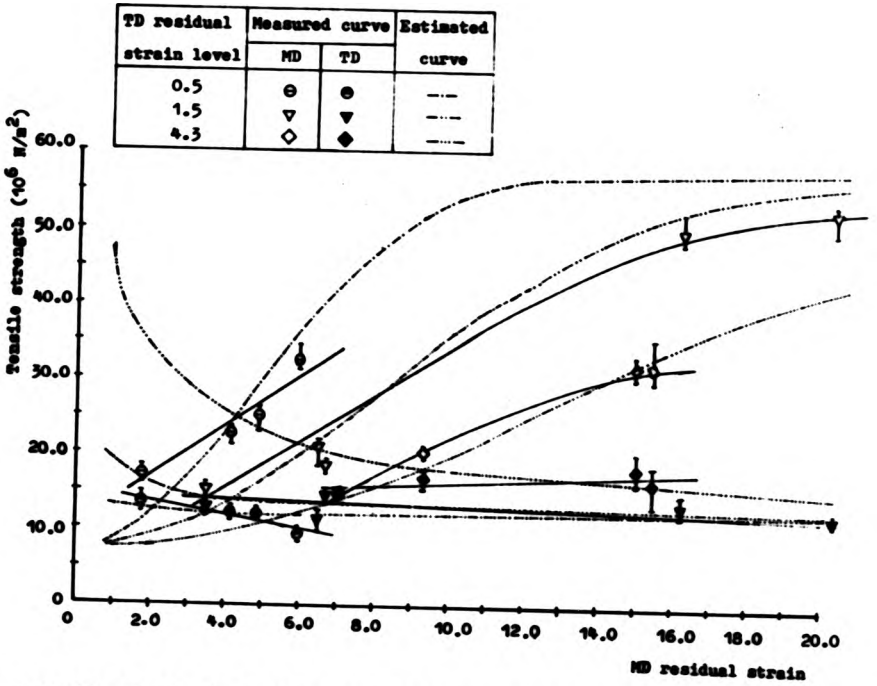

Figure 8.29. Estimated and measured curves of the effect of MD residual strain on the tensile strength of LDPE films.

The effect of increasing TS_{max}, TS_o and k on the TS for a range of values of ε_t and ε_p can be studied by choosing theoretical values of the above parameters. This is shown in Figures 8.30 to 8.32.

From Figure 8.30, it can be seen that increasing TS_{max} for a range of values of ε_t and ε_p produces steeper curves.

Increasing TS_o, Figure 8.31, for a range of values of ε_t shifts the initial part of the curves vertically. However, increasing TS_o for a range of values of ε_p produces straight lines which are shifted vertically with increasing TS_o.

Figure 8.32 shows the effect of increasing k on the tensile strength. It can be seen that increasing k shifts the initial part of the curves vertically and makes them steeper.

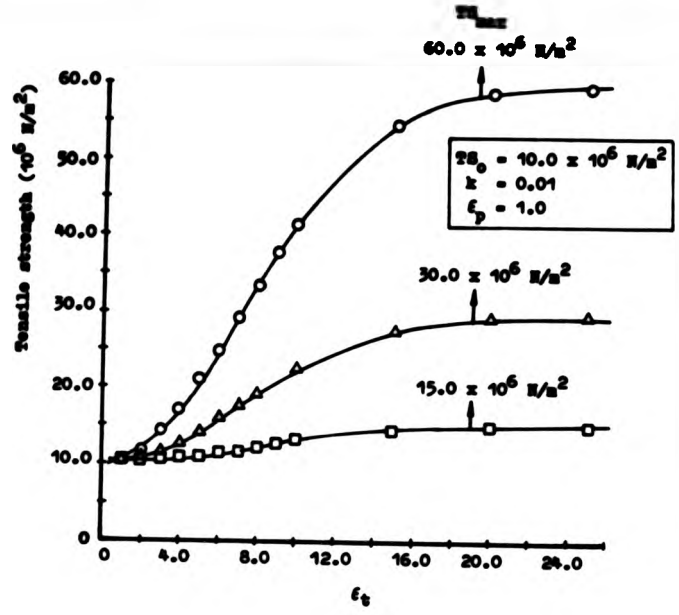

(a)

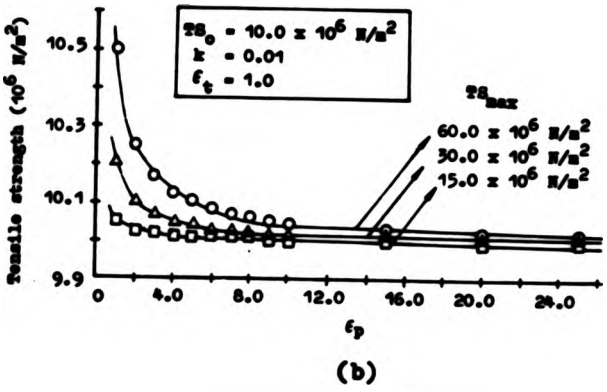

(b)

Figure 8.30. Effect of changing TS_{max} on the tensile strength at constant TS_o and k for a range of values of: (a) ϵ_t and (b) ϵ_p.

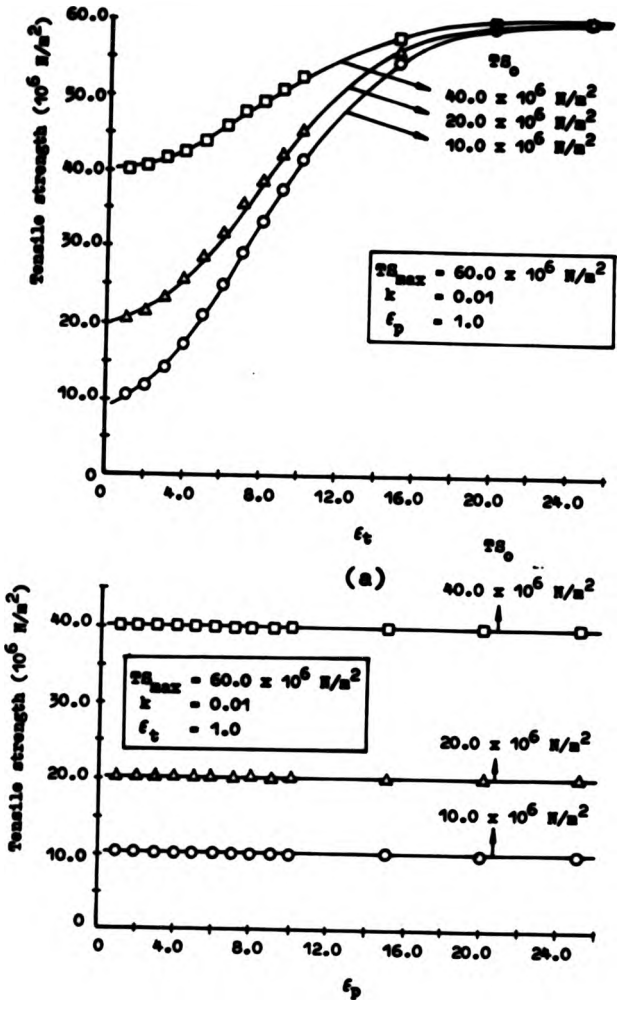

Figure 8.31. Effect of changing TS_o on the tensile strength at constant TS_{max} and k for a range of values of: (a) ε_t and (b) ε_p.

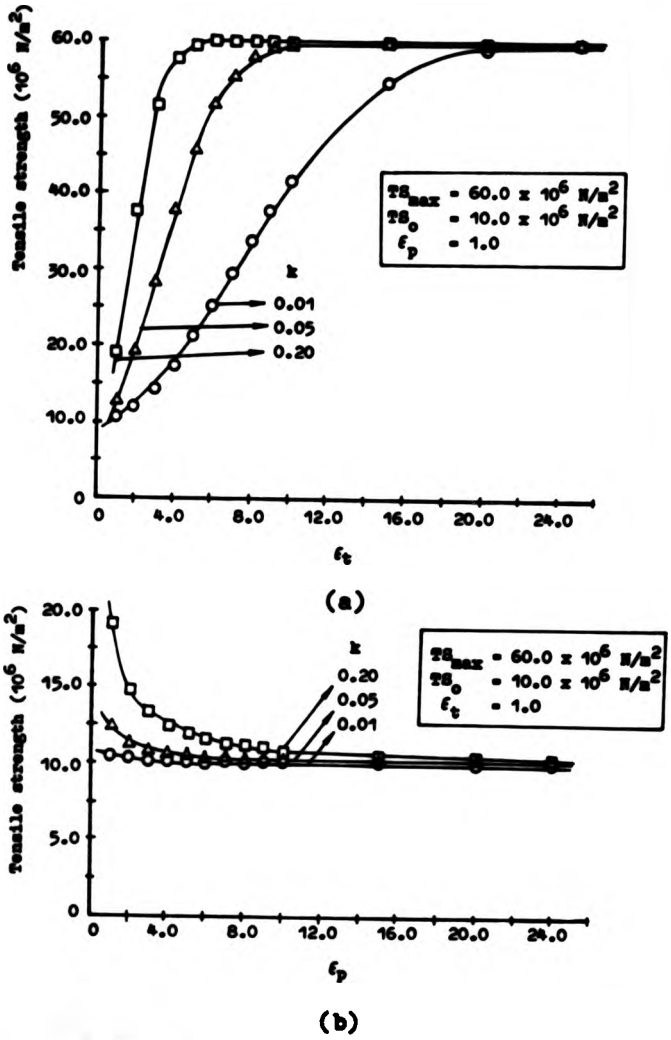

Figure 8.32. Effect of changing k on the tensile strength at constant TS_{max} and TS_o for a range of values of: (a) ϵ_t and (b) ϵ_p.

8.6 Discussion

The work on the relationship between *TS* and residual strain of PE films shows that *TS* of the films depends on $\varepsilon^2_t / \varepsilon_p$. That is the residual strain ratio, $\varepsilon_t / \varepsilon_p$ multiplied by the level of residual strain in the test direction, ε_t. The residual strain ratio determines the proportion of molecules oriented in the test direction compared to the direction perpendicular to the test direction, as pointed out earlier in Chapter 5.0. Therefore, as this ratio increases the amount of molecules oriented in the test direction increases. The increase in the amount of molecules oriented in the test direction results in the increase in the *TS* in that direction. This is because *TS* is a property which depends on the number of molecules which can support the applied load during stretching.

The residual strain ratio, however, reflects the proportion of molecules oriented in the *MD* and the *TD* within a given film sample. To compare the proportion of molecules oriented along the *MD* and the *TD* between different samples of various residual strain levels, the residual strain level in the test direction ε_t need to be taken into consideration. This is because the sample with higher residual strain level in the test direction will have greater amount of molecules oriented in that direction and thus has greater *TS*. This is evident from

the plot of TS_t against $\varepsilon^2_t/\varepsilon_p$, shown earlier.

It could be argued that the relationship obtained between *TS* and residual strain could also be due to different crystal morphology in the films. This is due to the same reason mentioned in Chapter 7.0 for Eb results. Doing the same procedure as in Chapter 7.0, *TS* of several unannealed LDPE films, shown in Table 8.12, are plotted into Figures 8.33 and 8.34. The curves drawn in Figures 8.12 and 8.13 are also included for comparison. From these figures it could be seen that the *TS* of these films are distributed along the curves. This means that the relationship obtained between *TS* and residual strain is due to different residual strain in the films and not due to different morphology. If the relationship obtained is due to different morphology then the tensile strength of the unannealed LDPE films should fall into one group anywhere on the curve because these films are expected to have the same morphology while the annealed films should fall into another group corresponding to their morphology. This, however, is not observed.

The difference in morphology between annealed and blown films is due to the difference in the crystallisation conditions. In the case of annealed films, crystallisation takes place by allowing the heated polymer to cool to room temperature. In the case of blown films, crystallisation takes place in a flowing melt with faster cooling rate than that encountered in annealing process.

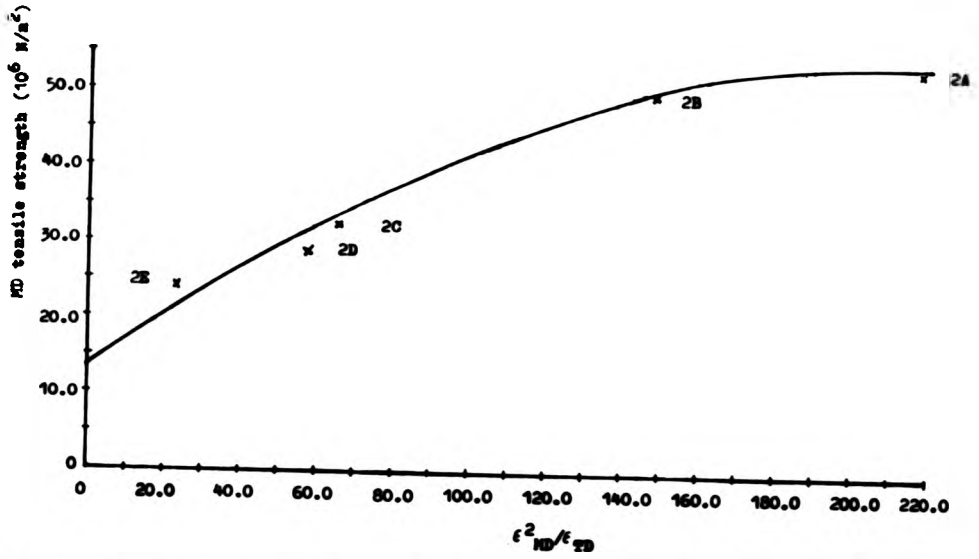

Figure 8.33. Tensile strength in MD of unannealed LDPE films as a function of $\epsilon^2_{MD}/\epsilon_{TD}$.

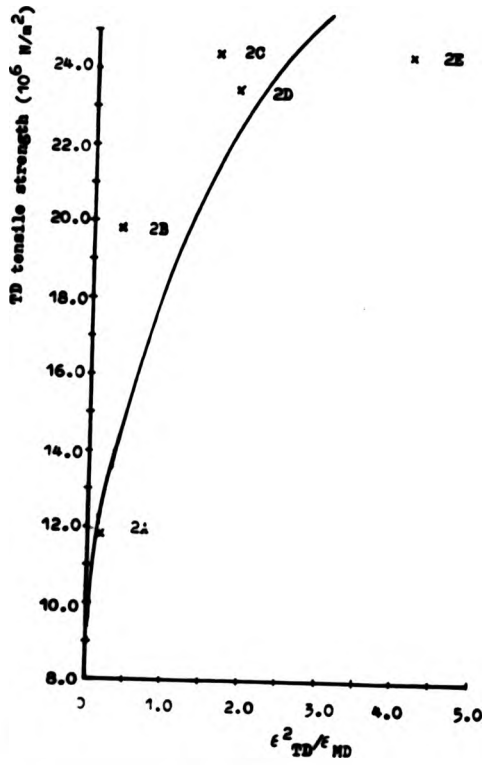

Figure 8.34. Tensile strength in TD of unannealed LDPE films as a function of $\epsilon^2_{TD}/\epsilon_{MD}$.

The *TS* of PE films also depends on the composition of LLDPE in the blend. Increasing LLDPE composition in the blend increases the *TS* of the film.

The value of TS_o, from Table 8.11, increases with increasing LLDPE composition in the films. This is expected because LLDPE-rich films have greater *TS* than LDPE-rich films. The values of TS_{max}, however, are not much affected by blending.

The constant k represents the rate at which *TS* changes from TS_o to TS_{max} as $\varepsilon^2_t/\varepsilon_p$ is increased. The greater the value of k, the greater is the rate of change, as shown by Figure 8.32. This explains the observed increase in the value of k with increasing LLDPE composition as shown in Table 8.11. This is because LLDPE-rich films have greater *TS* than LDPE-rich films eventhough they have lower residual strains. The greater *TS* is due to greater values of k of these films.

It was also observed that the value of k in *TD* is greater than that in *MD*, from Table 8.11. The possible reason for this is due to great scattering of the *TD* data which introduces errors into the estimated k values. Further work, however, is needed to confirm this.

CHAPTER 9.0

EFFECT OF RESIDUAL STRAINS ON THE YIELD STRESS OF POLYETHYLENE FILMS

9.1 Introduction

The effect of *MD* residual strain, ε_{MD}, and *TD* residual strain, ε_{TD}, on the yield stress, *YS*, of films made from LDPE, LLDPE and blends of the two is discussed in this chapter.

9.2 Effect of Residual Strains on the Yield Stress of Low Density Polyethylene Films

The *YS* of LDPE films as a function of ε_{TD} is shown in Table 9.1 and plotted in Figure 9.1. It can be seen that, eventhough the points are scattered, increasing ε_{TD} decreases *YS* in both directions.

The effect of increasing ε_{MD} on *YS* of LDPE films is shown in Table 9.2 and plotted in Figure 9.2. It could be seen that increasing ε_{MD} increases *YS* in both directions of the films.

Table 9.1. Effect of TD residual strain on the yield stress of LDPE films. The MD residual strain and film thickness were kept constant (within experimental error).

			MD		TD	
Sample	Residual strain		Thick-ness (10^{-6} m)	Yield stress (10^6 N/m^2)	Thick-ness (10^{-6} m)	Yield stress (10^6 N/m^2)
	MD	TD				
6A	7.82	0.70	33.7	16.65	36.3	13.90
6B	7.24	1.27	34.6	11.82	34.3	12.77
6C	6.68	1.41	33.3	11.84	33.3	12.97
6D	6.87	3.67	32.3	10.51	30.7	9.91
6E	12.84	1.19	32.3	19.88	33.3	13.65
6F	12.23	1.38	31.7	14.81	33.3	13.05
6G	13.04	3.10	31.7	9.95	31.7	11.40
6H	12.93	3.66	31.3	11.61	32.3	12.80
6I	13.06	7.38	37.3	8.59	37.7	9.10
6J	16.05	1.37	37.0	17.89	35.3	11.94
6K	16.27	1.84	35.0	15.13	36.7	12.88
6L	16.19	4.20	32.3	10.88	34.0	10.82
6M	15.47	4.68	33.0	11.75	33.3	11.52

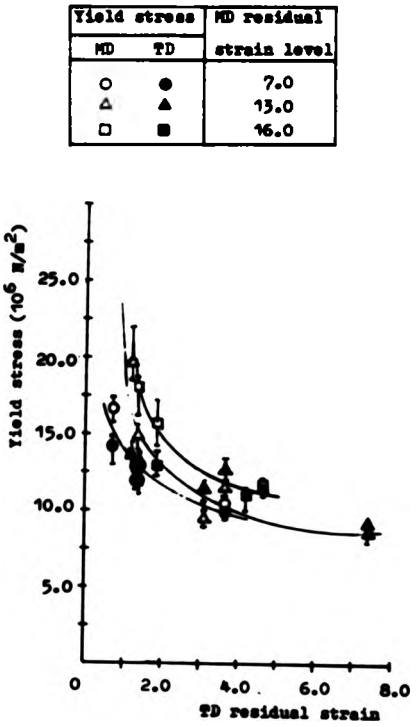

Figure 9.1. Effect of TD residual strain (at constant MD residual strain and thickness) on the yield stress of LDPE films.

Table 9.2. Effect of MD residual strain on the yield stress of LDPE films. The TD residual strain and film thickness were kept constant (within experimental error).

Sample	Residual strain		MD		TD	
	MD	TD	Thickness (10^{-6} m)	Yield stress (10^6 N/m^2)	Thickness (10^{-6} m)	Yield stress (10^6 N/m^2)
7A	1.75	0.68	36.3	10.96	35.0	12.09
7B	4.17	0.51	33.0	11.52	31.3	13.13
7C	4.83	0.72	34.0	11.18	34.7	12.07
7D	5.94	0.33	34.3	13.52	34.0	13.18
7E	3.52	1.40	35.0	10.55	36.7	11.35
7F	6.49	1.48	33.3	10.31	31.7	11.51
7G	6.68	1.41	33.3	11.84	33.3	12.97
7H	16.27	1.84	35.0	15.13	36.7	12.88
7I	20.33	1.89	34.0	15.96	35.0	8.92
7J	7.05	3.82	32.3	10.51	30.7	9.91
7K	9.33	4.71	32.7	9.23	32.3	10.14
7L	15.07	4.34	33.7	11.65	32.3	12.03
7M	15.49	3.90	31.3	13.28	31.7	12.62

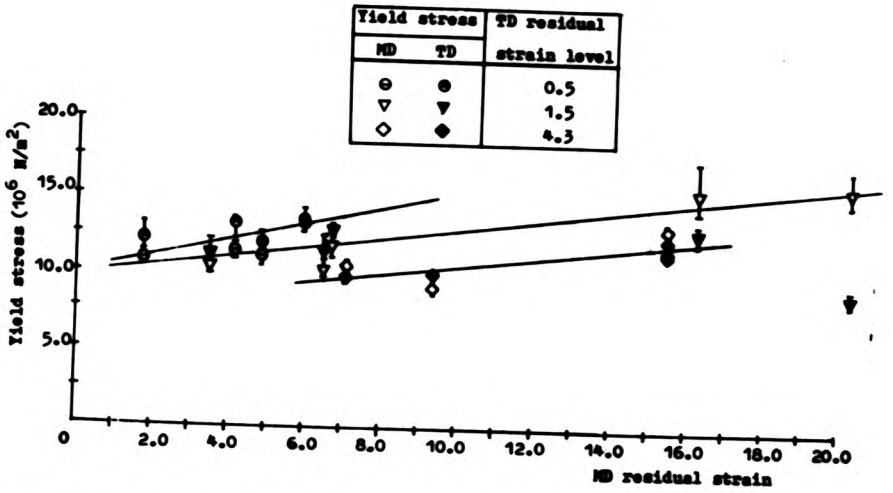

Figure 9.2. Effect of MD residual strain (at constant TD residual strain and thickness) on the yield stress of LDPE films.

9.3 Effect of Residual Strains on the Yield Stress of Blended and Linear Low Density Polyethylene Films

The results of increasing ε_{TD} and ε_{MD} on YS of 75% LDPE/25% LLDPE, 25% LDPE/75% LLDPE blend films and LLDPE films are shown in Tables 9.3 to 9.8 and plotted in Figures 9.3 to 9.8.

The results show the same trend as observed with LDPE films except LLDPE films which show that ε_{MD} has little effect on the YS.

Table 9.3. Effect of TD residual strain on the yield stress of 75% LDPE/25% LLDPE blend films. The MD residual strain and film thickness were kept constant (within experimental error).

Sample	Residual strain		MD		TD	
	MD	TD	Thickness (10^{-6} m)	Yield stress (10^6 N/m^2)	Thickness (10^{-6} m)	Yield stress (10^6 N/m^2)
8A	9.38	0.60	36.3	11.94	36.0	11.79
8B	9.65	0.69	38.7	13.33	37.0	11.36
8C	9.42	1.62	35.3	10.35	38.0	10.52
8D	9.65	2.07	36.0	10.76	35.7	10.20
8E	9.83	2.18	34.7	10.45	35.0	10.31

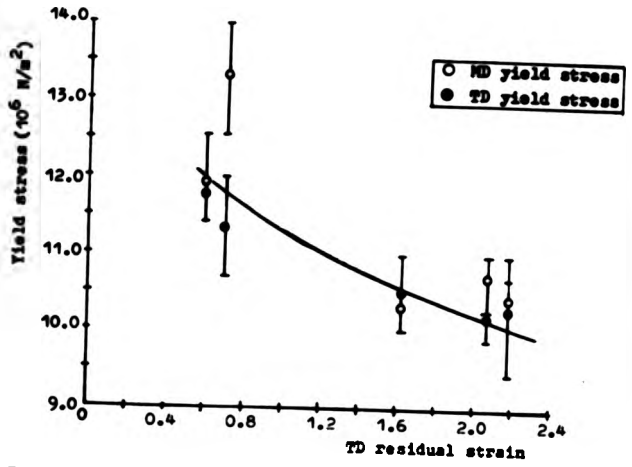

Figure 9.3. Effect of TD residual strain (at constant MD residual strain and thickness) on the yield stress of 75% LDPE/25% LLDPE blend films.

Table 9.4. Effect of MD residual strain on the yield stress of 75% LDPE/25% LLDPE blend films. The TD residual strain and film thickness were kept constant (within experimental error).

Sample	Residual strain		MD		TD	
	MD	TD	Thickness (10^{-6} m)	Yield stress (10^6 N/m^2)	Thickness (10^{-6} m)	Yield stress (10^6 N/m^2)
9A	5.98	0.92	36.7	9.36	36.7	9.49
9B	6.31	1.09	37.0	9.65	36.3	10.12
9C	11.49	0.89	37.3	12.79	38.3	10.44
9D	12.61	1.06	36.3	13.48	38.3	10.76
9E	12.77	1.08	37.3	13.70	37.0	11.57

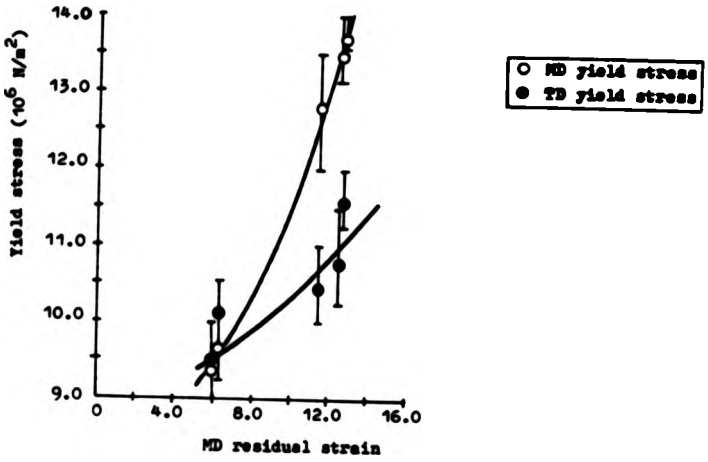

Figure 9.4. Effect of MD residual strain (at constant TD residual strain and thickness) on the yield stress of 75% LDPE/25% LLDPE blend films.

Table 9.5. Effect of TD residual strain on the yield stress of 25% LDPE/75% LLDPE blend films. The MD residual strain and film thickness were kept constant (within experimental error).

Sample	Residual strain		MD		TD	
	MD	TD	Thickness (10^{-6} m)	Yield stress (10^6 N/m^2)	Thickness (10^{-6} m)	Yield stress (10^6 N/m^2)
10A	8.95	0.80	37.3	11.46	37.7	12.84
10B	9.05	2.01	34.3	10.70	35.0	11.41
10C	8.76	2.20	35.7	10.26	36.3	11.46
10D	9.40	2.30	34.7	10.25	33.7	11.40

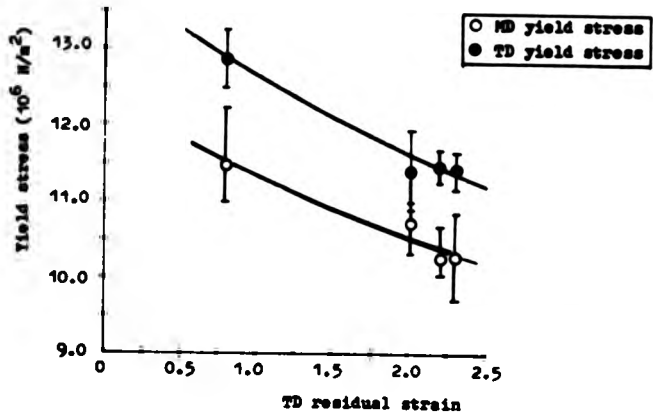

Figure 9.5. Effect of TD residual strain (at constant MD residual strain and thickness) on the yield stress of 25% LDPE/75% LLDPE blend films.

Table 9.6. Effect of MD residual strain on the yield stress of 25% LDPE/75% LLDPE blend films. The TD residual strain and film thickness were kept constant (within experimental error).

Sample	Residual strain		MD		TD	
	MD	TD	Thickness (10^{-6} m)	Yield stress (10^6 N/m^2)	Thickness (10^{-6} m)	Yield stress (10^6 N/m^2)
11A	4.32	0.98	34.3	10.66	35.0	10.68
11B	7.52	0.94	37.3	12.25	36.3	12.74
11C	10.47	1.05	37.7	12.37	38.0	11.28
11D	11.26	1.16	37.3	14.32	37.7	12.21

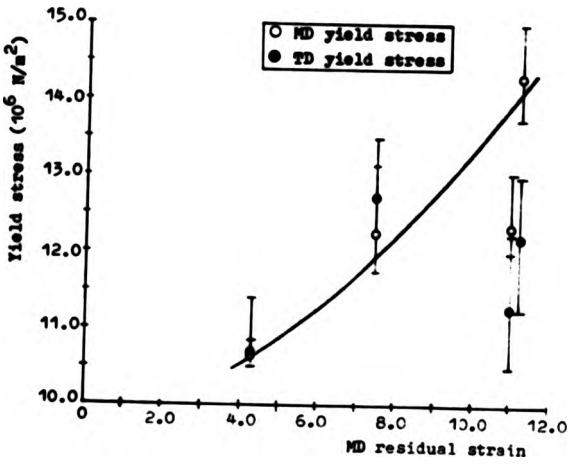

Figure 9.6. Effect of MD residual strain (at constant TD residual strain and thickness) on the yield stress of 25% LDPE/75% LLDPE blend films.

Table 9.7. Effect of TD residual strain on the yield stress of LLDPE films. The MD residual strain and film thickness were kept constant (within experimental error).

Sample	Residual strain		MD		TD	
	MD	TD	Thickness (10^{-6} m)	Yield stress (10^6 N/m^2)	Thickness (10^{-6} m)	Yield stress (10^6 N/m^2)
12A	6.34	0.68	35.7	11.74	35.0	11.65
12B	6.23	0.83	33.7	11.73	34.0	12.28
12C	6.31	1.42	34.0	10.90	35.7	11.27
12D	6.54	1.47	34.3	10.20	34.7	11.66
12E	6.63	1.59	35.7	10.32	35.3	11.80

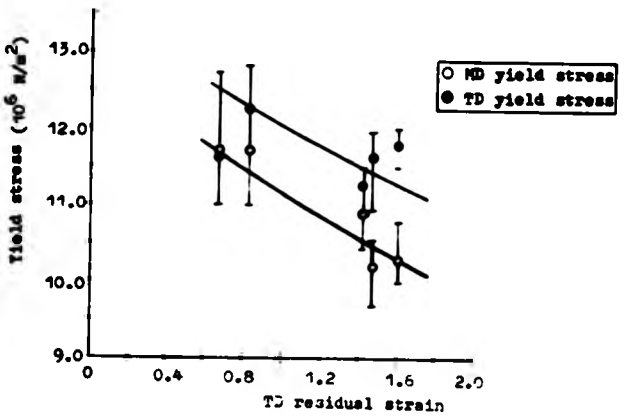

Figure 9.7. Effect of TD residual strain (at constant MD residual strain and thickness) on the yield stress of LLDPE films.

Table 9.8. Effect of MD residual strain on the yield stress of LLDPE films. The TD residual strain and film thickness were kept constant (within experimental error).

Sample	Residual strain		MD		TD	
	MD	TD	Thickness (10^{-6} m)	Yield stress (10^6 N/m^2)	Thickness (10^{-6} m)	Yield stress (10^6 N/m^2)
13A	5.01	1.04	33.0	11.93	33.7	11.96
13B	5.14	1.13	31.3	11.53	37.3	10.98
13C	7.41	0.85	36.0	10.00	37.0	11.41
13D	7.85	1.05	36.0	10.70	38.3	11.76

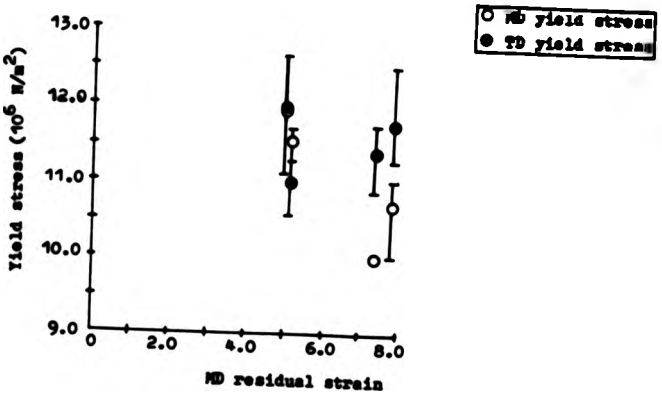

Figure 9.8. Effect of MD residual strain (at constant TD residual strain and thickness) on the yield stress of LLDPE films.

9.4 Discussion

Eventhough the results are scattered, it can be seen that increasing ε_{MD} increases the *YS* of the films in both directions. The increase in *YS*, however, is small. On the other hand, increasing ε_{TD} produces the opposite effect, reducing *YS* in both directions. Also it is observed that the *YS* in both directions are almost the same.

Because of the above observations, *YS* was plotted against $\varepsilon_{MD}/\varepsilon_{TD}$ to see if the data fell on a single curve. the results were scattered, Figure 9.9, indicating a more complex pattern of behaviour.

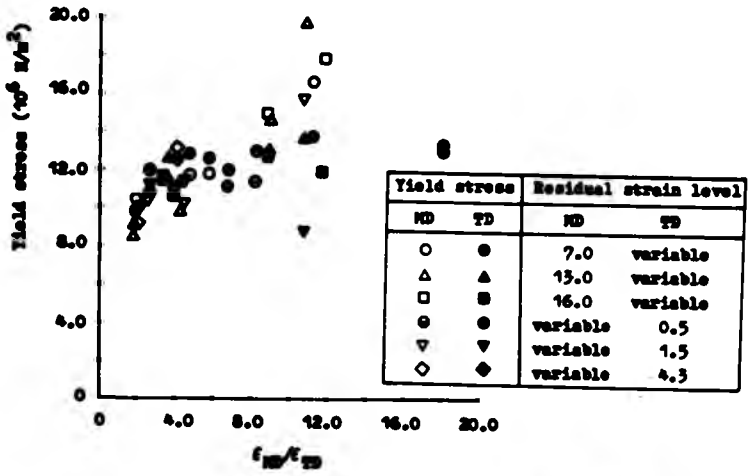

Figure 9.9. Plot of yield stress against $\varepsilon_{MD}/\varepsilon_{TD}$ of LDPE films.

In Chapter 1.0, section 1.5.5, it was explained that when the film sample is stretched lamellae separation will take place. The separation results in lamellae slip. The disruption of the lamellae causes the yield process. Therefore explanation of the observed behaviour is likely to involve consideration of the crystalline regions of the material rather than just the amorphous molecular chains between crystalline regions which have been postulated to control the ultimate properties. The present study did not investigate the effect of melt strain on the orientation of the lamellae but this would be an interesting topic for further investigation.

CHAPTER 10.0

EFFECT OF RESIDUAL STRAINS ON THE TENSILE MODULUS OF POLYETHYLENE FILMS

10.1 Introduction

The effect of ε_{MD} and ε_{TD} on the tensile modulus, *TM*, of LDPE, LLDPE and blends of the two films is studied in this chapter.

10.2 Effect of Residual Strains on the Tensile Modulus of Low Density Polyethylene Films

The effect of ε_{TD} on *TM* of LDPE films is shown in Table 10.1 and the results are plotted in Figure 10.1. It can be seen that, eventhough the points are scattered, the effect of increasing ε_{TD} is to reduce *TM* in both directions of the films. Also, it is observed that TM_{MD} and TM_{TD} are almost the same.

Increasing ε_{MD} has an opposite effect on *TM* of the films. It seems that increasing ε_{MD} increases *TM* in both directions of LDPE films. These results are shown in Table 10.2 and Figure 10.2.

Table 10.1. Effect of TD residual strain on the tensile modulus of LDPE films. The MD residual strain and film thickness were kept constant (within experimental error).

Sample	Residual strain		MD		TD	
	MD	TD	Thickness (10^{-6} m)	Tensile modulus (10^7 N/m^2)	Thickness (10^{-6} m)	Tensile modulus (10^7 N/m^2)
6A	7.82	0.70	33.7	22.28	36.3	25.87
6B	7.24	1.27	34.6	19.79	34.3	26.25
6C	6.68	1.41	33.3	20.08	33.3	21.20
6D	6.87	3.67	32.3	13.02	30.7	14.04
6E	12.84	1.19	32.3	21.29	33.3	14.26
6F	12.23	1.38	31.7	19.27	33.3	21.26
6G	13.04	3.10	31.7	16.61	31.7	16.84
6H	12.93	3.66	31.3	17.19	32.3	21.69
6I	13.06	7.38	37.3	12.32	37.7	13.06
6J	16.05	1.37	37.0	25.27	35.3	22.66
6K	16.27	1.84	35.0	23.14	36.7	23.64
6L	16.19	4.20	32.3	18.03	34.0	14.85
6M	15.47	4.68	33.0	11.82	33.3	13.61

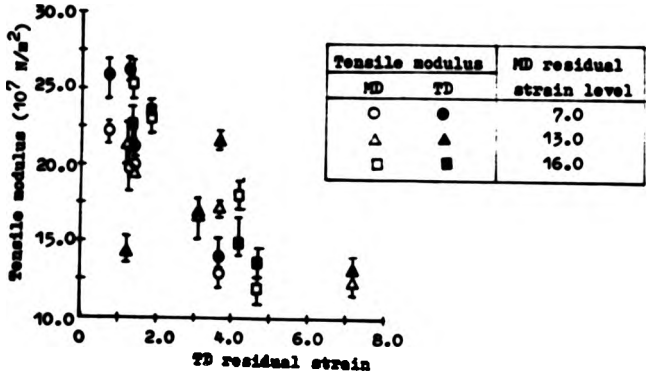

Figure 10.1. Effect of TD residual strain (at constant MD residual strain and thickness) on the tensile modulus of LDPE films.

Table 10.2. Effect of MD residual strain on the tensile modulus of LDPE films. The TD residual strain and film thickness were kept constant (within experimental error).

Sample	Residual strain		MD		TD	
	MD	TD	Thickness (10^{-6} m)	Tensile modulus (10^7 N/m^2)	Thickness (10^{-6} m)	Tensile modulus (10^7 N/m^2)
7A	1.75	0.68	36.3	16.00	35.0	13.23
7B	4.17	0.51	33.0	18.16	31.3	19.17
7C	4.83	0.72	34.0	17.55	34.7	17.34
7D	5.94	0.33	34.3	19.45	34.0	18.56
7E	3.52	1.40	35.0	16.61	36.7	14.98
7F	6.49	1.48	33.3	16.84	31.7	19.30
7G	6.68	1.41	33.3	20.08	33.3	21.20
7H	16.27	1.84	35.0	23.14	36.7	23.64
7I	20.33	1.89	34.0	23.85	35.0	21.70
7J	7.05	3.82	32.3	13.02	30.7	14.04
7K	9.33	4.71	32.7	12.59	32.3	11.50
7L	15.07	4.34	33.7	13.17	32.3	15.71
7M	15.49	3.90	31.3	12.65	31.7	12.69

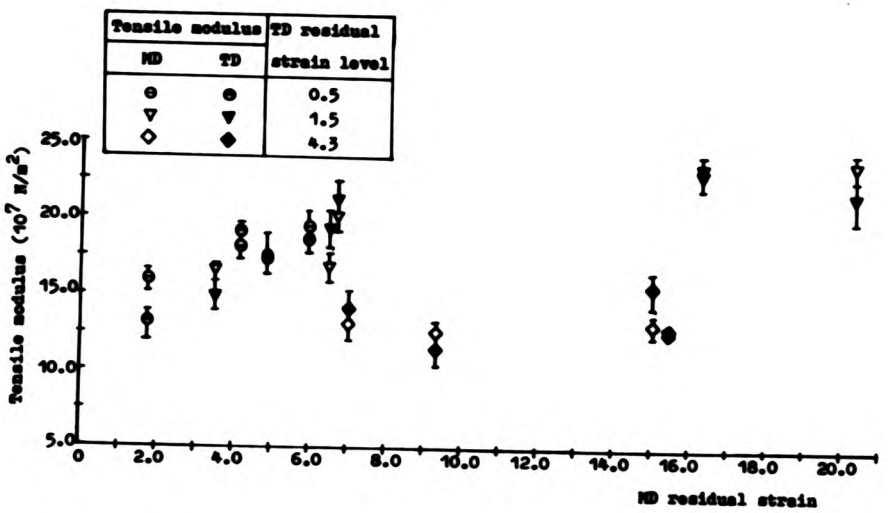

Figure 10.2. Effect of MD residual strain (at constant TD residual strain and thickness) on the tensile modulus of LDPE films.

10.3 Effect of Residual Strains on the Tensile Modulus of Blended and Linear Low Density Polyethylene Films

The results of ε_{TD} and ε_{MD} on the *TM* of 75% LDPE/25% LLDPE, 25% LDPE/75% LLDPE blend films and LLDPE films are shown in Tables 10.3 to 10.8 and plotted in Figures 10.3 to 10.8.

The general trend that is observed is that the results of *TM* as a function of ε_{TD} are scattered. The results of *TM* as a function of ε_{MD} show that increasing ε_{MD} increases the *TM*.

Table 10.3. Effect of TD residual strain on the tensile modulus of 75% LDPE/25% LLDPE blend films. The MD residual strain and film thickness were kept constant (within experimental error).

Sample	Residual strain		MD		TD	
	MD	TD	Thickness (10^{-6} m)	Tensile modulus (10^7 N/m^2)	Thickness (10^{-6} m)	Tensile modulus (10^7 N/m^2)
8A	9.38	0.60	36.3	14.22	36.0	16.92
8B	9.65	0.69	38.7	12.94	37.0	15.81
8C	9.42	1.62	35.3	13.71	38.0	11.90
8D	9.65	2.07	36.0	16.15	35.7	14.65
8E	9.83	2.18	34.7	14.18	35.0	12.59

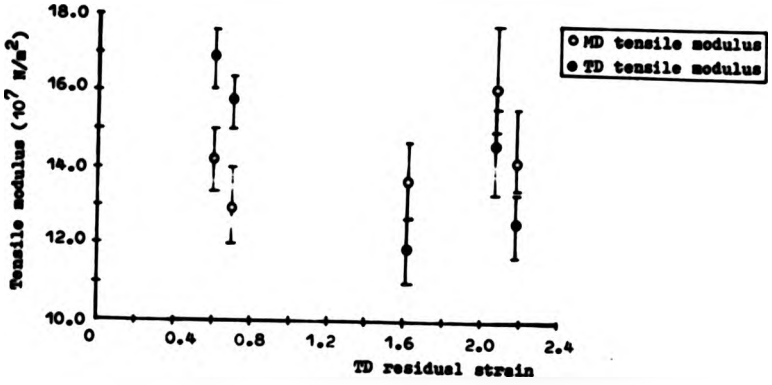

Figure 10.3. Effect of TD residual strain (at constant MD residual strain and thickness) on the tensile modulus of 75% LDPE/25% LLDPE blend films.

Table 10.4. Effect of MD residual strain on the tensile modulus of 75% LDPE/25% LLDPE blend films. The TD residual strain and film thickness were kept constant (within experimental error).

Sample	Residual strain		MD		TD	
	MD	TD	Thickness (10^{-6} m)	Tensile modulus (10^7 N/m^2)	Thickness (10^{-6} m)	Tensile modulus (10^7 N/m^2)
9A	5.98	0.92	36.7	11.56	36.7	11.78
9B	6.31	1.09	37.0	13.61	36.3	11.42
9C	11.49	0.89	37.3	16.97	38.3	13.44
9D	12.61	1.06	36.3	13.34	38.3	14.45
9E	12.77	1.08	37.3	16.89	37.0	13.75

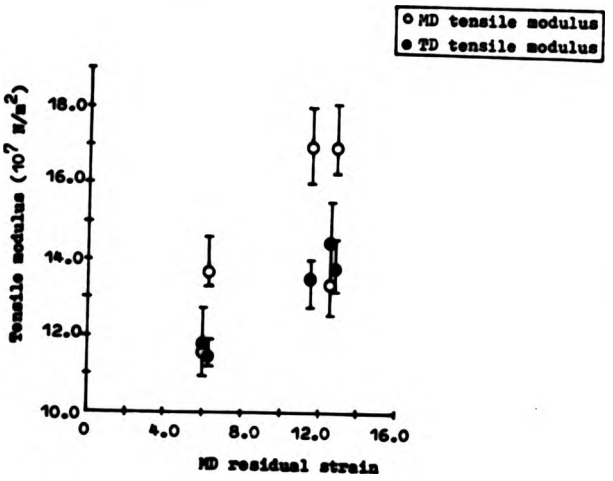

Figure 10.4. Effect of MD residual strain (at constant TD residual strain and thickness) on the tensile modulus of 75% LDPE/25% LLDPE blend films.

Table 10.5. Effect of TD residual strain on the tensile modulus of 25% LDPE/75% LLDPE blend films. The MD residual strain and film thickness were kept constant (within experimental error).

Sample	Residual strain		MD		TD	
	MD	TD	Thickness (10^{-6} m)	Tensile modulus (10^7 N/m^2)	Thickness (10^{-6} m)	Tensile modulus (10^7 N/m^2)
10A	8.95	0.80	37.3	16.94	37.7	13.89
10B	9.05	2.01	34.3	16.98	35.0	17.81
10C	8.76	2.20	35.7	10.98	36.3	13.58
10D	9.40	2.30	34.7	12.54	33.7	17.61

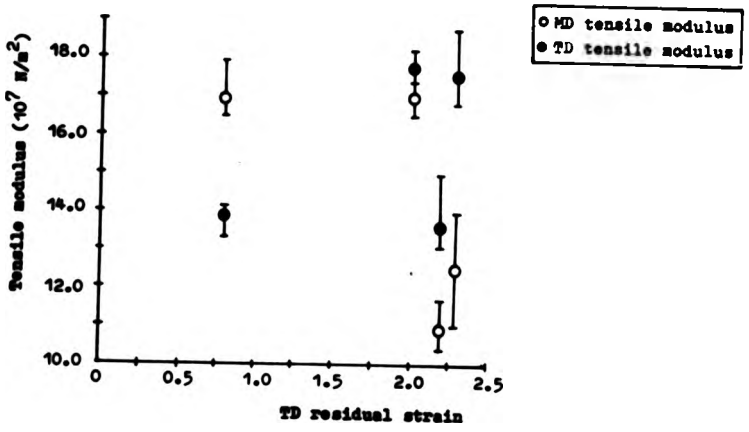

Figure 10.5. Effect of TD residual strain (at constant MD residual strain and thickness) on the tensile modulus of 25% LDPE/75% LLDPE blend films.

Table 10.6. Effect of MD residual strain on the tensile modulus of 25% LDPE/75% LLDPE blend films. The TD residual strain and film thickness were kept constant (within experimental error).

Sample	Residual strain		MD		TD	
	MD	TD	Thickness (10^{-6} m)	Tensile modulus (10^7 N/m^2)	Thickness (10^{-6} m)	Tensile modulus (10^7 N/m^2)
11A	4.32	0.98	34.3	12.27	35.0	10.87
11B	7.52	0.94	37.3	15.04	36.3	17.18
11C	10.47	1.05	37.7	12.62	38.0	17.35
11D	11.26	1.16	37.3	13.76	37.7	11.98

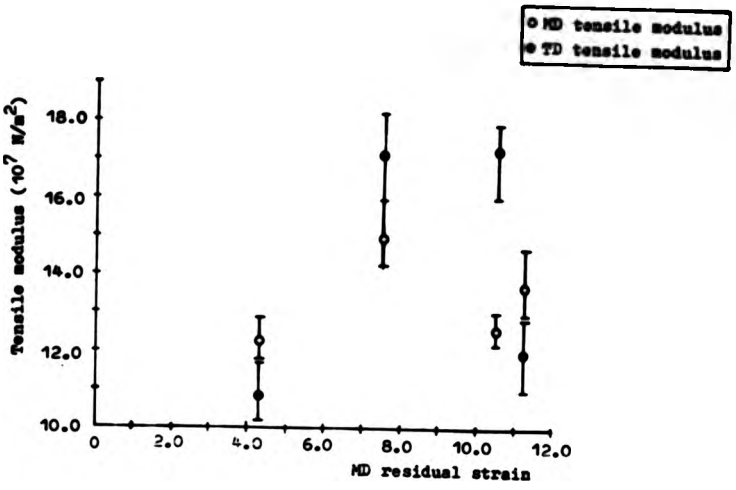

Figure 10.6. Effect of MD residual strain (at constant TD residual strain and thickness) on the tensile modulus of 25% LDPE/75% LLDPE blend films.

Table 10.7. Effect of TD residual strain on the tensile modulus of LLDPE films. The MD residual strain and film thickness were kept constant (within experimental error).

Sample	Residual strain		MD		TD	
	MD	TD	Thickness (10^{-6} m)	Tensile modulus (10^7 N/m^2)	Thickness (10^{-6} m)	Tensile modulus (10^7 N/m^2)
12A	6.34	0.68	35.7	10.89	35.0	13.67
12B	6.23	0.83	33.7	15.50	34.0	14.06
12C	6.31	1.42	34.0	12.50	35.7	11.32
12D	6.54	1.47	34.3	14.51	34.7	18.30
12E	6.63	1.59	35.7	12.53	35.3	12.42

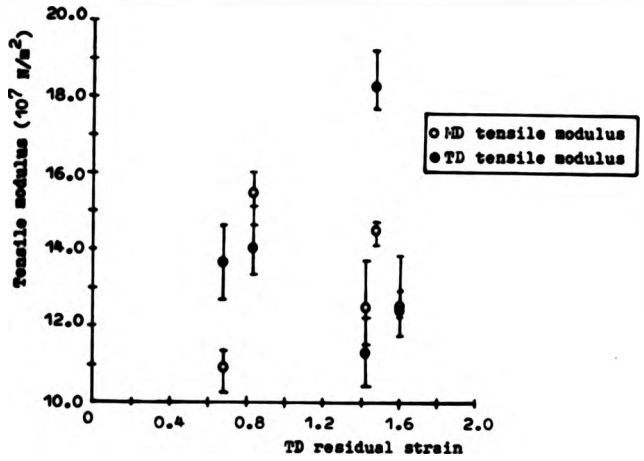

Figure 10.7. Effect of TD residual strain (at constant MD residual strain and thickness) on the tensile modulus of LLDPE films.

Table 10.8. Effect of MD residual strain on the tensile modulus of LLDPE films. The TD residual strain and film thickness were kept constant (within experimental error).

Sample	Residual strain		MD		TD	
	MD	TD	Thickness (10^{-6} m)	Tensile modulus (10^7 N/m^2)	Thickness (10^{-6} m)	Tensile modulus (10^7 N/m^2)
13A	5.01	1.04	33.0	15.04	33.7	15.34
13B	5.14	1.13	31.3	15.46	37.3	12.54
13C	7.41	0.85	36.0	14.50	37.0	14.38
13D	7.85	1.05	36.0	15.14	38.3	11.52

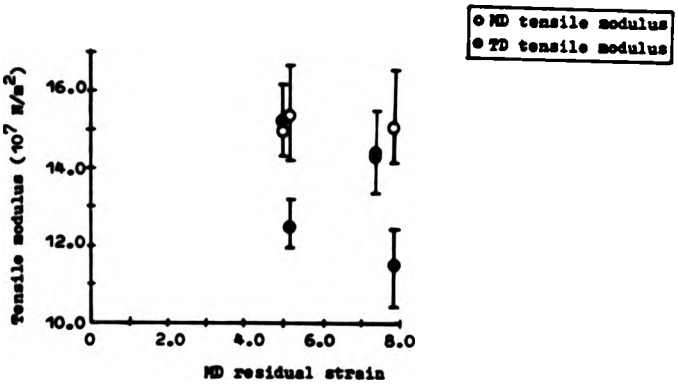

Figure 10.8. Effect of MD residual strain (at constant TD residual strain and thickness) on the tensile modulus of LLDPE films.

10.4 Discussion

The results of the effect of residual strain on *TM* of PE films show that there is a clear trend in the case of LDPE films, that is *TM* increases with ε_{MD} and decreases with increasing ε_{TD}. However, as the proportion of LLDPE in the films increases, the residual strain appears to have less and less effect on the *TM*. The results also show that LDPE films have greater *TM* than the blend and LLDPE films.

The *TM* of the films is a measure of small strain elastic response of the amorphous and crystalline regions of the films *(121)*. The modulus depends on orientation of each region and the modulus of the crystalline region is greater than that of the amorphous region. Therefore it can be said that modulus is controlled by the orientation of the crystalline region. The present studies did not investigate the orientation of the crystalline region and therefore no conclusion could be drawn it without further studies.

CHAPTER 11.0

EFFECT OF RESIDUAL STRAINS ON THE TEAR STRENGTH OF POLYETHYLENE FILMS

11.1 Introduction

The tear strength, TrS, of the films made from LDPE, LLDPE and the blends of the two is evaluated using the method described in Chapter 2.0.

The tear strength in the *MD*, TrS_{MD}, is the tear strength when the tear is initiated in the *MD*, whilst that in the *TD*, TrS_{TD}, is the tear strength when the tear is initiated in the *TD*.

11.2 Effect of Residual Strains on the Tear Strength of Low Density Polyethylene Films

The effect of ε_{TD} on TrS of LDPE films is shown in Table 11.1 and plotted in Figure 11.1. It can be seen that increasing ε_{TD} reduces TrS_{MD} of the films. The effect on TrS_{TD}, however, is smaller but again tends to reduce TrS_{TD}.

Increasing ε_{MD} showed the opposite effect on TrS of LDPE films, as shown in Table 11.2 and Figure 11.2. Increasing ε_{MD} increases TrS_{MD} and has smaller but similar effect on TrS_{TD}.

It is noticed from the results that $Tr\mathcal{S}_{MD}$ is greater than $Tr\mathcal{S}_{TD}$. Also it was observed during tearing test that the tear initiated along the *MD* changed the direction of tear propagation towards the *TD*. Those that were initiated along the *TD* did not change the direction of propagation.

Table 11.1. Effect of TD residual strain on the tear strength of LDPE films. The MD residual strain and film thickness were kept constant (within experimental error).

Sample	Residual strain		MD		TD	
	MD	TD	Thickness (10^{-6} m)	Tear strength (10^4 N/m)	Thickness (10^{-6} m)	Tear strength (10^4 N/m)
6E	12.84	1.19	32.2	11.31	33.0	5.46
6F	12.23	1.38	37.0	12.00	35.7	4.89
6G	13.04	3.10	31.3	8.09	31.3	4.89
6H	12.93	3.66	35.0	7.88	34.3	5.11
6I	13.06	7.38	32.0	3.59	31.0	3.47

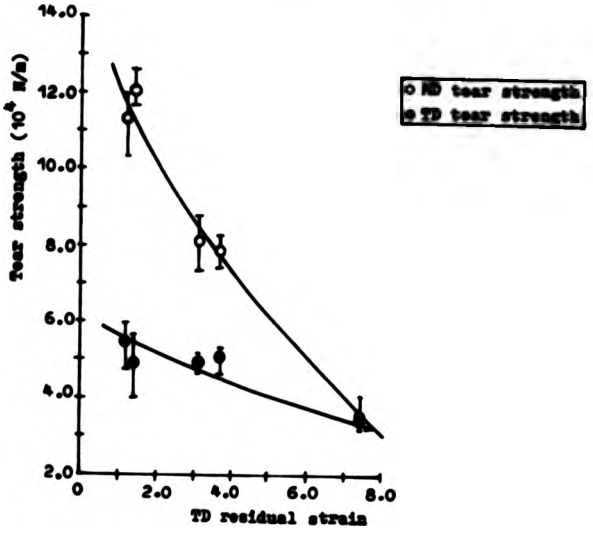

Figure 11.1. Effect of TD residual strain (at constant MD residual strain and thickness) on the tear strength of LDPE films.

Table 11.2. Effect of MD residual strain on the tear strength of LDPE films. The TD residual strain and film thickness were kept constant (within experimental error).

Sample	Residual strain		MD		TD	
	MD	TD	Thickness (10^{-6} m)	Tear strength (10^4 N/m)	Thickness (10^{-6} m)	Tear strength (10^4 N/m)
7J	7.05	3.82	31.7	4.80	32.0	4.46
7K	9.33	4.71	36.3	5.43	34.3	4.80
7L	15.07	4.34	30.7	7.24	32.0	5.90
7M	15.49	3.90	31.3	8.12	31.0	5.35

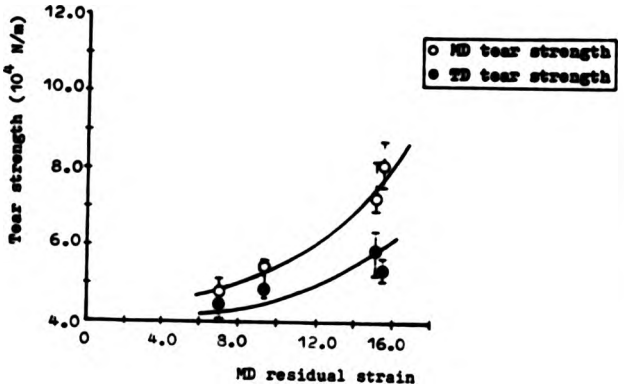

Figure 11.2. Effect of MD residual strain (at constant TD residual strain and thickness) on the tear strength of LDPE films.

11.3 Effect of Residual Strains on the Tear Strength of Blended and Linear Low Density Polyethylene Films

The effect of ε_{TD} and ε_{MD} on TrS of blended films and LLDPE films is shown in Tables 11.3 to 11.8 and plotted in Figure 11.3 and 11.8. The results show that 75% LDPE/25% LLDPE blend films show similar behaviour to LDPE films but 25% LDPE/75% LLDPE blend films and LLDPE films do not. In the cases where the proportion of LLDPE is greater than that of LDPE, TrS_{MD} is less than TrS_{TD} (the opposite case to LDPE films).

The effect of increasing the residual strain in both directions on the TrS of 25% LDPE/75% LLDPE blend films show that increasing the residual strain in both directions decreases the TrS_{MD} but has little effect on the TrS_{TD}, Tables 11.5 and 11.6 and Figures 11.5 and 11.6.

Eventhough the plots of TrS against the residual strains of LLDPE films, Figures 11.7 and 11.8, show that the TrS in both directions is affected by the residual strain, the change in the TrS values with residual strain is small. This is because the range of residual strain values is less in these films.

It is observed that increasing the LLDPE composition in the blends increases the TrS in both directions of the films. The tear initiated along the MD also showed the same behaviour as observed with LDPE films.

Table 11.3. Effect of TD residual strain on the tear strength of 75% LDPE/25% LLDPE blend films. The MD residual strain and film thickness were kept constant (within experimental error).

Sample	Residual strain		MD		TD	
	MD	TD	Thickness (10^{-6} m)	Tear strength (10^{4} N/m)	Thickness (10^{-6} m)	Tear strength (10^{4} N/m)
8A	9.38	0.60	35.3	13.96	35.3	11.07
8B	9.65	0.69	34.3	17.66	35.7	10.95
8C	9.42	1.62	36.0	11.81	36.0	11.15
8D	9.65	2.07	37.3	11.40	36.0	10.99
8E	9.83	2.18	35.0	12.89	37.0	11.03

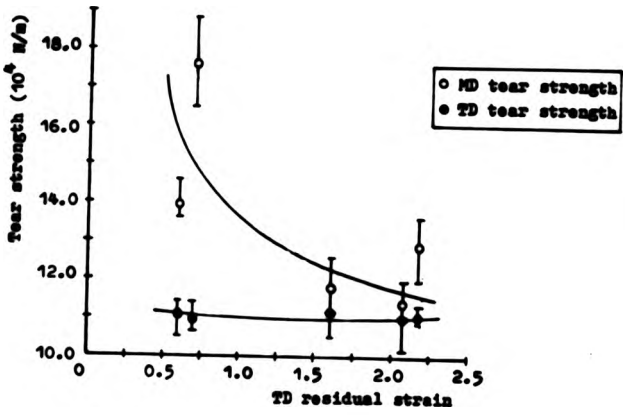

Figure 11.3. Effect of TD residual strain (at constant MD residual strain and thickness) on the tear strength of 75% LDPE/25% LLDPE blend films.

Table 11.4. Effect of MD residual strain on the tear strength of 75% LDPE/25% LLDPE blend films. The TD residual strain and film thickness were kept constant (within experimental error).

Sample	Residual strain		MD		TD	
	MD	TD	Thickness (10^{-6} m)	Tear strength (10^{4} N/m)	Thickness (10^{-6} m)	Tear strength (10^{4} N/m)
9A	5.96	0.92	34.0	11.48	34.0	11.00
9B	6.31	1.09	36.0	11.97	36.0	10.66
9C	11.49	0.89	36.7	13.94	36.3	10.01
9D	12.61	1.06	36.3	15.23	35.7	10.10
9E	12.77	1.08	37.3	16.34	36.0	9.95

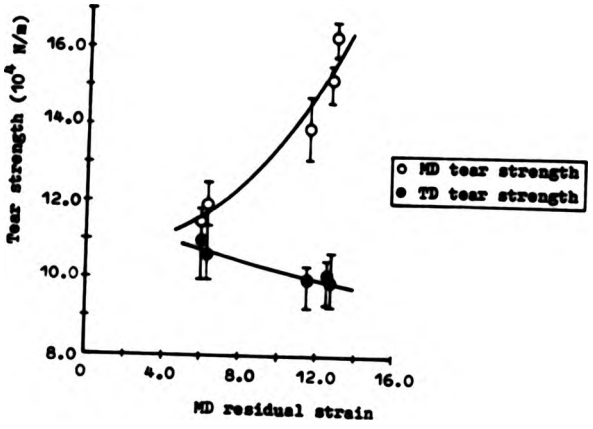

Figure 11.4. Effect of MD residual strain (at constant TD residual strain and thickness) on the tear strength of 75% LDPE/25% LLDPE blend films.

Table 11.5. Effect of TD residual strain on the tear strength of 25% LDPE/75% LLDPE blend films. The MD residual strain and film thickness were kept constant (within experimental error).

Sample	Residual strain		MD		TD	
	MD	TD	Thickness (10^{-6} m)	Tear strength (10^{4} N/m)	Thickness (10^{-6} m)	Tear strength (10^{4} N/m)
10A	8.95	0.80	36.7	12.40	37.7	12.71
10B	9.05	2.01	37.3	11.07	35.7	12.46
10C	8.76	2.20	34.3	10.34	35.6	12.95
10D	9.40	2.30	34.7	9.81	34.3	12.46

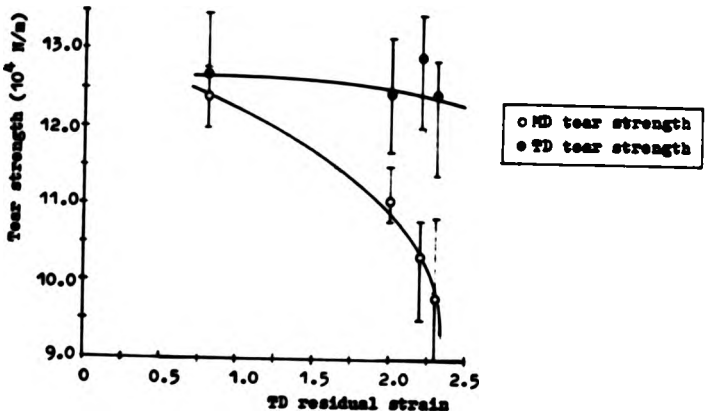

Figure 11.5. Effect of TD residual strain (at constant MD residual strain and thickness) on the tear strength of 25% LDPE/75% LLDPE blend films.

Table 11.6. Effect of MD residual strain on the tear strength of 25% LDPE/75% LLDPE blend films. The TD residual strain and film thickness were kept constant (within experimental error).

Sample	Residual strain		MD		TD	
	MD	TD	Thickness (10^{-6} m)	Tear strength (10^4 N/m)	Thickness (10^{-6} m)	Tear strength (10^4 N/m)
11A	4.32	0.98	38.0	11.21	37.3	12.42
11B	7.52	0.94	38.0	10.80	39.0	12.62
11C	10.47	1.05	36.7	8.81	36.7	12.44
11D	11.26	1.16	36.3	6.31	37.3	12.96

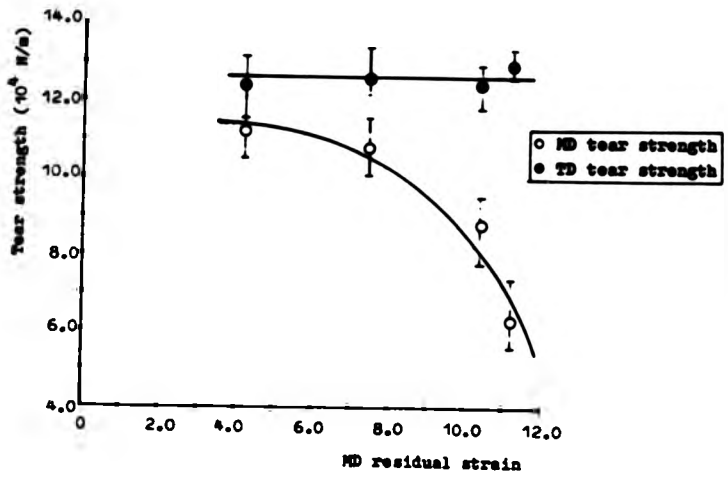

Figure 11.6. Effect of MD residual strain (at constant TD residual strain and thickness) on the tear strength of 25% LDPE/75% LLDPE blend films.

Table 11.7. Effect of TD residual strain on the tear strength of LLDPE films. The MD residual strain and film thickness were kept constant (within experimental error).

Sample	Residual strain		MD		TD	
	MD	TD	Thickness (10^{-6} m)	Tear strength (10^4 N/m)	Thickness (10^{-6} m)	Tear strength (10^4 N/m)
12A	6.34	0.68	36.3	12.03	33.7	12.30
12B	6.23	0.83	36.3	11.95	33.7	12.61
12C	6.31	1.42	34.0	10.85	34.7	13.34
12D	6.54	1.47	33.3	10.79	34.7	12.87
12E	6.63	1.59	32.7	11.51	33.0	13.56

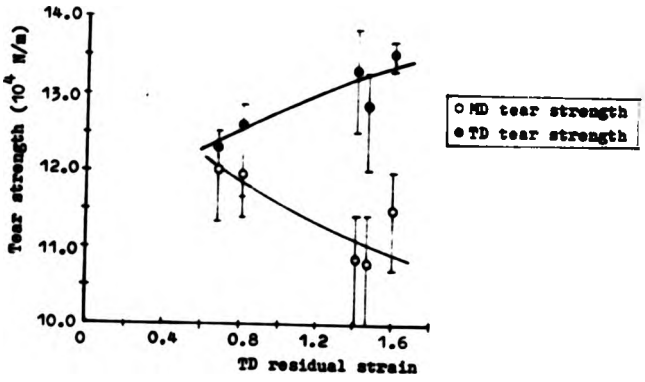

Figure 11.7. Effect of TD residual strain (at constant MD residual strain and thickness) on the tear strength of LLDPE films.

Table 11.8. Effect of MD residual strain on the tear strength of LLDPE films. The TD residual strain and film thickness were kept constant (within experimental error).

Sample	Residual strain		MD		TD	
	MD	TD	Thickness (10^{-6} m)	Tear strength (10^4 N/m)	Thickness (10^{-6} m)	Tear strength (10^4 N/m)
13A	5.01	1.04	32.7	11.56	33.0	13.87
13B	5.14	1.13	32.7	11.70	34.4	13.51
13C	7.41	0.85	34.7	11.82	36.3	13.63
13D	7.85	1.05	37.0	12.18	36.0	12.88

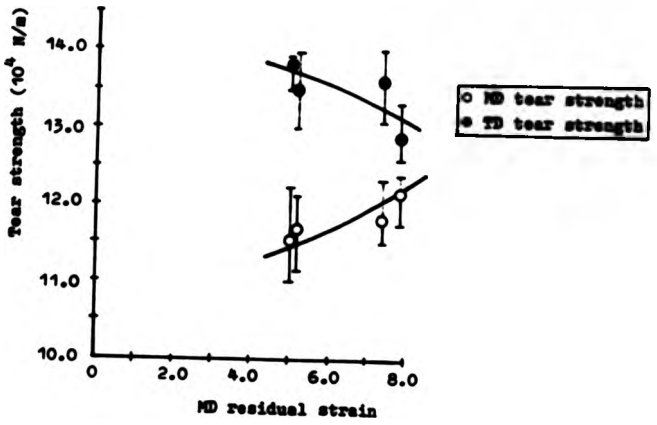

Figure 11.8. Effect of MD residual strain (at constant TD residual strain and thickness) on the tear strength of LLDPE films.

11.4 Discussion

The general trend that is observed from the results is that TrS_{MD} is affected by the residual strain. The TrS_{TD}, on the other hand, is not affected by the residual strain except in the case of LDPE films.

The TrS_{MD} seems to increase with increasing ε_{MD} and decreases with increasing ε_{TD}. The possible reason for this is the direction of tear propagation. As mentioned before in section 11.2, the tear initiated along the *MD* changed the direction of propagation towards the *TD*, whilst that initiated along the *TD* did not. The possible reason for this behaviour is the energy needed for tearing. The tear may propagate in a direction which minimises the energy needed to deform and fracture the film ahead of the tear. This energy can be evaluated by calculating the area under the tensile test curves for samples stressed along the *MD* and the *TD*. The results of this treatment is shown in Table 11.9. The results show that the energy needed to break the sample stressed in the *TD* is greater than that of the samples stressed in the *MD*.

Table 11.9. The energy under the stress-strain curves of LDPE films samples stressed in MD and TD.

Film sample	Residual strain		Energy (Nm)	
	MD	TD	MD	TD
6D	6.87	3.67	1.91	2.46
6E	12.84	1.19	0.96	3.42
6M	15.47	4.68	1.62	3.88
7L	15.07	4.34	1.80	3.03
7M	15.49	3.90	1.16	2.68

In the tear test, the *MD* samples had their tear initiated in the *MD* direction, Figure 11.9. For the tear to propagate in this direction the material ahead of the tear has to be stretched to failure in the *TD*. Table 11.9 shows that more energy is needed to break the sample by pulling in the TD than by pulling in the *MD*. Therefore the tear takes the most energetically favourable route and propagates in the *TD* where the material ahead of the tear is deformed in the *MD*. Therefore the tear which is initiated along the *MD* will change direction towards the *TD*.

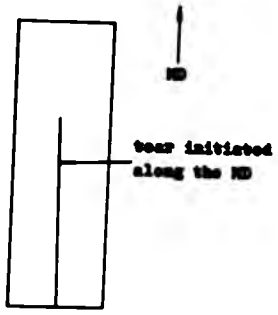

Figure 11.9. The direction of the initiated tear for sample cut along the MD.

From the above observation, it can be said that the TrS in both directions is the measure of the force per unit test piece thickness needed to break the molecular chains that are oriented along the MD. Therefore TrS will increase with increasing ϵ_{MD} and decrease with increasing ϵ_{TD}. This is because increasing ϵ_{MD} will increase the amount of molecular chains oriented along the MD, while increasing the ϵ_{TD} will reduce it.

The above argument explains the change of TrS_{MD} with the residual strain in both directions but not TrS_{TD}. Also since the tear propagated along the same direction, the TrS in both directions should be the same. This, however, is not observed. It was observed that TrS_{MD} of LDPE-rich films is greater than TrS_{TD} but that of LLDPE-rich films is the opposite. Further work is needed to explain this.

CHAPTER 12.0

EFFECT OF RESIDUAL STRAINS ON THE IMPACT STRENGTH OF POLYETHYLENE FILMS

12.1 Introduction

The effect of ε_{MD} and ε_{TD} on the impact strength, *IS*, of the films made from LDPE, LLDPE and the blends of the two is discussed in this chapter. The films were produced using the annealing conditions shown in Chapter 6.0.

The impact force or failure energy of the samples can be used as a measure of impact strength. In this project both are examined.

12.2 Effect of Transverse Direction Residual Strain on the Impact Strength of Low Density Polyethylene, Blended and Linear Low Density Polyethylene Films

The effect of increasing ε_{TD} on *IS* of LDPE films is shown in Table 12.1 and plotted in Figures 12.1 and 12.2. It could be seen that increasing ε_{TD} increases the *IS* of the films.

The results of increasing ε_{TD} on the *IS* of the blended and LLDPE films are also shown in Table 12.1 and plotted in Figures 12.1 and 12.2. It can be seen that these films show the same trend as observed with LDPE

films.

Table 12.1. Effect of TD residual strain on the impact strength of LDPE, LLDPE and blends of LDPE and LLDPE films. The MD residual strain and film thickness were kept constant (within experimental error).

Film	Sample	Residual strain		Average thickness (10^{-6} m)	Impact strength	
		MD	TD		Impact force (10^5 N/m)	Failure energy (10^4 J/m)
LDPE	6E	12.84	1.19	32.0	13.26	3.97
	6F	12.23	1.38	33.8	14.61	3.44
	6G	13.04	3.10	32.0	15.92	6.43
	6H	12.93	3.66	33.4	15.94	7.92
	6I	13.06	7.38	33.6	19.41	9.12
75% LDPE/ 25% LLDPE	8A	9.38	0.60	37.0	6.03	1.58
	8B	9.65	0.69	37.2	6.89	2.06
	8C	9.42	1.62	37.8	10.50	2.80
	8D	9.65	2.07	37.6	8.67	2.14
	8E	9.83	2.18	38.5	7.91	3.71
25% LDPE/ 75% LLDPE	10A	8.95	0.80	37.6	5.94	1.85
	10B	9.05	2.01	38.6	12.09	7.86
	10C	8.76	2.20	35.0	11.60	5.89
	10D	9.40	2.30	39.0	11.33	7.68
LLDPE	12A	6.34	0.68	32.8	8.14	2.42
	12B	6.23	0.83	34.8	9.67	2.82
	12C	6.31	1.42	36.2	12.43	7.17
	12D	6.54	1.47	35.2	12.80	6.72
	12E	6.63	1.59	36.0	13.11	8.65

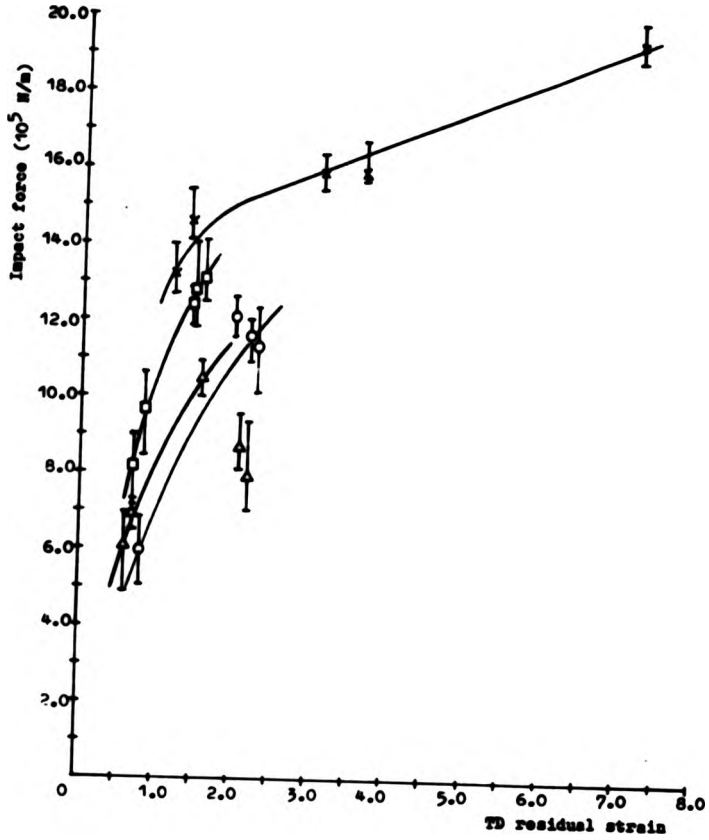

Figure 12.1. Effect of TD residual strain on the impact strength (impact force) of: (×) LDPE, (△) 75% LDPE/25% LLDPE, (○) 25% LDPE/75% LLDPE and (□) LLDPE films. The MD residual strain and film thickness were kept constant (within experimental error).

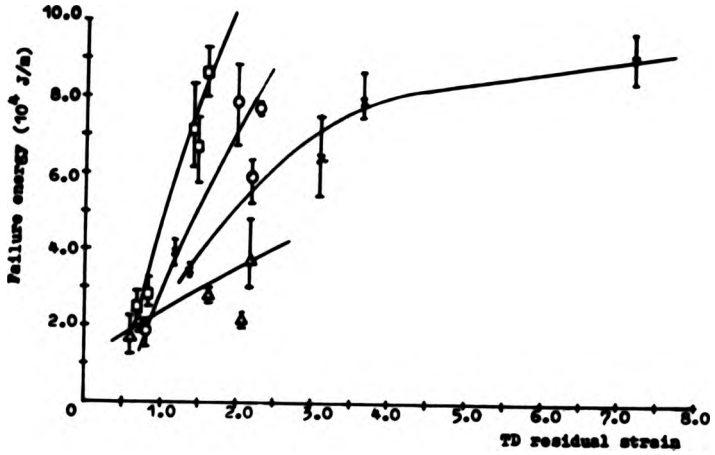

Figure 12.2. Effect of TD residual strain on the impact strength (failure energy) of: (×) LDPE, (△) 75% LDPE/25% LLDPE, (○) 25% LDPE/75% LLDPE and (□) LLDPE films. The MD residual strain and film thickness were kept constant (within experimental error).

12.3 Effect of Machine Direction Residual Strain on the Impact Strength of Low Density Polyethylene, Blended and Linear Low Density Polyethylene Films

The effect of increasing ϵ_{MD} on the *IS* of LDPE films is shown in Table 12.2 and plotted in Figures 12.3 and 12.4. It could be seen that increasing ϵ_{MD} decreases the impact force but has little effect on the failure energy.

The same behaviour is observed with the blended and

LLDPE films, as shown in Table 12.2 and Figures 12.3 and 12.4.

Table 12.2. Effect of MD residual strain on the impact strength of LDPE, LLDPE and blends of LDPE and LLDPE films. The TD residual strain and film thickness were kept constant (within experimental error).

Film	Sample	Residual strain		Average thickness	Impact strength	
		MD	TD	(10^{-6} m)	Impact force (10^5 N/m)	Failure energy (10^4 J/m)
LDPE	7J	7.05	3.82	32.4	18.17	5.78
	7K	9.33	4.71	35.6	18.53	5.83
	7L	15.07	4.34	32.0	17.58	6.44
	7M	15.49	3.90	31.0	16.14	6.59
75% LDPE/ 25% LLDPE	9A	5.98	0.92	39.7	8.19	2.21
	9B	6.31	1.09	39.2	8.87	2.44
	9C	11.49	0.89	37.0	5.49	1.44
	9D	12.61	1.06	37.0	7.20	4.63
	9E	12.77	1.08	35.2	6.78	2.16
25% LDPE/ 75% LLDPE	11A	4.32	0.98	36.2	9.47	3.25
	11B	7.52	0.94	37.4	5.59	1.65
	11C	10.47	1.05	36.2	7.77	2.37
	11D	11.26	1.16	38.7	8.36	3.73
LLDPE	13A	5.01	1.04	35.5	12.02	7.21
	13B	5.14	1.13	36.0	12.93	6.79
	13C	7.41	0.85	32.6	10.56	7.36
	13D	7.85	1.05	33.7	9.82	8.25

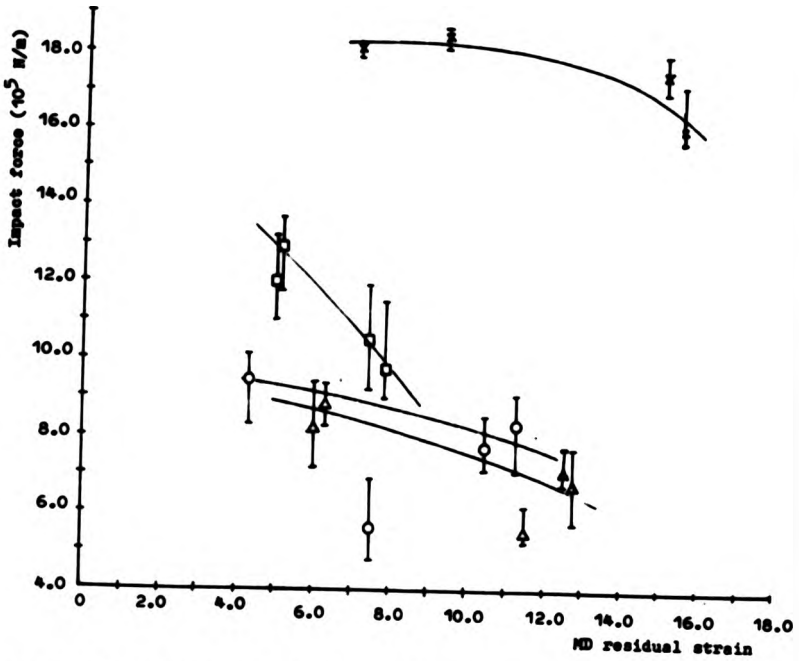

Figure 12.3. Effect of MD residual strain on the impact strength (impact force) of: (×) LDPE, (△) 75% LDPE/25% LLDPE, (○) 25% LDPE/75% LLDPE and (□) LLDPE films. The TD residual strain and film thickness were kept constant (within experimental error).

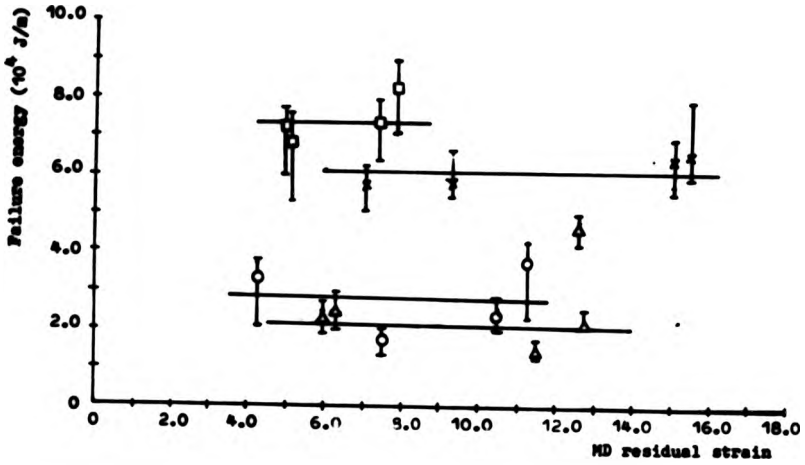

Figure 12.4. Effect of MD residual strain on the impact strength (failure energy) of: (×) LDPE, (△) 75% LDPE/25% LLDPE, (○) 25% LDPE/75% LLDPE and (□) LLDPE films. The TD residual strain and film thickness were kept constant (within experimental error).

12.4 Discussion

The results of *IS* as a function of residual strain show that *IS* increases with increasing ε_{TD} and decreases with increasing ε_{MD}. The reason for the observed dependent is due to the fact that *IS* is dependent on the balance of orientation in the films. Films with balanced orientation, same level of ε_{MD} and ε_{TD} in the sample, will have high *IS*. Balanced films will puncture during impact,

whereas unbalanced films will split along the direction of molecular orientation. Since the films manufactured in this project have high ϵ_{MD} and low ϵ_{TD}, increasing ϵ_{TD} will result in more balanced films. Therefore, *IS* will increase with increasing ϵ_{TD}. On the other hand, increasing ϵ_{MD} will result in unbalanced films and thus *IS* decreases with increasing ϵ_{MD}.

The effect of blending on *IS* is variable. This is in agreement with the results published in the literature.

CHAPTER 13.0

CONCLUSION AND SUGGESTIONS FOR FURTHER WORK

13.1 Introduction

In this project the effect of changing the processing conditions on the mechanical properties of blown PE films was studied. It was observed that changing the processing conditions changes the orientation in the films. This change in orientation affects the mechanical properties of the films.

The orientation of the films was evaluated by a shrinkage method. With this method the residual strain in the films was evaluated and used as a measure of orientation.

The work done in this project can be classified into three areas. These are:

a) measurement of residual strain;
b) factors affecting residual strain; and
c) effect of residual strain on the mechanical properties of the films.

The conclusion reached in each area is discussed in the following sections.

13.2 Measurement of Residual Strains

The basis of this work has been the development of a novel method to assess the degree of residual strain in the *MD* and the *TD* of the films. The method is based on shrinkage measurement and is described in Chapter 2.0 and Appendix 1.0.

The residual strain values give a clearer measure of orientation than the shrinkage values. This is because it is possible to obtain negative shrinkage values and these are physically difficult to interpret. On the other hand, residual strain values are always positive and thus give a clearer molecular picture of the degree of orientation.

The residual strain in one direction is dependent on the residual strain in the other direction. If the value in one direction is increased the value in the other direction will also increase. The reason for this has been explained in Chapter 3.0.

The residual strain is not a direct measure of orientation but related to the orientation and length of the strained molecules. For a given level of orientation, longer molecules will give higher residual strain values.

13.3 Factors Affecting Residual Strain

The factors that affect residual strain were studied in the preliminary work of this project which was

summarised in Chapter 3.0. The conclusion that can be drawn from this study is that the residual strain of the films depends on:

a) the processing conditions;
b) blending; and
c) annealing temperature and time of the films.

The effect of changing the processing conditions on the residual strain of the films was shown in Chapter 3.0. The results showed that increasing the blow-up ratio or the haul-off speed increased the residual strain in both direction of the films. Increasing the freeze line height or the screw speed, on the other hand, reduced the residual strain in both directions of the films.

The amount of residual strain depends on both the stretching and relaxation processes during film formation. The above observations on the effect of changing processing conditions are consistent with this explanation as elaborated in section 3.3.

The type of resin used also affected the residual strain values of the films. If the processing conditions and the film thickness were kept constant, increasing LLDPE composition in the blend resulted in the reduction of the residual strain. The reduction is due to the linear structure of LLDPE which is thought to allow greater rate of molecular relaxation.

The residual strain of the films could also be affected by an annealing process. Annealing the films at several temperatures, in the temperature range of 105-130^{o}C, for a range of annealing time resulted in the reduction of residual strain. The rate of residual strain reduction was greater at higher annealing temperatures.

A number of studies *(120)* have examined the effect of annealing, at temperatures close to the melting point, on the crystalline regions of polyethylene. They showed thickening of the lamellae which form the crystallites. For this to occur there must be molecules rearrangement within, on the surface and between the lamellae.

It is postulated that in the present case where there is residual strain in the molecules between the lamellae, once the temperature is raised to a value where molecular rearrangement can occur the tendency is for the strained molecules or oriented chain ends to become less strained (i.e. relax). Thus, this reduction in strain will occur at temperatures similar to those where lamellae thickening has been observed.

13.4 Effect of Residual Strains on the Mechanical Properties

To study the effect of residual strain on the mechanical properties, the residual strain in one direction and the film thickness were kept constant by using the annealing method. Thus the effect of changing

residual strain in one direction only could be determined.

The mechanical properties of the films are affected by the residual strain. The properties like the elongation at break, tensile strength and impact strength showed clear trends but with scattering of the points. Others, like the yield stress, tensile modulus and tear strength need further work before any conclusion could be drawn.

The elongation at break and tensile strength results showed an exponential relationship with the residual strain. In both cases the value of the property changed between a value at zero residual strain and approached a limitting value at high levels of residual strain. Equations were derived and used to estimate the properties. The estimated and measured values showed a good agreement. This comparison is shown in Chapters 7.0 and 8.0. This implies that a shrinkage test can be used to estimate the likely ultimate tensile properties of the films.

The molecular characteristics that control the shrinkage also control the tensile strength and elongation at break. It is postulated that this molecular cause is the strain in the molecules between the lamellae in the semi-crystalline material.

The results of increasing residual strain on the impact strength showed that impact strength depends on the balance of residual strain in the films. Films with balanced residual strain have higher impact strength. A

model to show the relationship between impact strength and residual strain, however, cannot be drawn due to limited data.

Tear testing involved a complicated stress pattern in the sample but the trend for tears initiated in the *MD* to change direction and propagate in the *TD* can be explained in terms of the differing energy requirements to break the film in the two directions.

13.5 Comparison With Previous Work

Comparing the results obtained in this project with the results published in the literature, it was observed that there are similarities.

The effect of shrinkage temperature and time on the shrinkage of the films was similar with the results published in the literature *(52-54,56-59)*. The results showed that the shrinkage increased with increasing shrinkage temperature and time.

The results of tensile strength, elongation at break and impact strength as a function of residual strain of the films followed the same pattern as observed with the results of those properties against orientation, published in the literature *(107,108,111-116)*.

In the literature it was reported that increasing the blow-up ratio or the haul-off speed increased the orientation in one direction and decreased in the other.

In this project, however, it was observed that increasing the blow-up ratio or the haul-off speed increased the residual strain in both directions. Also it was observed that increasing the freeze line height or the screw speed reduced the residual strain in both directions.

The difference between this project and the work done previously is that in this project the mechanical properties of the films and the processing conditions are related through a quantitative measure of film structure, in this case the residual strain. In the previous work *(22-46,106-116)*, the relationship between properties and processing conditions was explained in term of factors, such as the orientation, which are inferred rather than measured.

13.6 Suggestions for Further Work

While analysing the results, several observations were made. These observations could not be explained within the scope of this project. Therefore further work is needed to explain the above observations. It is expected that the results of this work will allow greater understanding of the blown film process than has been obtained in the previous work.

The predicted curves of the elongation at break of LDPE films against the residual strain, Figures 7.21 and 7.22, showed that at the point where the *MD* and *TD* curves

met, corresponding to samples of equal residual strain in both directions, the elongation at break of the films with different levels of residual strain falls within the same range. This is surprising because the elongation at break in a given direction of the films decreased with increasing residual strain. Since this is observed with predicted results, it is interesting to see whether the same behaviour will hold in practice. To study this equibiaxially oriented films of several levels of residual strains are needed.

The above films can be produced by building an apparatus which can stretch and cool molten films in a controlled way. This would mean that films of various levels of residual strains could be made without the complicated extruding process. With this apparatus, it is also possible to study in detail the effect of stretching on the residual strain and properties of the films.

The equations derived to described the relationship between tensile strength and elongation at break with the residual strains contains the constant k. In the elongation at break data, this constant was observed to be independent of the direction of test and blending but in tensile strength data it was not. Further work is needed to defined this constant and to see whether this constant is a structural parameter or not. This can be done by calculating the value of k with films produced by different methods so the the structure of the films are

different.

The results obtained for yield stress, tensile modulus and tear strength did not show a clear trend with residual strain. Probably these results depend on the orientation of the crystallites rather than the residual strain. Therefore further work using x-rays method is necessary to study the crystallite orientation-properties relationship.

It is also interesting to see whether the relationship obtained between tensile strength and elongation at break with residual strain hold in flat LDPE and LLDPE films. The rate of cooling of these films can be varied by varying the temperature of the chill roll, and can therefore be different from those found in the blown film method.

The effect of density on the films properties should be studied. This can be achieved by using LLDPE resins of different comonomer concentration.

APPENDIX 1.0

DERIVATION OF THE EQUATION TO EVALUATE RESIDUAL STRAINS FROM SHRINKAGE RESULTS

The equations to calculate the residual strain from the shrinkage results were derived based on the calculated stretching needed to return the shrunk sample to its original dimensions. To do the calculations, it is assumed that this is achieved by stretching the shrunk sample in two stages.

Consider the shrunk sample shown in Figure A1.1(a). The volume of this sample is given by

$$V = L.B.T \qquad \text{(A1.1)}$$

where L is its length, B is its breadth and T is its thickness.

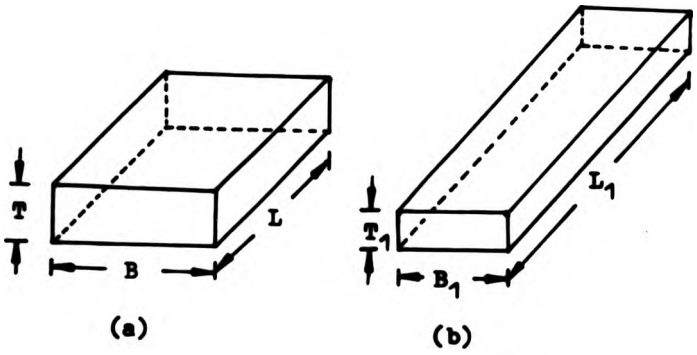

Figure A1.1. The dimensions of the shrunk sample: (a) before stretching; and (b) after stretching along L direction.

During the first stage of extension, the shrunk sample is stretched along its length, in L direction, as shown in Figure A1.1(b). During this stretching, it is assumed that the breadth and thickness of the sample contract in the same ratio because the sample is not clamped and thus can contract freely. The extension ratio in L direction, λ_L, is given by

$$\lambda_L = \frac{L_1}{L} \qquad \text{(A1.2)}$$

By rearranging equation A1.2, the new length of the stretched sample, L_1, is obtained as shown by equation A1.3.

$$L_1 = L.\lambda_L \qquad \text{(A1.3)}$$

Since the sample contracts in the same ratio in the other two directions, the new dimensions in the other two directions are given by equations A1.4 and A1.5.

$$T_1 = \frac{T}{X} \qquad \text{(A1.4)}$$

$$B_1 = \frac{B}{X} \qquad \text{(A1.5)}$$

where X is some constant.

The volume of the stretched sample is given by

$$V_1 = L_1.B_1.T_1 \qquad \text{(A1.6)}$$

and substituting equations A1.3, A1.4 and A1.5 into A1.6 get equation A1.7.

$$V_1 = L.\lambda_L.(BT/X^2) \qquad \text{(A1.7)}$$

Assuming that the sample is incompressible, the volume before and after the first stage of stretching are equal. Therefore equation A1.1 is equal to equation A1.7.

$$L.B.T = L.\lambda_L.(BT/X^2) \qquad \text{(A1.8)}$$

Simplifying equation A1.8 results in equation A1.9.

$$X = (\lambda_L)^{1/2} \qquad \text{(A1.9)}$$

Substituting equation A1.9 into equations A1.4 and A1.5 get the equation for the new breadth and thickness after the first stage of stretching.

$$B_1 = \frac{B}{(\lambda_L)^{1/2}} \qquad \text{(A1.10)}$$

$$T_1 = \frac{T}{(\lambda_L)^{1/2}} \qquad \text{(A1.11)}$$

The second stage of stretching involves stretching the sample along its breadth, B direction, as shown in Figure A1.2. The extension ratio along the B direction is given by

$$\lambda_B = \frac{B_2}{B_1} \qquad \text{(A1.12)}$$

or

$$B_1 = \frac{B_2}{(\lambda_B)} \qquad \text{(A1.13)}$$

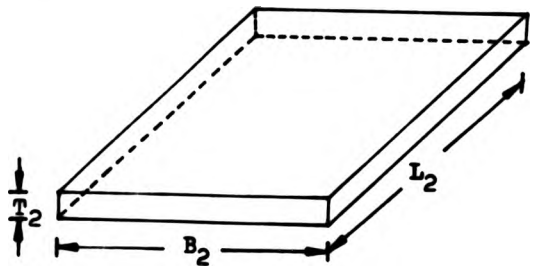

Figure A1.2. The dimensions of the shrunk sample after the second stage of stretching along B direction.

During the second stage of stretching, it is assumed that the sample contracts in the same ratio in thickness and length directions. Using the same argument as before, the new length, L_2, and new thickness, T_2, are given by

$$L_2 = \frac{L_1}{(\lambda_B)^{1/2}} \qquad \text{(A1.14)}$$

$$T_2 = \frac{T_1}{(\lambda_B)^{1/2}} \qquad \text{(A1.15)}$$

Substituting equation A1.10 into equation A1.13 results in equation A1.16.

$$\frac{B_2}{\lambda_B} = \frac{B}{(\lambda_L)^{1/2}} \qquad \text{(A1.16)}$$

and rearranging equation A1.16 yields equation A1.17.

$$B_2 = \frac{B\lambda_B}{(\lambda_L)^{1/2}} \qquad \text{(A1.17)}$$

Also substituting equation A1.3 into A1.14 and equation A1.11 into A1.15 yields the new length, L_2, and new thickness, T_2, of the sample after the second stage of stretching.

$$L_2 = \frac{L\lambda_L}{(\lambda_B)^{1/2}} \qquad \text{(A1.18)}$$

and

$$T_2 = \frac{T}{(\lambda_L \lambda_B)^{1/2}} \qquad \text{(A1.19)}$$

Now consider the shrink ratio of the sample. The shrink ratio is given by the ratio of the original dimension to the shrunk dimension. The shrink ratio in the L direction is given by

$$S_L = \frac{L_2}{L} \qquad \text{(A1.20)}$$

where L_2 is the original length and L is the shrunk length of the sample. Similarly, the shrink ratio in the B direction is given by

$$S_B = \frac{L_2}{B} \qquad \text{(A1.21)}$$

where B_2 and B denote the original and shrunk breadth of the sample, respectively.

Substituting equation A1.18 into equation A1.20 and simplifying results in

$$(\lambda_L)^2 = (S_L)^2 . \lambda_B \qquad \text{(A1.22)}$$

Also substituting equation A1.17 into equation A1.21 and rearranging gives

$$\lambda_B = s_B(\lambda_L)^{1/2} \qquad \text{(A1.23)}$$

Finally, by substituting equation A1.23 into equation A1.22 and rearrange get

$$\lambda_L = (s_L)^{4/3}.(s_B)^{2/3} \qquad \text{(A1.24)}$$

Equation A1.24 is the extension ratio in L direction. The extension ratio along B direction is obtained by substituting equation A1.24 into equation A1.23 to give

$$\lambda_B = (s_B)^{4/3}.(s_L)^{2/3} \qquad \text{(A1.25)}$$

In general, the extension ratio in any given direction is given by

$$\lambda_X = \frac{X + \Delta X}{X} \qquad \text{(A1.26)}$$

The term $\Delta X/X$ is the strain term and therefore the extension ratio is given by

$$\lambda_X = 1 + \epsilon_X \qquad \text{(A1.27)}$$

where ϵ_X is the strain term.

Applying this argument to equations A1.24 and A1.25,

the residual strain along L and B directions is given by

$$\varepsilon_L = (S_L)^{4/3}.(S_B)^{2/3} - 1 \qquad \text{(A1.28)}$$

and

$$\varepsilon_B = (S_B)^{4/3}.(S_L)^{2/3} - 1 \qquad \text{(A1.29)}$$

Replacing L by MD and B by TD to denote the machine and transverse directions, the equations to evaluate the residual strain in MD and TD are obtained.

$$\varepsilon_{MD} = (S_{MD})^{4/3}.(S_{TD})^{2/3} - 1 \qquad \text{(A1.30)}$$

and

$$\varepsilon_{TD} = (S_{TD})^{4/3}.(S_{MD})^{2/3} - 1 \qquad \text{(A1.31)}$$

APPENDIX 2.0

EVALUATION OF THE TRUE RESIDUAL STRAINS VALUES OF THE FILMS AFTER ANNEALING

It was mentioned in Chapter 2.0 that the true residual strain of the films was evaluated using the extrapolation method. This is done by doing the shrinkage test for each sample at three shrinkage times; 10.0, 20.0 and 30.0 minutes. The apparent residual strain value evaluated at each shrinkage time was evaluated and plotted as shown by Figure A2.1. The points A, B and C denote the apparent residual strain values at 10.0, 20.0 and 30.0 minutes shrinkage time, respectively. The true residual strain of this sample is the value at zero shrinkage time, found by extrapolation.

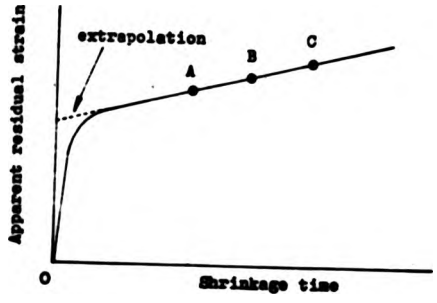

Figure A2.1. The extrapolation method used to evaluate the true residual strain of the films.

APPENDIX 3.0

EVALUATION OF THE VELOCITY OF THE MELT AT THE DIE LIP

The velocity of the melt leaving the die, V_o, is different from the velocity of the solid film at the freeze line, V_1. The value of V_1 is given by the *HOS* used to make the film. This comparison is shown in Figure A3.1.

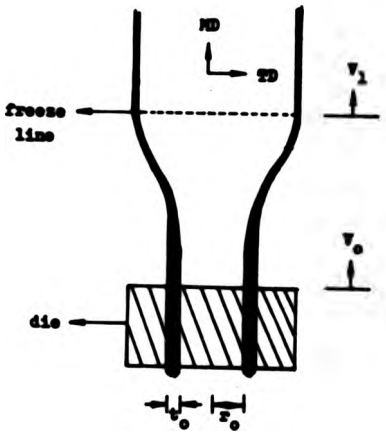

Figure A3.1. Sketch showing V_1 and V_o of a blown film bubble.

If the die has a radius of r_o mm and the die gap is t_o mm, then the cross-section of the die is given by:

$$\text{Cross-section} = 2\pi r_o t_o \qquad \text{(A3.1)}$$

The volumetric output of the die is the product of its cross-section and V_o. Thus

$$\text{Volumetric output} = 2\pi r_o t_o V_o \qquad \text{(A3.2)}$$

The unit of the volumetric output is mm^3/s if the unit of V_o is mm/s.

If the output rate of the extruder is Q, then the volumetric output can be calculated by dividing Q with the density of the melt, ρ_m, as shown below:

$$\text{Volumetric output} = \frac{Q}{\rho_m} \qquad \text{(A3.3)}$$

Changing the unit of equations A3.3 to mm^3/s and substitute into equation A3.2 and rearrange results in:

$$V_o = \frac{Q \times 10^9}{3600 \times \rho_m 2\pi r_o t_o} \qquad \text{(A3.4)}$$

Equation (A3.4) can be used to evaluate V_o if the value of ρ_m at a given temperature is known. The LDPE films investigated were extruded at 163°C and the value of ρ_m of LDPE melt at this temperature was obtained from published literature as 769.0 kg/m^3.

REFERENCES

1) A. Whelan and D.J. Dunning; *Development in Plastics Technology-1*; Chapter 3, Applied Science Publishers Ltd.

2) J.R.A. Pearson and C.J.S. Petrie; *J. Fluid Mech.*; 40(1), 1-19(1970)

3) J.R.A. Pearson and C.J.S. Petrie; *J. Fluid Mech.*; 42(3), 609-625(1970)

4) C.J.S. Petrie; *AIChE J.*; 21(2), 275-282(1975)

5) C.J.S. Petrie; *Polym. Eng. Sci.*; 15(10), 708-724(1975)

6) R.K. Gupta, A.B. Metzner and K.F. Wissbrun; *Polym. Eng. Sci.*; 22(3), 172-181(1982)

7) X-L Luo and R.I. Tanner; *Polym. Eng. Sci.*; 25(10), 620-629(1985)

8) J.R.A. Pearson and C.J.S. Petrie; *Plast. Polym.*; 85-94(1970)

9) C.J.S. Petrie; *Rheol. Acta*; 12, 92-99(1973)

10) R. Farber and J. Dealy; *Polym. Eng. Sci.*; 14(6), 435-440(1974)

11) T. Kanai and J.L. White; *Polym. Eng. Sci.*; 24(15), 1185-1201(1984)

12) T.A. Huang and G.A. Campbell; *Adv. Polym. Tech.*; 5(3),181-192(1985)

13) T. Kanai and J.L. White; *J. Polym. Eng.*; 5(2), 135-157(1985)

14) T.A. Huang and G.A. Campbell; *J. Plast. Film Sheet.*; 2, 30-39(1986)

15) T. Kanai, M. Kimura and Y. Asano; *J. Plast. Film Sheet.*; 2, 224-241(1986)

16) C.D. Han and J.Y. Park; *J. Appl. Polym. Sci.*; 19, 3257-3276(1975)

17) C.D. Han and J.Y. Park; *J. Appl. Polym. Sci.*; 19, 3277-3290(1975)

18) W.A. Holmes-Walker and B. Martin; *Brit. Plast.*; 232-236(1966)

19) L.E. Dowd; *SPE J.*; 28, 22-26(1972)

20) W. Ast; *Kunststoffe*; 63, 427-433(1973)

21) C.J.S. Petrie; *Plast. Polym.*; 259-264(1974)

22) M.H. Wagner; *Kunststoffe*; 68(6), 361-366(1978)

23) D.R. Holmes, R.G. Miller, R.P. Palmer and C.W. Bunn; *Nature*; 1104-1106(1953)

24) A. Keller; *J. Polym. Sci.*; 15, 31-49(1955)

25) P.A. Bettelheim and R.S. Stein; *J. Polym. Sci.*; 27(115), 567-569(1958)

26) D.R. Holmes and R.P. Palmer; *J. Polym. Sci.*; 31, 345-358(1958)

27) G. Raumann and D.W. Saunders; *Proc. Phys. Soc.*; 77, 1028-1037(1961)

28) P.H. Lindenmeyer and S. Lustig; *J. Appl. Polym. Sci.*; 227-240(1965)

29) V.B. Gupta and I.M. Ward; *J. Macromol. Sci.-Phys.*; B1(2), 373-400(1967)

30) V.B. Gupta, A. Keller and I.M. Ward; *J. Macromol. Sci.-Phys.*; B2(1), 139-146(1968)

31) V.B. Gupta and I.M. Ward; *J. Macromol. Sci.-Phys.*; B4(2), 453-459(1970)

32) C.R. Desper; *J. Appl. Polym. Sci.*; 13(1), 169-191(1969)

33) T. Nagasawa, T. Matsumura and S. Hoshino; *Appl. Polym. Symp.*; 20, 275-293(1973)

34) A. Keller; *Shell Polym.*; 2(3), 86-89(1978)

35) W.P. Maddams and J.E. Preedy; *J. Appl. Polym. Sci.*; 22, 2721-2737(1978)

36) W.P. Maddams and J.E. Preedy; *J. Appl. Polym. Sci.*; 22, 2739-2749(1978)

37) W.P. Maddams and J.E. Preedy; *J. Appl. Polym. Sci.*; 22, 2751-2759(1978)

38) M.A. McRae and W.P. Maddams; *J. Appl. Polym. Sci.*; 22, 2761-2768(1978)

39) M. Pietralla and H.G. Kilian; *J. Polym. Sci. Polym. Phys. Ed.*; 18, 285-290(1980)

40) R.J. Samuels; *J. Appl. Polym. Sci.*; 26, 1383-1412(1981)

41) K.J. Choi, J.E. Spruiell and J.L. White; *J. Polym. Sci. Polym. Phys. Ed.*; 20, 27-47(1982)

42) J.J.C. Picot; *Polym. Eng. Sci.*; 24(6), 415-420(1984)

43) N. Ashizawa, J.E. Spruiell and J.L. White; *Polym. Eng. Sci.*; 24(13), 1035-1042(1984)

44) J.L. Pezzutti and R.S. Porter; *J. Appl. Polym. Sci.*; 30, 4251-4259(1985)

45) M. Gilbert, D.A. Hemsley and S.R. Patel; *Brit. Polym. J.*; 19, 9-23(1987)

46) J.L. White and M. Cakmak; *Adv. Polym. Tech.*; 8(1), 27-61(1988)

47) D.R. Parikh and G.W. Knight; *Plast. Eng.*; 47-49(1988)

48) W. Seifried; *Kunststoffe*; 78(10), 948-952(1988)

49) C.T. Mathawny; *SPE J.*; 17(6), 567-570(1961)

50) R.J. Samuels; *Structured Polymer Properties*; Chapter 4.0, John Wiley and Sons.(1974)

51) K.C. Steffen; *Mod. Plast.*; 145-148(1966)

52) P.R. Pinnock and I.M. Ward; *Trans. Faraday Soc.*; 62, 1308-1320(1966)

53) B.N. Gregory; *Plastics*; 165-168(1969)

54) G. Menges and W.O. Predohl; *Polym. Eng. Sci.*; 15(5), 394-400(1975)

55) E. Fischer; *Kunststoffe*; 71(6), 380-385(1981)

56) T. Pakula and M. Trznadel; *Polymer*; 26, 1011-1018(1985)

57) T. Pakula and M. Trznadel; *Polymer*; 26, 1019-1024(1985)

58) A. Siegmann and Y. Nir; *Polym. Eng. Sci.*; 27(3), 225-231(1987)

59) T. Liu and I.R. Harrison; *Polym. Eng. Sci.*; 28(8), 517-521(1988)

60) H.D. Keith and F.J. Padden,Jr.; J. Polym. Sci.; 41(138), 525-528(1959)

61) A. Peterlin; J. Polym. Sci. Part C; 9, 61-89(1965)

62) K. Kobayashi and T. Nagasawa; J. Polym. Sci. Part C; 15, 163-183(1966)

63) A. Peterlin; J. Polym. Sci. Part C; 15, 427-443(1966)

64) G. Meinel and A. Peterlin; Polym. Letters; 5, 613-618(1967)

65) R.G. Vadimsky, H.D. Keith and F.J. Padden,Jr.; J. Polym. Sci. Part A-2; 7, 1367-1378(1969)

66) H.D. Keith, F.J. Padden,Jr. and R.G. Vadimsky; J. Appl. Phys.; 42(2), 4585-4592(1971)

67) T. Nagasawa, T. Matsumura and S. Moshino; Appl. Polym. Symp.; 20, 295-313(1973)

68) T. Tagawa and K. Ogura; J. Polym. Sci. Polym. Phys. Ed.; 18, 971-979(1980)

69) B.J. Jungnickel; Polym. Eng. Sci.; 27(4), 1021-1034(1987)

70) H. Leder; Kunststoffe; 73(5), 251-254(1983)

71) D.H. Sebastian and J.R. Dearborn; Polym. Eng. Sci.; 23(10), 572-575(1983)

72) F. De Candia, A. Perullo and V. Vittoria; J. Appl. Polym. Sci.; 28, 1815-1817(1983)

73) C.D. Han and T.H. Kwack; J. Appl. Polym. Sci.; 28, 3399-3418(1983)

74) T.H. Kwack and C.D. Han; J. Appl. Polym. Sci.; 28,

3419-3433(1983)

75) G. Attalla and P. Bertinotti; *J. Appl. Polym. Sci.*; 28, 3503-3511(1983)

76) S.A. Montes; *Polym. Eng. Sci.*; 24(4), 259-263(1984)

77) D. Constantin; *Polym. Eng. Sci.*; 24(4), 268-274(1984)

78) S. Bork; *Kunststoffe*; 74(9), 474-485(1984)

79) J. Gray; *Prog. Rub. Plast. Tech.*; 1(1), 1-12(1985)

80) F.P. La Mantia and D. Acierno; *Polym. Eng. Sci.*; 25(5), 279-283(1985)

81) A. Furumiya, Y. Abana, Y. Ushida, T. Masuda and A. Nakajima; *Pure Appl. Chem.*; 824-832(1985)

82) J.A. Torkington; *Polycon.*; 1-13(1985)

83) D.E. James; *Encyclo. Polym. Sci. Eng.*; 6, 429-454, John Wiley and Sons(1985)

84) A. Naber and M.R. Kamal; *Plast. Eng.*; 43-46(1987)

85) R. Muller, J.L. Barea and P. Sanseau; *J. Appl. Polym. Sci.*; 33, 289-303(1987)

86) A. Siegmann and Y. Nir; *Polym. Eng. Sci.*; 27(15), 1182-1186(1987)

87) J.L. White and H. Yamane; *Pure Appl. Chem.*; 59(2), 193-216(1987)

88) D.M. Kalyon, D.W. Yu and F.H. Moy; *Polym. Eng. Sci.*; 28(23), 1542-1550(1988)

89) D.M. Kalyon and F.H. Moy; *Polym. Eng. Sci.*; 28(23), 1551-1558(1988)

90) J.A. Torkington; *Macplas*; 48-51(1982)

91) C.S. Speed; *Plast. Eng.*; 39-42(1982)

92) J. Mancekivell; Canadian Plast.; 27-30(1982)

93) F. Arch; Paper, Film and Foil Convert.; 88-94(1982)

94) J. Johnson; Paper Synthet. Confr.; 85-91(1982)

95) M. Nelmy; Paper Synthet. Confr.; 93-102(1982)

96) S. Bonotto, G.S. Cieloszyk, W.D. Heitz and F.A. Ruiz; Paper Synthet. Confr.; 103-112(1982)

97) P.A. Davies; Polycon.; 40-53(1984)

98) F.P. La Mantia and D. Acierno; Eur. Polym. J.; 21(9), 811-813(1985)

99) E.W. Veazey; J. Plast. Film Sheet.; 1, 60-67(1985)

100) D. Acierno, D. Curto, F.P. La Mantia and A. Valenza; Polym. Eng. Sci.; 26(1), 28-33(1986)

101) F.P. La Mantia, A. Valenza and D. Acierno; Eur. Polym. J.; 22(8), 647-652(1986)

102) P. Vadhar and T. Kyn; Polym. Eng. Sci.; 27(3), 202-210(1987)

103) M. Schule and R. Wolff; Kunststoffe; 77(8), 744-750(1987)

104) V. Musil, B. Pregrad and B. Zerjal; Intern. Polym. Process.; 2(3/4), 182-184(1988)

105) F.P. La Mantia, A. Valenza and D. Acierno; Polym. Eng. Sci.; 28(2), 90-95(1988)

106) P.L. Clegg and N.D. Huck; Plastics; 26(4), 114-120(1961)

107) P.L. Clegg and N.D. Huck; Plastics; 26(5), 107-110(1961)

108) J.P. Pilaro, R.J. Kramer, L.A. Kuhlmann; Mod. Plast.;

123-220(1961)

109) M.J. Hughes and M.J. Cawkwell; *Plastics*; 31(3), 274-277(1966)

110) I. Sirevic, M. Cvjeticanin and I. Catic; *SPE 38th Annual Confr.*; 41-43(1980)

111) D.A. Williamson; *Plast. Polym.*; 169-174(1970)

112) E. Paschke, H. Ploenes and H. Dans; *Kunststoffe*; 67(7), 377-380(1977)

113) O. Hollricher, D. Lockner and H. Zimmermann; *Kunststoffe*; 70(1), 2-4(1980)

114) C.V. Datter; *Plast. Eng.*; 29-30(1982)

115) E. Fischer: *Kunststoffe*; 76(2), 117-122(1986)

116) T. Kanai; *Intern. Polym. Process.*; 1(3), 137-143(1987)

117) M.A. Brunt; *Plastica*; 20(7), 275-285(1967)

118) E.S. Shermann; *Polym. Eng. Sci.*; 24(11), 895-907(1984)

119) D.J. Dunning and W.B. Burger: *Private Communication*; L.S.P.T.(1988)

120) D.C. Bassett; *Principles of Polymer Morphology*; Chapter 5.0, Cambridge University Press(1981)

121) I.M. Ward; *Structure and Properties of Oriented Polymers*; Chapters 7.0 and 8.0, Applied Science Publishers Ltd.(1975)

TITLE AN INVESTIGATION INTO THE RELATIONSHIPS BETWEEN PROCESSING, ORIENTATION AND PROPERTIES OF LOW DENSITY POLYETHYLENE FILMS

AUTHOR BAHARIN BIN AZAHARI

INSTITUTION and DATE Polytechnic of North London (1990) (CNAA)